doi.org/10.1002/batt.202000022

Special Collection

Electrolytes for Lithium (Sodium) Batteries Based on Ionic Liquids: Highlighting the Key Role Played by the Anion

Thomas Rüther,*[a] Anand I. Bhatt,[a] Adam S. Best,[a] Kenneth R. Harris,*[b] and Anthony F. Hollenkamp[a]

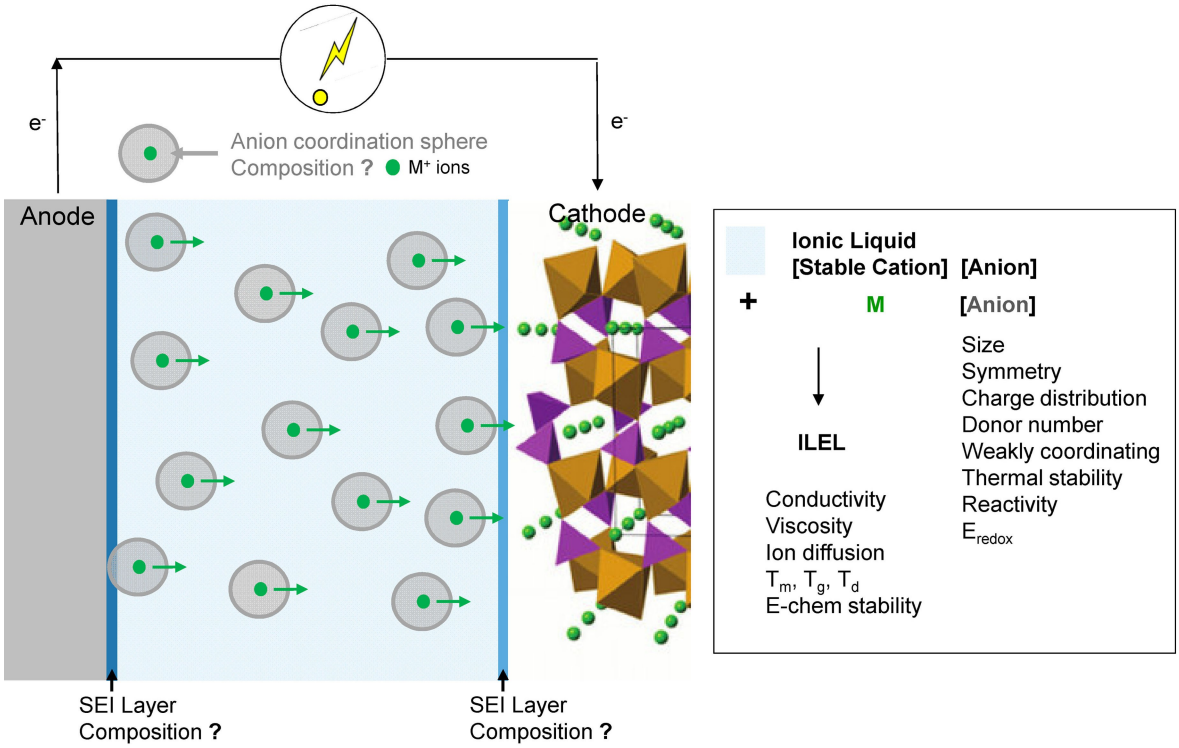

Research since 2000 has clearly shown that ionic liquids (ILs) and their metal salt containing mixtures have good potential to be considered as electrolytes (ILELs) in lithium and other electropositive metal (ion) batteries. This outcome is particularly relevant for the operation of such devices in elevated temperature regimes where ILELs would have a significant advantage over the conventional organic carbonate solvent/$LiPF_6$ electrolytes that, due to their limited thermal stability and flammability, cause concerns about the safety of current LIB technology. There is evidence from a number of review articles that physicochemical properties can be tailored such that ILELs could meet requirements for operating in batteries at lower temperature regimes. By drawing on a broad range of cation/anion combinations, there is further evidence from these papers that within a particular family of cations, the physicochemical properties of ILs and ILELs are largely defined by the anion component. Despite the key role of the anion there are few reviews that have sections dedicated to this aspect. This review surveys the physicochemical, transport and structural properties of ILs (mainly pyrrolidinium salts) and ILELs employing prominent and representative anion classes.

1. Introduction

With the re-exploration of water- and air-stable low temperature molten salts (Ionic Liquids or ILs) in recent times,[1] after a hiatus following their initial reports in 1914[2] many applications opened up for this interesting class of materials.[3] The key advantages of ILs compared to many molecular solvents are their negligible vapor pressure, general non-flammability and combustibility and the prospect of tailoring of their physicochemical properties due to flexibility in choosing and designing the structures of their constituent cations and anions. This permits "tuning" of their properties and, if desired, properties such as wide liquid ranges, high thermal and redox stabilities, and remarkable ionic conductivity can be achieved.[4] Due to these features, mixtures of ILs with metal salts have become very attractive as alternative electrolytes (Ionic Liquid based electrolytes, or ILELs) for electrochemical applications involving the redox chemistry of very electropositive metal ion species. Of these, lithium battery technology is the target application of this review.[4c,5]

There are two broad areas in which lithium battery technology draws ionic liquid electrolytes into consideration. First, contemporary lithium-ion technology is plagued by concerns about the thermal instability, vapor pressure and flammability of the organic carbonate solvent-based electrolyte systems containing $Li[PF_6]$ that are in almost universal usage.[6] This 'thermal sensitivity' makes cooling of lithium-ion batteries mandatory in most new applications involving larger scale units.[7] This not only diminishes the specific energy density achievable (per weight or volume) but also increases cost due to the additional engineering required to mitigate the risk of thermal runaway (and possible fire or explosion). Currently, large battery system costs are largely dictated by the associated system hardware compared to cells (80% system costs vs. 20% for electric vehicles and 60% systems costs vs. 40% for residential storage batteries). As we will see in more detail below, lithium-ion batteries with ILELs have been built and because of their superior properties they do not require elaborate control systems for thermal management. While ILs and their binary or ternary metal salt mixtures may have wide electrochemical windows and sufficiently high conductivity above room temperature, they are hampered by poor low-temperature charge- transport performance, which has prevented their successful commercial application so far.[8] To some degree this is difficult to comprehend, given that cooling battery systems is comparably more difficult and energy intensive. Applying gentle heating in conjunction with good insulation is less costly to engineer and build compared to provision of cooling systems. Further effects such as reduced parasitic energy requirements for heating systems are typically lower than the corresponding energy requirements for cooling, which can, if designed appropriately, result in overall improved system efficiency and hence better lifetime economics.

The second, and arguably more significant, area of impact of ILELs is in the domain of next generation batteries that use lithium metal anodes.[9] Notable amongst this group are lithium-sulfur[10] and lithium air (oxygen)[11] batteries, along with on-going interest in replacing the graphite anode in lithium-ion with metallic lithium. As described in more detail below, some of the anions that provide the best liquid properties in ILELs also greatly enhance the efficiency with which lithium can be reversibly oxidized and reduced. This provides the basis for what is the ultimate negative electrode (in terms of energy density) for example in Li-S batteries. Here, many of the cations and anions that are common constituents of ILs possess properties of salts already employed in Li-S batteries and hence ILs and mixtures thereof with other solvents and additives have been investigated as respective electrolytes.[10b] Studies of IL based electrolytes in LiS batteries have also revealed that their performance is strongly dependent on the chemical nature of the anion component, i.e. insulating Li sulfate and sulfide species are generated when $[FSI]^-$ is present whereas such species are absent if the IL anion is $[TFSI]^-$.[10c] Furthermore, for future battery development there is much interest in the

[a] *Dr. T. Rüther, Dr. A. I. Bhatt, Dr. A. S. Best, Dr. A. F. Hollenkamp*
Commonwealth Scientific and Industry Research Organisation (CSIRO)
Research Way, Clayton, VIC, 3168, Australia
E-mail: thomas.ruether@csiro.au
[b] *Assoc. Prof. K. R. Harris*
School of Science, University of New South Wales
Australian Defence Force Academy
PO Box 7916, Canberra BC, ACT 2610, Australia
E-mail: k.harris@adfa.edu.au

Supporting information for this article is available on the WWW under https://doi.org/10.1002/batt.202000022

Special Collection *An invited contribution to a Special Collection on Electrolytes for Electrochemical Energy Storage*

doi.org/10.1002/batt.202000022

application and development of solid state polymer electrolytes (SSEP)[12] because, compared with liquid electrolytes, SSEP offer advantages such as higher safety, transition metal ion dissolution suppression from cathodes, lithium dendrite suppression close to anodes and interaction reduction between cathodes and anodes. This is particularly relevant to modern ternary cathode materials (TCM)[12b] in which conflicting requirements for energy density and safety in practical application need to be overcome. However, the inferior ion diffusion, poor mechanical performance of SSEP and long-term cycling capabilities remain a challenge. In order to address these obstacles, polymer/liquid hybrid electrolytes (amongst other polymer/composite electrolytes) have been developed where the liquid hybrid electrolyte component contains typically Li[TFSI], Li[BF_4] and Li[PF_6] salts and may comprise of an IL as a plasticizer and conductivity enhancing additive. ILELs may therefore ultimately provide the means for ensuring that these new battery technologies not only set high standards of performance, but also make the devices inherently safe.

The number of investigations into the physicochemical and transport properties of ILs and ILELs has continued to grow over the last two decades, to the point where a huge range of cations and anions have now been studied. However, few definitive studies are available that investigate correlations between the key physicochemical properties and specific ions. From the studies that have been carried out, it appears that within a particular family of cations, the physicochemical properties are, to a large extent, defined by the anion component of the salts present in the specific electrolyte system or ionic liquid type under examination. As an example, the work of Slattery et al.[13] on the assessment of conductivity shows that for imidazolium-, ammonium- and pyrrolidinium-based ILs, the cation dependence is much smaller than for the anions.

Thomas Rüther graduated from the Technical University of Aachen/Germany and was awarded a PhD in synthetic organometallic and electrochemistry in 1994. In the following he held positions at the Universities of Rennes (France, Postdoc), Tasmania (Hobart, Research Fellow), Monash (Melbourne, Research Fellow) and in the private industry (R&D chemist). He joined CSIRO in 2005 and is currently a senior research scientist and project leader in the CSIRO Energy business unit. His main research interests are the synthesis, physicochemical properties and application of ionic liquid-based electrolytes and solvent media for lithium batteries, metal electrodeposition and mineral recovery.

Anand Bhatt leads the Electrochemical Energy Storage Technologies (EEST) research team at CSIRO. The EEST team is developing next-generation batteries, Australian standards for commercial systems and on-shore battery recycling technology. A major EEST focus is in understanding how energy storage can be integrated into the Australian electricity grid and allowing increased penetration of solar PV generation whilst maintaining grid stability. This area investigates energy storage technological limitations for the unique Australian environment and geography. The EEST team is also investigating battery recycling technologies to extract valuable resources from all chemistries to decrease landfill disposal rates to (as close as practicable) zero.

Adam S. Best is a Principal Research Scientist at CSIRO Manufacturing. He has over 20 years of experience in materials for lithium batteries with significant experience in the formulation and application of ionic liquids for use in both lithium-ion and lithium metal batteries. He has published on all aspects of lithium batteries including cathode and anode materials, electrolytes including polymers, ceramics and composites thereof and novel battery concepts including flexible batteries.

Ken Harris is a graduate of the University of Adelaide, where he obtained his PhD in the under the supervision of Peter Dunlop. He held research positions at Simon Fraser University, Vancouver, the Diffusion Research Unit at the Australian National University, Canberra, and the Van der Waals Laboratory, Amsterdam, and lectureships at the Chelsea College, London, RMIT (Melbourne) and the Phillip Institute of Technology, Melbourne. He joined UNSW Canberra in 1987 and was Head of the School of Chemistry from 2001–2003. He is a Fellow of the Royal Society of Chemistry and a member of the International Association of Transport Properties. His research interest is the measurement of thermodynamic and transport properties of fluids and fluid solutions, and in relating these to statistical mechanical theory. Since 2004 he continues research as an Honorary Associate Professor.

A. F. Hollenkamp: after being awarded a Ph.D. (electrochemistry) from Deakin University in 1988, he joined CSIRO to lead a project in the development of energy storage devices for remote-area power supplies. Around 2000, his research shifted to new possibilities in rechargeable lithium batteries, which led to significant discoveries in the combination of room-temperature ionic liquid electrolytes with metallic lithium anodes. Recently this research has shown that ionic liquids can provide the basis for durable, high specific energy rechargeable lithium batteries that work well at above-ambient temperatures. He continues to work on new uses for the lithium electrode, such as lithium-sulfur and lithium air batteries, as well as exploring new applications for ionic liquids.

In terms of electrochemical applications, such as batteries, the list of essential properties which have to be met by ILs is extensive: sufficient electrochemical, chemical and thermal stability, wide liquid range; low viscosity; high ionic conductivity; good solubility of the electrolyte salt; low environmental impact; scalable production levels; and low cost. Hence the choices for suitable anions and cations are very limited and are further restricted by solution speciation effects of the metal ions in ILELs which may form complexes with the anion. In a simplistic picture, the size of the anion correlates with the viscosity and hence ionic conductivity of an IL,[14] but it is important to consider several other structure related factors, in particular when electroactive species are present. With respect to the mobility of the charge carrying metal ions in ILELs, Watanabe et al.[7a] pointed out that the design of the anion structure is critical since it significantly affects the viscosity of the electrolyte. How a metal ion species is transported through the solvent matrix (electrolyte) and eventually into the electrode structure will be a function of the nature of its solvation sphere: this will depend on the Lewis basicity, the number of potential donor centers, the donor number (DN), charge and charge distribution and the geometry of the anions. The aspect of solvation sphere may be somewhat simpler in ILELs where, to a first approximation, only the anion constituent has to be considered, whereas in molecular solvent based electrolytes the anion of the constituent metal salt (e.g. Li[PF_6], Li[TFSI], etc.) will be competing with solvent molecules (e.g. carbonates, acetonitrile, ethers, glymes) for coordination sites at the metal ion and the broader coordination sphere.[7a,15]

Since the physicochemical properties of a specific electrolyte system or IL are, to a large extent, defined by the nature of the anion component present,[16] and because its nature is defined by a multitude of factors, this review focuses exclusively on the properties of ILs and ILELs as a function of the anion component. Among the many reviews on ILs and ILELs, there are very few that have sections dedicated to the anion structure.[7a,16b,17] With the application of plating/stripping cycling of lithium in a battery system in mind, some electrochemical studies have concentrated on the role of the anion in ILs and, more pertinent, ILELs, by investigating the electrochemical behavior of different anions in the presence of a given cation for comparison.[14,16e,18] In order to maintain the focus of this review on the nature of the anion as the property determining entity, the IL examples selected primarily feature pyrrolidinium cations. This type of cation has been chosen as it exhibits, in terms of the targeted electrochemical application, the best electrochemical stability amongst the range of cations typically encountered in ILs[7a,18b,19,20] In several instances, imidazolium salts serve as examples in the absence of data for corresponding pyrrolidinium derivatives.

Despite being crucial, the development of new anions for LIB electrolyte applications has been moving at a slow pace,[16a–d] partly due to the demands of the requirement of suitable physicochemical properties and partly because of synthetic challenges. The latter are strikingly obvious when reviewing the fairly recent contributions to the field from Finze et al. on homo- and heteroleptic-borate-based anions (see section 2.3).

To introduce the anions, in terms of their properties in ILELs, they are grouped as follows: (i) 'simple' and highly symmetric anions: (ii) imide type anions; (iii) chelato borates; (iv) homoleptic and heteroleptic borates (with cyano, hydrido, perfluoroalkyl and fluoride ligands). Considering the body of work on ILELs, we have not included phosphinate- and phosphate-based anions,[21] thereby leaving more room to discuss the structural characterization of neat M(anion)$_n$ (M = Li, Na) salts and respective salts isolated from their binary IL mixtures in an important section relevant to ILELs (section 4). Discussion of the application of ILELs in batteries is mostly in terms of lithium batteries, along with some selected examples drawn from the relatively new literature on sodium batteries. Due to the on-going importance of development of lithium-salt-based electrolytes, we include a special section on the transport (diffusion) properties of selected ILELs (section 3).

2. Anion Types and their Properties

Why and how anions, in combination with a particular type of organic cation, impart the observed properties to the resulting IL is of considerable interest but at the same time it is associated with a high level of complexity due to a multitude of contributing factors originating from the properties of the anion itself, several of which are interrelated.[7a,16b] These are thermal stability, molar mass and size, symmetry, the presence of electron withdrawing groups or atoms, charge delocalization, chemical and electrochemical redox stability, Lewis basicity or acidity, donor number (DN), coordinating ability, i.e. whether it is weakly or strongly coordinating. In particular, the discussion of 'charge delocalization' and 'weakly coordinating' in relation to IL properties such as melting points is sometimes inconsistent and unclear in the literature.

For example, the anions $[BF_4]^-$, $[PF_6]^-$, $[AcO]^-$, $[TfO]^-$, $[TFSI]^-$ are all presented under the banner of 'weakly' or even 'very weakly complexing' anions[22] although there are significant differences in coordination ability found in a relative comparison of these anions (see paragraph below on donor numbers). On other occasions, $[BF_4]^-$ and $[PF_6]^-$ have been labelled 'moderately strong coordinating' anions.[23] To bring more clarity to the topic, the review article by Strauss[24] as well as that of Rupp and Krossing[17b] on weakly coordinating anions in conjunction with several studies of anion donor numbers (DN)[25] are most helpful here. Strauss noted a number of criteria that define weakly coordinating anions: low overall charge and a high degree of charge delocalization over the entire anion which implies that the larger the anion (the more atoms it contains), the more delocalized the charge and the more weakly coordinating it will be. Further, the presence of only very weakly basic sites on the periphery of the anion means that such anions featuring only hydrogen and fluorine atoms should be more weakly coordinating than anions that contain oxygen atoms in their structure. Complementing this assessment, the quantitative studies of Schmeisser et al.[25a] and

doi.org/10.1002/batt.202000022

Holzweber et al.[25b] have estimated anion donor numbers in imidazolium ILs in comparison with Kamlet-Abboud-Taft (KAT) parameters, α (hydrogen bond donating ability), β (hydrogen bond accepting ability), π* (dipolarity). According to Marcus,[26] the β-parameter, a measure for a molecule's electron pair (EP) donation ability (Lewis basicity), correlates well with Gutmann's concept of DNs as a measure for the tendency of an anion to donate EPs to an acceptor species, in the present context of IL based electrolytes for batteries a metal ion, namely Li^+. In the past some shortcomings of the KAT solvent descriptors have been noticed and hence the donor-acceptor approach of Gutmann is a quantitative measure of Lewis basicity and acidity through estimation of DN and ANs.

From the studies on DNs several important points emerge. Firstly, in the presence of the same cation, the measured DNs vary significantly with the anion (Figure 1). Many of the anions studied have been classified as weakly coordinating (or even 'innocent') relative to water. The comparative definition of weakly coordinating is likely to be misleading in actual electrolyte applications, where little or no 'competing' water (or other solvent) is present and when the relative basicity between, for example $[TFSI]^-$ and $[TfO]^-$ or $[DCA]^-$, becomes relevant; the DN of $[TfO]^-$ is two to four times higher than that of $[TFSI]^-$ and that of DCA four times higher still, although all anions have a clear degree of charge delocalization.[25] To some extent this difference is due to the presence of the electron-withdrawing CF_3 groups in $[TFSI]^-$. Another strong contributing factor is the nature of the donor group: it was observed in the Schmeisser study[25a] that a plot of β vs. DN shows two separate correlations of nearly straight lines, with one group of anions carrying O-donor atoms and the other group featuring N-donor and fluorine atoms. Two similar sets of dependencies were further observed with correlations between DNs and calculated interaction energies, with cyano-group containing anions all falling on one line and N- and O-donor anions on a second, with the O-donors at the higher end of the DN scale. The interrelated factors of charge delocalization – basicity – donor numbers – coordination ability also have an important bearing on the electrochemical stability since an increasing DN infers a stronger electron donating ability (Lewis basicity) and therefore the higher electron density at the donor center renders the anion more susceptible to oxidation.

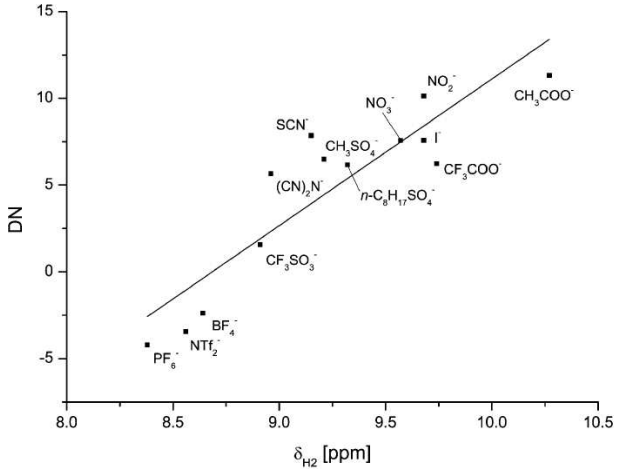

Figure 1. Linear correlation of DN with δH2 for [bmim][X], where X is the variation of the anion. Reprinted with permission from Ref. [25b]. Copyright 2012 Wiley-VCH.

2.1. Small, Simple Anions of High Symmetry

Although these anions appear, from a commercial and, to some extent, synthetic point of view, ideal candidates for ionic liquid-based battery electrolytes, the physicochemical properties of their respective ILs, notably high melting points, limit their use to a few select applications such as elevated temperature operation (discussed below, see examples of anions in Figure 2 and Table 1).

The fully fluorinated anions $[BF_4]^-$ and $[PF_6]^-$ are classified as weakly coordinating, due to high charge delocalization. However, their high symmetry, which is typically associated with higher lattice energies,[27] and the absence of any conformational degrees of freedom to increase entropy, facilitate crystallization and allow for closer packing,[28] thus increasing the melting temperature [Eq. (1)]:[17b,29]

Table 1. Selected physicochemical properties of small, simple anions of high symmetry.

Salt	T_d [°C]	T_g [°C]	T_m [°C]	$\sigma_{25°C}$ [mS·cm^{-1}]	ΔE [V]	E_{ox} [V]	E_{red} [V]
$Li[BF_4]$	160[a][48]	−119	296[1][48]	3.72 (EC: EMC)[49] ~2.5 (EC: DEC)[50]	4.5(Pt)[51]	4.5	n. r.
$[C_3mpyr][BF_4]$	n.r.	−85[30]	62–65		~4(GC)[30]		
$[C_4mpyr][BF_4]$	286[31]	n.o.	138[30] 152[6]	2×10^{-5}[34]	n.r.	n.r.	n.r.
$Li[PF_6]$	197[40]	−80	200[40]	~9 (30 °C, EC:DME)[52]	4.5(Pt)[36b] 3 (GC)	n.r.	n.r.
$[C_4mpyr][PF_6]$	n.r.	n.o.	70[22b]	~10^{-2} (> 41 °C)	n.r.	n.r.	n.r.
[$[C_4mpyr][DCA]$	250[22c]	106	−55	~11[44–45]	4.2(Pt)	0.59	−3.62
[$[C_4mpyr][Al(Ohfip)_4]$	~155		50	7.15 (70 °C)	4.5[b] (GC) $[Bu_4N][AlOpftb)]$[47]	2.2	−2.3
$[C_4mpyr][BH_4]$	n.r.	n.r.	162[53]	n.r.	~3 Bu_4N salt[54]	0	−3

[a] T_d and T_m inversely differ because T_m was obtained in sealed pans whereas TGA measurements involve heating the sample open to flowing N_2 gas; [b] *vs* Fc/Fc^+, recorded in CH_2Cl_2 solution.

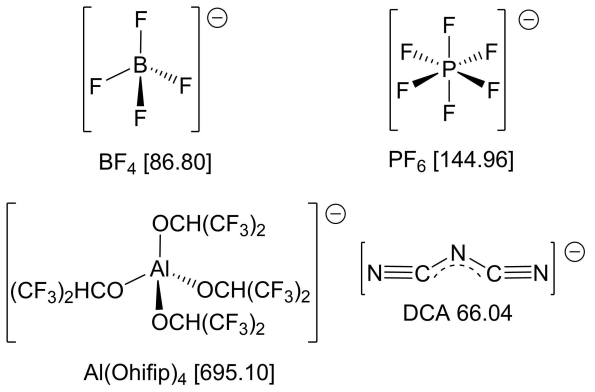

Figure 2. Small, simple anions of high symmetry and their molar masses in [g·mol^{-1}].

$$T_m = \frac{\Delta_{melt}H}{\Delta_{melt}S} \quad (1)$$

Consequently, the pyrrolidinium salts have relatively high melting points, which renders them unsuitable as ambient temperature liquid electrolytes. Pyrrolidinium $[BF_4]^-$ and $[PF_6]^-$ salts were first investigated with respect to potential usage as ILELs by Forsyth et al.[30] and Golding et al.,[22b] respectively. For both anions, the m.p. range from 390 (decomp.) to 60 °C with increasing alkyl chain length $C_{1\text{-}7}$mpyr, except for $[C_4mpyr][BF_4]$ and $[C_6mpyr][PF_6]$ which have (as yet unexplained) m.p. of 138 and 200 °C,[22b] respectively. $[C_3mpyr][BF_4]$ and $[C_7mpyr][PF_6]$ have the lowest m.p., 64 and 60 °C, respectively.

The decomposition temperatures, T_d, within the $[C_xmpyr][BF_4]$ series are relatively high, 280–350 °C, depending on the alkyl group pattern references.[17a,30–31]

Another important commonality is that several of these salts show plastic crystal behavior with one or more solid-solid phase transitions. This renders them interesting materials for application in solid-state electrolyte batteries.[32] These and other properties are discussed separately in the following sections.

While no conductivity data have been reported for $[C_3mpyr][BF_4]$ and $[C_4mpyr][BF_4]$, the former yields an electrochemical stability window (ESW) of approximately 4 V (at a glassy carbon electrode, GC), at 100 °C.[30] Given that the ESW is expected to be wider at lower temperatures,[17a,33] $[C_xmpyr][BF_4]$ salts were later considered for battery electrolyte applications. Indeed, a detailed electrochemical analysis of [pyrrolidinium][BF_4] electrolytes towards their application in all-solid-state batteries was conducted by Jin et al.[34] and our group[35] for Li[BF_4] mixtures with the shorter alkyl chain cation derivatives which possess ionic organic plastic crystal (IOPC) behavior.[32b,c] The ion conductivity of $[C_1mpyr][BF_4]$ is close to 2×10^{-5} S·cm^{-1} at 90 °C (solid state phase II) and increases by about one order of magnitude when doped with several wt% of Li[BF_4]. At this temperature, conductivities for $[C_2mpyr][BF_4]+Li[BF_4]$ are well above 10^{-4} S·cm^{-1} and exceed 10^{-3} S cm^{-1} when the concentration of Li[BF_4] is $\geq$10 mol%.

To obtain further data on suitability for use as lithium battery electrolytes, both of these pyrrolidinium derivatives (with 10 mol% Li BF_4) were evaluated in Li|Li symmetrical cells. This provides a broad measure of how well they support reversible charging/discharging of a lithium metal anode. Combined with impedance data, the results suggested that good cycling performance over hundreds of cycles is possible at a current density of 0.1 mA·cm^{-2}. For the ethyl derivative reversible lithium plating and stripping could also be demonstrated voltammetrically in a symmetrical Li| Li cell (v = 5 mV·s^{-1}, 50 °C) as well as for a thin disc of solid-state electrolyte in an all Pt electrode arrangement (v = 50 mV·s^{-1}, 50 °C). In an early demonstration of the concept of using IOPCs to enable all-solid-state batteries, cycle data were recorded at a 0.1 C rate of battery cells consisting of a Li metal anode, $LiFePO_4$ cathode and IOPC electrolyte. Discharge capacities close to 140 mA·h·g^{-1} (c.f. theoretical maximum discharge capacity of 168 mA·h·g^{-1}) were achieved at 100 °C and nearly 50% of theoretical capacity was attainable at 80 °C.[35]

2.1.1. Hexafluorophosphate, $[PF_6]^-$

Li[PF_6] is still the most common lithium salt in commercial lithium-ion batteries (LIBs) due to several factors. It presents a good compromise in meeting many of an extensive list of physico- and electrochemical performance criteria as well as scalable, low cost of production. It has the ability to form a stable solid electrolyte interface layer (SEI) on graphite anodes and a protective layer on the aluminum current collector.[16b,36] Apart from hydrolytic instability,[37] the major problems are its considerable thermal instability and the equilibrium with its molecular dissociation compounds LiF and PF_5, even at room temperature.[38,39] The salt decomposes above 177 °C,[40] however, decomposition reactions beginning above 55 °C are sufficient to affect lithium and lithium ion battery cycling.[41]

Li[PF_6] shows excellent electrochemical stability in conventional carbonate based electrolytes (E_{red} ~ 0.5, E_{ox} ~ 5 V on Pt vs. Li/Li^+) and notably, its oxidative stability is better than that of bis-imide Li salts under the same conditions (section 2.2. on imide-type anions). However, its stability is significantly reduced in contact with high surface area carbons, with an ESW around 3 V.[36b]

As noted earlier, the ILs based on hexafluorophosphate have not received a great deal of attention, due to their generally higher relative melting points. For [pyrrolidinium][PF_6] molten salts, data for conductivities have not been tabulated and had to be read from a plot[32a] but surprisingly they show that despite the lower m.p. of $[C_4mpyr][PF_6]$, the conductivity appears to be almost two orders of magnitude lower compared to that of the propyl derivative of higher m.p., at temperatures up to 41 °C. This observation is due to the phase behavior of $[C_4mpyr][PF_6]$ where a solid-solid phase transition at 41 °C leads to a sharp rise in conductivity to ~10^{-5} S·cm^{-1} before melting at 70 °C where it surpasses the conductivity of the propyl derivative until its melting at 113 °C. The availability of electrochemical data is limited to the liquid imidazolium derivatives

due to the relative high melting points.[17a] The ESWs of the $[C_x mpyr][PF_6]$ series can be expected to be comparatively wide, given the high electrochemical stability of both the cation and the anion. Indeed, it was shown in a comparison of conventional carbonate/Li$[PF_6]$ electrolytes with the same electrolyte but doped with additives Li[TFSI,] Li[FTFSI], Li[FSI] that the latter electrolyte formulation showed higher current densities in the range 4.5–5 V and are therefore less stable to electrochemical oxidation.[36b] These experimental data also support the computational studies by Ong et al. which concluded that the relative stabilities follow the order $[PF_6]^- > [BF_4]^- > [TFSI]^-$ if a high-quality computational model is applied.[42]

2.1.2. Dicyanamide, $[N(CN)_2]^-$

In searching for ILs with low melting point and low viscosity, the group of MacFarlane[22c] introduced ILs containing dicyanamide ($[DCA]^-$), as another relatively small anion with a relatively high degree of charge delocalization (proton affinity $-590\ kJ\cdot mol^{-1}$),[17c] albeit lower than that of $[TFSI]^-$ (Data for proton affinities for representative anions are given in Table 3). Notably, conformational flexibility of this anion and its reduced symmetry relative to $[BF_4]^-$ and $[PF_6]^-$, are contributing factors which tend to decrease melting temperatures, T_m, since they impede efficient packing in the solid state. Indeed, $[C_4mpyr]$[DCA] has one of the lowest glass transition temperatures, T_g, $-106\,^\circ C$, with a weak melting transition at approximately $-55\,^\circ C$. The thermal stability is reasonably good, $250\,^\circ C$, but considerably lower than that of the corresponding $[TFSI]^-$ salt (see below). The lower degradation temperature is, in part, associated with a favored pathway for degradation that involves abstraction of a methyl group and formation of dicyanomethylamine. This is in agreement with the relative basicity and hence nucleophilicity of $[DCA]^-$.[43] The dynamic behavior of $[C_4mpyr]$[DCA] has been investigated by Simons et al.[44] who have confirmed the expected high ionic conductivity, approximately $11\ mS\cdot cm^{-1}$ ($25\,^\circ C$, data not tabulated).

The electrochemical stability (and application as an IL based battery electrolyte) of $[C_4mpyr]$[DCA] on a Pt substrate has been investigated in some detail by us.[45] The ESW was estimated to be 4.2 V (threshold current density $0.014\ mA\cdot cm^{-2}$) with boundary potentials of $E_{red} = 3.62$ and $E_{ox} = 0.59$ V (vs. Ag/Ag^+); a value for E_{ox} of approx. 2 V (vs. Ag/Ag^+) was reported for [emim][DCA] on a glassy carbon electrode, but no threshold current was given and on closer inspection of the CV trace provided it has to be concluded that E_{ox} is at best 1 V when ignoring a not small current rise observed above 0.5 V. (We also note that the electrochemical data for $[C_4mpyr]$[DCA] listed in a review paper[17a] do not appear in the corresponding ref. [77] and neither does the compound). Hence, the E_{red} in the DCA-IL is limited by the electrochemical stability of the cation (we note that E_{red} in the corresponding imidazolium salt is approximately 1.6 V less[22c]) while E_{ox} is limited by the anion. The oxidative instability is, to some extent, associated with the formation of the dimer $(CN)_2N{-}N(CN)_2$[22c] but this is not surprising considering the relatively high DN (Lewis basicity) and hence high electron density at the donor center, according to the studies of Schmeisser et al.[25a] and Holzweber et al.[25b] Consistent with this assessment, E_{ox} determined under the same conditions for the tricyanomethanide anion (not discussed any further in this article) is even lower, approx. 0 V. Although the DCA anion is also very attractive from an economic and environmental point of view (having no fluorine), the comparatively low oxidative stability imparted by this anion on its salts limits the scope for using these ILs in conjunction with common high voltage cathodes such as NMC, NCA or LNMO. In CV and symmetrical Li|Li cell cycling experiments it was shown that successful deposition and dissolution of Li is dependent on the amount of residual water present in the $[C_4mpyr]$[DCA]/Li[DCA] electrolyte;[45] 100–200 ppm appeared to be optimum to generate a sufficiently stable SEI to protect against electrolyte degradation. With this prerequisite, Li|$LiFePO_4$ cells containing $[C_4mpyr]$[DCA]/Li[DCA] electrolyte showed over $130\ mA\cdot h\cdot g^{-1}$ of discharge capacity without a significant capacity reduction over 20 cycles and, perhaps more intriguing, a solid state organic ionic plastic crystal variant, $[C_1mpyr]$[DCA],[45] achieved $150\ mA\cdot h\cdot g^{-1}$ discharge capacity with the same electrode combination without any significant capacity fade for up to 200 cycles at $80\,^\circ C$.

2.1.3. Tetrakis(polyfluoroalkoxy)aluminate, $[Al(OR^F)_4]^-$

The lithium salts of tris- and tetrakis(polyfluoroalkoxy)aluminate superweak anions have been considered as adequate replacements for the thermally unstable Li$[PF_6]$ and hence their properties were studied in detail by Ivanova et al.[46] Indeed, Li$[Al(Ohfip)_4]$ and also solutions thereof in EC-DMC mixtures do not show any signs of decomposition below $100\,^\circ C$. Furthermore, solutions of this lithium salt show sufficiently high conductivity and ESWs exceeding 5 V (vs. Li).

Tetrakis(polyfluoroalkoxy)aluminates ionic liquids[27,47] were thoroughly reviewed in an interesting paper by Rupp and Krossing.[17b] which presented an analysis of the principles governing the physical properties of this IL class with minimized interactions, basic principles that could be extended, for example, to the prediction of the principal properties of a wide variety of typical ILs. In the abstract the authors further state that *"…especially the $[Al(Ohfip)_4]^-$ anions in combination with asymmetric organic cations turned out to be very well suited for the synthesis of ILs with very low melting points, some even far below 0 °C."* However, when surveying the respective data listed in the accompanying table, it becomes clear that out of the 29 IL examples there are nine that have $T_m < 20\,^\circ C$, half of which are imidazolium ILs. The classic $[C_2mim]^+$, $[C_4mim]^+$ and $[C_4mpyr]^+$ cations give relatively high melting salts when combined with $[Al(Ohfip)_4]^-$; e.g. $[C_4mpyr][Al(Ohfip)_4]$ has a m. p. of $50\,^\circ C$ ($T_c = 39\,^\circ C$) which may be compared with the low melting $[C_4mpyr][TFSI]$ ($-6.3\,^\circ C$, see respective chapter). Therefore, conductivity data are only available above $70\,^\circ C$ ($\sigma = 7.15\ mS\cdot cm^{-1}$). The T_d of $155\,^\circ C$ observed for $[C_4mpyr][Al(Ohfip)_4]$ is

comparatively low and, due to the central Al atom, the anion is very sensitive to hydrolysis. Electrochemical data were reported for the $[Bu_4N]^+$ salts of fluorinated *t*-butyl anion derivatives (pftb, hftb)[47] and the Li-salts:[46b] the ESWs of the former do not exceed 4.5 V (at $I_{threshold} = 7 \times 10^{-5}$ A·cm^{-2}) in CH_2Cl_2, whereas the latter are greater than 5 V.

2.2. Imide-Type Anions

For the group of imide-type anions we discuss the properties of Li/Na and pyrrolidinium based ILs composed of the symmetric and asymmetric anions bis(trifluoromethanesulfonyl)imide, ([TFSI]$^-$), fluorosulfonyl-(trifluoromethanesulfonyl)imide, ([FTFSI]$^-$), bis(fluorosulfonyl)imide, ([FSI]$^-$), trifluoromethanesulfonylcyanoamide [TFSAM]$^-$, 2,2,2-trifluoro-*N*-(trifluoromethylsulfonyl)acetamide, ([TSAC]$^-$), and methoxycarbonyltrifluorosulfonylimide ([MCTFSI]$^-$) (Figure 3 shows their structures; for selected physicochemical properties of imide-type anion salts, refer to Table 2). Due to their structural similarities, this series of anions lends itself to an assessment of how variation of the functional groups at the nitrogen and therefore changes of the charge distribution, coordination ability, donor numbers, electrochemical and thermal stability affect the physicochemical properties of their respective salts. In this section we first present the properties of the individual anion salts before discussing their performance as battery electrolytes.

Since the early interest in applying ionic liquids as possibly safer electrolytes in lithium batteries, the symmetric perfluorinated [TFSI]$^-$ and [FSI]$^-$ anions have taken centre stage since when combined with pyrrolidinium cations, the corresponding Ils possess transport properties and electrochemical stabilities suitable for this intended application.

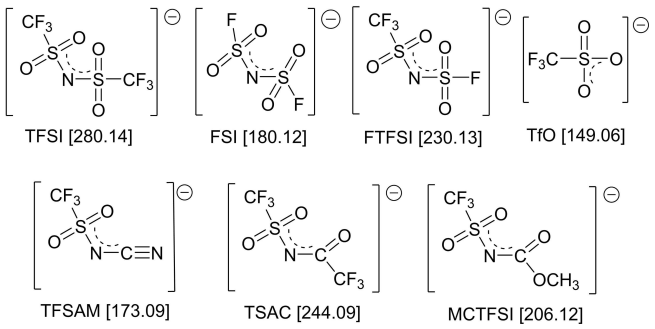

Figure 3. Imide-type anions and their molar masses in [ ].

2.2.1. Bis(trifluoromethanesulfonyl)imide, [TFSI]$^-$

The protonated form of [TFSI]$^-$ was first synthesized by Fotopoulos and DesMarteau.[55] This was an attempt to arrive at a very acidic organic amine acid by exploiting the strong electron withdrawing nature of the sulfonyl group. Its chemistry was further explored in subsequent papers by the same group and the favorable electrochemical properties of its Li-salt such as a wide ESW, reversible Li plating and stripping and a relatively high conductivity were investigated initially in polymer matrixes[56] and later in liquid solution.[57] This was partly driven by an interest in replacing the unstable Li[PF_6] with a chemically more stable lithium salt having similar transport properties in solution. Owing to the low basicity, high degree of charge delocalization[17c] and perfluorinated nature imparted by the two trifluoromethylsulfonyl groups on the [TFSI]$^-$ anion, the group of MacFarlane in 1999,[20a] could introduce very thermally and electrochemically stable ILs based on the pyrrolidinium cation. These ILs have remarkably low melting points despite the relatively high molar mass of the

Table 2. Selected physicochemical properties of lithium and pyrrolidinium imide type anion salts.

Salt	T_d [°C]	T_g [°C]	T_m [°C]	σ(25 °C) [mS cm^{-1}]	Δ*E* [V]	E_{ox} [V]	E_{red} [V]
Li[TFSI]	360[57b]		236–237[57b]	12.5 (PC:DME)[57c] 2–15 (glymes)[57a]	4.5(EC/DMC)(Pt)[36b] 5.2–5.5 (glymes)[57a] (GC)	1.6	−2.9
[C_4mpyr][TFSI]	~400[28,77]	−85[28,77]	−6.3[28,77]	2.2–2.7[20a,58]	5.76 (Pt)[20b] 5.5 (GC)[20a]	2.05 2.5	−3.71 −3.0
Li[FSI]	>230[a]	−103	132–145[71–72]	9.73 (EC/EMC)[49]			
[C_3mpyr][FSI]	219–231[75]	n.o.	−9[99]	6.4[75] 8.2[74] 8.7[76c]	5.3 (GC)[74] 5.07(Pt)[99] ~6 (Pt)[18d]	2.3 1.97 ~2	−3.0 −3.1 ~−4
[C_4mpyr][FSI]	189–198[75]	−104[75]	−18[75]	4.8[75] 5.25[15]	5.35(Pt)[75]	1.95	−3.4
[C_3mpyr][FTFSI][83a]	285	−107	n.o.	4.97 (20 °C)	5.97	2.36	−3.61
[C_4mpyr][FTFSI][83a]	256	−103	n.o.	3.5 (20 °C)	5.86	2.31	−3.55
[C_3mpyr][TFSAM][84]	285	−12[b]	n.o.	6.6	4.1(Pt)	2.4	−1.7
[C_4mpyr] [TFSAM][85]	283	−97.7	n.o.	3.8	2.6	1.1(Pt)	−1.5(Ni)
[C3mpip][TSAC][18b]	n.r.	−83	n.o.	2.1	4.8	n. r.	n. r.
Na[MCTFSI][16d]	279	n.r.	190	1.8 (EC:PC)	4.79 (Pt)	2.03	−2.76
[C_4mpyr][MCTFSI][16d]	270	n.r.	n.r.	~0.3			
[C_4mpyr][TfO][89b]	n.r.	n.o.	5.6	1.3	5.38	2.03	−3.35

[a] In presence of water traces some exothermic behaviour is observed around 180 °C. [b] Probably an artefact.

anion. In the following years, key physicochemical properties of [pyrrolidinium][TFSI] and also the 6-membered ring [piperidinium][TFSI] ILs have been investigated by the groups of MacFarlane, Matsumoto, Henderson, our own and, notably, Passerini[20b] who published a systematic study of [1-alkyl-mpyr][TFSI] where the alkyl group ranged from methyl to *n*-decyl.

Comparing the physicochemical data of [$C_n$mpyr][TFSI] ILs to those of the corresponding salts of the simpler, smaller and highly symmetrical anions $[BF_4]^-$ and $[PF_6]^-$, the $[TFSI]^-$ ILs have a larger liquid range and good conductivity (2.2–2.75 $mS \cdot cm^{-1}$ at 25 °C).[20a,58] Although there is some inconsistency about how thermal stability for ILs should be estimated and referenced,[43b,59] the short-term thermal stability of [C_4mpyr][TFSI] is around 400 °C. For the corresponding $[PF_6]^-$ salts only the decomposition of [C_1mpyr][PF_6] at 390 °C before melting has been reported. There is some discrepancy about the relative anion stabilities since they are generally assumed to follow the order $[PF_6]^- > [TFSI]^- \sim [BF_4]^- > [AsF_6]^-$, halides[60] but in some cases short-term stabilities of salts composed of $[TFSI]^-$ are higher than those consisting of $[PF_6]^-$; i.e. in open chain symmetrically substituted ammonium and butyl-methyl imidazolium ILs.[43b] While the $[PF_6]^-$ anion shows significant self-decomposition over time (disproportionation with release of the conjugated Lewis acid[57b,c]), at 271 °C [C_4mpyr][TFSI] shows not more than 1 wt% mass loss over 10 h using the re-definition of the decomposition temperature introduced by Wooster et al.[61] From thermal analysis studies of a variety of ILs, it was noted that weakly coordinating anions have a higher thermal stability, with (perfluoroalkylsulfonyl)imides and $[PF_6]^-$ showing the best stabilities.[43b]

There is further ambiguity around the electrochemical stability of the imide anions compared to $[PF_6]^-$ and $[BF_4]^-$. The ESW of [$C_n$mpyr][TFSI] ILs is close to 6 V[20b] which is larger than that of conventional carbonate Li[PF_6] electrolytes and therefore such ILs are of interest for application in batteries constituting of high-voltage cathodes.[42] However, from computational modelling, Ong et al.[42] found that [C_3mpy][TFSI] has, depending on the level of calculations, both lower cathodic and anodic stability limits than [bmim][PF_6], or the ESWs of [bmim][PF_6], [bmim][BF_4], [bmim][TFSI] and [C_3mpy][TFSI] to follow the order 4.9, 5.1, 5.5 and 6.1 V, respectively at a higher level of calculations. Probably due to being solid at room temperature, sound electrochemical ESW data for [$C_n$mpyr][PF_6] ILs are not available and the problem of a meaningful comparison is further exacerbated by the fact that the limiting reductive and oxidative potentials are strongly substrate and scan rate dependent, amongst other factors. Electrochemical data were obtained by MacFarlane et al.[20a] and Appetecchi et al.[20b] on GC and Pt substrates, respectively, but at different scan rates, 100 and 5 $mV \cdot s^{-1}$, and hence the reported ESW (5.5 vs. 5.76 V) differ due to discrepancies in E_{red} −3.0 *vs.* −3.71 V and E_{ox} +2.5 vs. 2.05 V arising from scan rate dependencies; we note that the cut-off current density was not defined in the MacFarlane work, whereas Appetecchi et al. reported limiting potentials for 0.05 and 0.1 $mA \cdot cm^{-2}$ thresholds where the difference in E_{red} was 0.1 V.

The first studies of lithium electrochemistry in TFSI ILs were conducted by Katayama et al.[62] and Matsumoto et al.[63] Reversible plating and stripping of lithium was observed on several substrate materials and it was suggested that the well-defined behavior was due to the formation, in situ, of a protective (semi-passivating) solid electrolyte interphase (SEI). Studies soon followed in which a variety of spectroscopic techniques was employed to characterize the SEI that forms on lithium electrodes.[64] Subsequently, many groups have sought to show how a lithium metal electrode can work successfully in a device with an electrolyte based on a $[TFSI]^-$ IL.[65] More recently, this effort has also been part of the development of lithium-sulfur batteries as this technology seeks to move away from the contemporary configuration in which Li[TFSI] is dissolved in flammable ether solvents.[10]

Despite a great deal of effort, only limited success has been achieved with $[TFSI]^-$ ILs. Overall it appears that: (i) the conductivity of mixtures of lithium salts and $[TFSI]^-$ ILs is only just sufficient for low rates of charge-discharge duty; (ii) at typical concentrations, lithium ion transport is sub-optimal, thereby further limiting higher rate performance; (iii) the SEI formed in the presence of $[TFSI]^-$, with a wide range of counter-cations, does not provide long term stability to the lithium electrode. A further limitation of thermally stable $[TFSI]^-$ salts is that they are unable to protect the aluminum current collector commonly used in LIBs beyond 3.7 V vs. Li^+/Li.[66] This issue is exacerbated at elevated temperature due to cracking of the passivation layer and enhanced solubility of surface species. It has been shown that at the initial stage of Al corrosion $Al_x[TFSI]_y$ complexes are formed from reaction with the protecting Al_2O_3 layer. While these complexes are relatively soluble in traditional carbonate solvents and therefore have no passivation activity, some ILs may inhibit their dissolution.[67] For these reasons, the literature on ILs in lithium batteries features a number of attempts to find anions that promote improved behavior of the lithium electrode.

2.2.2. Bis(fluorosulfonyl)imide[FSI]$^-$

The smaller and more acidic anion $[FSI]^-$ was first synthesized in its acid form by Appel and Eisenhauer[68] and later in a more economic manner by Beran and Prihoda.[69] The thermal properties of lithium (and other alkali) bis(fluorosulfonyl)imide(s) (Na, K, Rb, Cs) have been investigated by Kubota et al.,[70] Kerner et al.,[71] Han et al.[49] and us.[72] This is a very controversial topic because Li[FSI] is increasingly being seen as an alternative to Li[PF_6], notably due to the established thermal instability of Li[PF_6]. Depending on the (synthetic) origin and associated purity of the Li[FSI] under investigation,[71] the observed melting points (124–128 °C, Beran 2006;[207] 130 °C Kubota et al.;[70] 132–145 °C, Huang et al.,[70] Han[49]) and, more importantly, the T_d differ. Thus, decomposition temperatures ranging from 70–300 °C have been reported, with T_d around 203–233 °C being a more realistic temperature range,[71] although some samples may show some small weight loss at around 178–187 °C prior to bulk decomposition.[49,71,72] It has to be pointed out that only

one salt was stable (< 0.2 % total mass loss) for 20 h at 125 °C in isothermal TGA analyses.[71] Instability is primarily related to residual impurities, notably $[ClO_4]^-$, which is commonly used in the synthesis of Li[FSI] from K[FSI], the general product in the synthesis of the anion. Despite the differences in the quality of the salts, no significant differences were observed during cycling of Li/LFP cells using IL-based electrolytes, however, no more than 50 cycles were conducted which does not permit to make an assessment on the impact of impurities on long-term cycling.[71]

Li[FSI] was proposed as a conducting salt with good anticorrosive properties for lithium-ion batteries in the mid 90's[73] and has been studied, in comparison with other Li-salts, as a conducting salt for lithium-ion batteries (Figure 4), in terms of the physico- and electrochemical properties in ethylene carbonate (EC)/ethyl methyl carbonate (EMC) of the neat Li[FSI] salt.[49] Among five salts studied, Li[FSI] shows the highest conductivity, which is attributed to its higher dissociation (though the supposition of association in aprotic ILs is questionable: see section 3), the relatively low viscosity of its solutions, and the medium size of the anion; the specific conductivities generally decrease in the order of Li[FSI] > Li[PF_6] > Li[TFSI] > Li[ClO_4] > Li[BF_4] .[49] Unlike Li[TFSI], Li[FSI] is able to match the capability of Li[PF_6] in forming a stable electrolyte/electrode interface at graphite anodes, thereby allowing for good cycling behavior of LCO/Li half-cells near 100 % CE and LCO/Graphite full cells.[49,74]

Ionic liquids derived from the $[FSI]^-$ anion were introduced by Michot et al.[73] and the groups of Matsumoto,[74] Passerini[16e,75] and our own[76] further investigated the neat pyrrolidinium (and piperidinium) ILs in more detail in subsequent publications, together with binary[77] and ternary[78] IL/lithium salt mixtures having [Pyr_{14}][TFSI] as the second IL component. Due to its smaller size, while maintaining a high degree of charge delocalization, the liquid range of the $[FSI]^-$ based ILs is even wider than that of their $[TFSI]^-$ counterparts and they are also superior, in terms of ion transport properties,[16e,74,76c] to the $[TFSI]^-$- system, primarily due to lower viscosity due to the $[FSI]^-$ anion. Thus, the conductivities of the neat [$C_n$mpyr][FSI] are nearly two times higher than those of the corresponding $[TFSI]^-$ ILs.

An inferior thermal stability of $[FSI]^-$ anion compared to $[TFSI]^-$ was observed, i.e. the onset point for mass loss (1 wt%) is about 219–231 °C for [C_3mpyr][FSI].[75] In previous stability studies on ILs it has been noted that, independent of the cation, a decrease in nucleophilicity by fluorinating the anion is directly translated into greater thermal stability.[43b] Thus, Han et al.[79] noticed a decrease of the thermal stability when stable CF_3 groups in $[TFSI]^-$ are replaced by F in $[FSI]^-$. Hence, the reduced thermal stability suggests that the FSO_2-groups have a greater lability towards pyrolysis than the perfluorinated CF_3SO_2 groups.[80]

Because the measurement of the electrochemical stability of electrolyte solvents and ions is not trivial, a comparison of reductive and anodic stabilities of the $[FSI]^-$ salt relative to the corresponding $[TFSI]^-$ salt is a difficult task. Nevertheless, the ESW data of [C_3mpyr][FSI] measured by Matsumoto et al.[74] (5.3 V) and Zhou et al. (5.37 V)[75] are in relatively good agreement despite being obtained on different substrates, GC and Pt, respectively. Therefore, the electrochemical stability of the $[FSI]^-$-IL appears to be slightly inferior to its $[TFSI]^-$ analogue. According to cyclic voltammetric analyses (Figure 5) on a Pt substrate under identical conditions (*v*,*T*, RE), the E_{red}, mainly determined by the nature of the cation, is significantly better and the E_{ox}, determined mainly by the nature of the anion, slightly better for [C_4mpyr][TFSI] compared to [C_3mpyr][FSI][78] we note, however, that in each case the alkyl chain length of the pyrrolidinium cation was different which has been demonstrated to have an effect on the E_{red}.[20b]

Nevertheless, due to the relative ease of mineralization of the reduced anion,[81] [C_3mpyr][FSI]/Li-salt mixtures have been

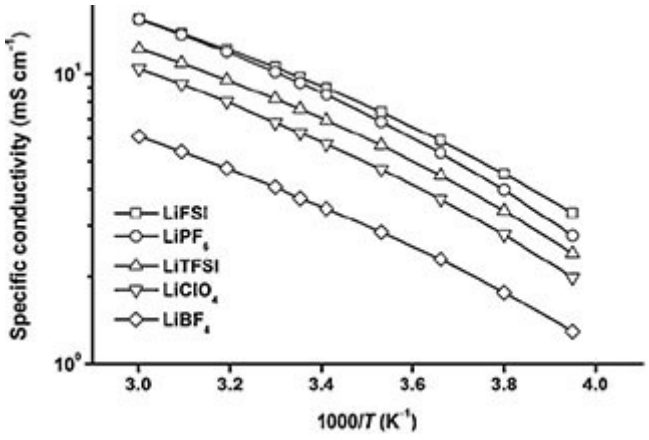

Figure 4. Arrhenius plots of the conductivity of 1.0 M Li[FSI], Li[PF_6], Li[TFSI], Li[ClO_4], and Li[BF_4] in a mixture of EC/EMC (3 : 7, v/v). Reprinted with permission from Ref. [49]. Copyright 2011 Elsevier.

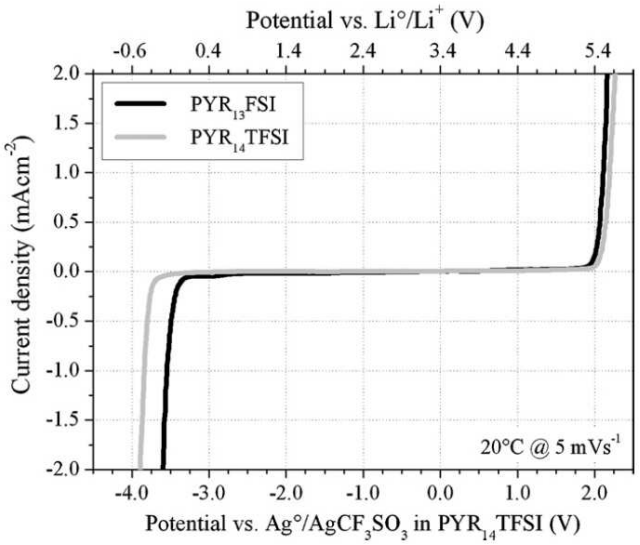

Figure 5. Linear sweep voltammetry of neat [C_3mpyr][FSI] and [C_4mpyr][TFSI] ionic liquids at 20 °C. Platinum was used for the working and counter electrodes. The reference electrode was a silver wire immersed in a 0.01 M solution of Ag[CF_3SO_3] in [C_4mpyr][TFSI]. Scan rate: 5 mV·s^{-1}. Reprinted with permission from Ref. [78]. Copyright 2009 Elsevier.

shown to be among the most suitable electrolytes for lithium plating and stripping (and has been termed a "magic anion)[76a,b,81] to a large degree due to ist ability to form a stable SEI on various substrates, including graphite and metallic Li surfaces. This allows for highly reversible long term electrodeposition and stripping of Li.[18d,81–82] From these studies an order of stability for the substrate Li SEI system regarding various different Li-salts dissolved in [C_3mpyr][FSI] can be assigned based on decreasing current density values and cycle numbers achieved. Indeed, cyclic voltammetric analyses of electrodeposition/stripping of lithium from these solutions on Pt (Figure 6, top panel) revealed that the coulombic efficiency for these systems follows the order Li[FSI] > Li[TFSI] > Li[BF_4] > Li[PF_6] > Li[AsF_6]. It was further observed in multicycle voltammograms that with the hexafluoro salts, a thick SEI forms rapidly which degrades the CV. When cycling at the lithium electrode (Figure 6, bottom panel), the electrochemical behavior of the investigated systems is different. In this case, the rate of SEI formation, based on CV data, follows the order Li[BF_4] > Li[AsF_6] > Li[PF_6] > Li[TFSI] > Li[FSI]. However, although in the instances of Li[PF_6] and Li[AsF_6] rapid SEI formation was observed, the voltammetric studies showed that these SEIs are not stable, while the SEI formed when Li[BF_4] is present in the electrolyte system is very stable.

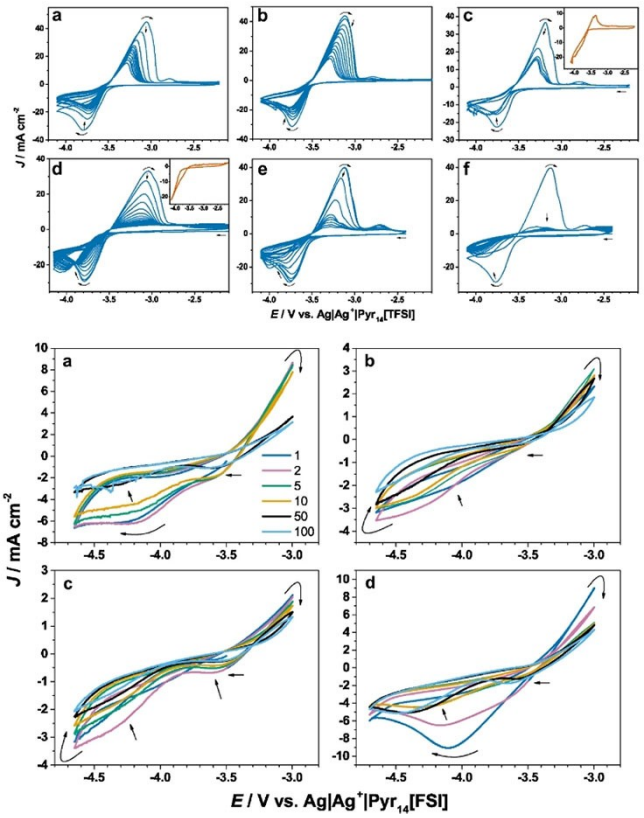

Figure 6. Top: Cyclic voltammetric data measuring the current response over 100 cycles (1st then every 9th scan) for the reduction/oxidation of Li^+/Li^0 at a Pt electrode in [C_3mpyr][FSI] at 50 mV·s^{-1} from 0.5 M a) Li[FSI], b) Li[TFSI], c) Li[BF_4], (1st to 37th scan) and inset 73rd scan, d) Li[AsF_6] (first 20 scans) and inset 88th scan, e) Li[PF_6] (first 20 scans) and f) Li[PF_6] (1st to 100th scan). Bottom: Cyclic voltammetric data measuring the current response over 100 cycles for the reduction/oxidation of Li^+/Li^0 at a Li electrode from 0.5 M a) Li[TFSI], b) Li[BF_4], c) Li[PF_6] and d) Li[AsF_6] in [C_3mpyr][FSI] at 50 mV·s^{-1}. Reprinted from Ref. [18d]. Copyright 2016 Elsevier.

2.2.3. Asymmetric Imide-Type Anions $[FTFSI]^-$, $[TFSAM]^-$, $[TSAC]^-$ and $[MCTFSI]^-$

Trends in thermal and transport behavior found between $[TFSI]^-$ and $[FSI]^-$ are also observable for the hybrid anion fluorosulfonytrifluoromethylsulfonyl imide $[FTFSI]^-$ for which ILs were first synthesized by Matsumoto et al.[18a] Further research by this group and others revealed their exceptional physico- and electrochemical properties.[83] In TGA studies of its pyrrolidinium salts, a very small weight loss was detected below 200 °C and in all cases, decomposition reaction occurred at 250–285 °C. Because $[FTFSI]^-$ is half fluorosulfonyl and half trifluoromethylsulfonyl, the T_{dS} of the pyrrolidinium salts lie, as expected, between those of the $[TFSI]^-$ and $[FSI]^-$ derivatives. Owing to the highly asymmetric structure of this anion, the corresponding pyrrolidinium ionic liquids have remarkable properties,[83a] in that they do not crystallize above −150 °C, so imparting an exceptionally wide liquid range while maintaining high ionic conductivities above 10^{-4} S·cm^{-1} even at −40 °C, both essential performance parameters for battery electrolytes. Although the $[FSI]^-$ based ILs have somewhat higher conductivities they have the disadvantage of early crystallization between −10–0 °C. Therefore, the example of $[FTFSI]^-$ ILs represents convincing evidence that ILs can be applied in low temperature operations, a critical point for their utilization as lithium battery electrolyte systems. The ESWs of $[FTFSI]^-$ ILs are very similar to or slightly better than the respective $[TFSI]^-$ ILs. Apparently differences most likely fall within margin for error in these determinations, which are notoriously susceptible to variability due to changes in electrode materials, scan rates, temperature and different levels of residual impurities (e.g. halide, water; impossible to assure are at the same level in different samples).

Recognizing symmetry and conformational flexibility as determining factors for arriving at wide liquid range ILs, there are three other instructive examples where one of the sulfonyl groups has been replaced with other potentially electron withdrawing groups, that is the series of imide type anions: trifluoromethanesulfonyl cyano amide $[TFSAM]^-$, 2,2,2-trifluoro-*N*-(trifluoromethylsulfonyl)acetamide, $[TSAC]^-$ and methylcarbonate(trifluoromethanesulfonyl)imide, $[MCTFSI]^-$. Studies of compounds (esp. salts) featuring these anions illustrate the effects of structure, symmetry and electronic nature (freedom of charge delocalization, electrochemical stability) on the resulting properties and also highlight the advantage of the sulfonyl group in terms of electrochemical stability.

Salts derived from the asymmetric hybrid anion $[TFSAM]^-$, first synthesized and studied in detail by Shaplov et al.[84] and later by Hoffknecht et al.[85] display quite similar physicochemical behavior to those of $[FTFSI]^-$. Notably, [C_4mpyr][TFSAM] has a wide liquid range as there is no crystallization before its T_g of −97.7 °C and it has a high T_d of 283 °C (we note that for [C_3mpyr][TFSAM] the T_d of 285 °C is the same as for [C_3mpyr]

[FTSFI]). Given these values, the thermal stability lies in between those of the corresponding $[TFSI]^-$ and $[FSI]^-$ ILs. The conductivity of $[C_4mpyr][TFSAM]$ (in our view, and considering experimental errors, somewhat overstated by Hoffknecht) is slightly less compared to the symmetric but smaller $[FSI]^-$ derivative, marginally better than that of $[C_4mpyr][FTFSI]$ and significantly higher than that of the symmetrical $[C_4mpyr][TFSI]$. Reviewing the electrochemical stabilities is less straightforward, not only for the reasons given earlier, but because of inconsistencies and lack of clarity in the description by Hoffknecht et al.[85] Considering the voltammogram presented, it appears that the ESW of $[C_4mpyr][TFSAM]$ is no wider than 2.6 V whereas Shaplov et al.[84] report 4.1 V for $[C_3mpyr][TFSAM]$. Further, in their conclusion Hoffknecht et al. claim a higher anodic stability compared to the corresponding $[TFSI]^-$ and $[FTFSI]^-$ derivatives. Clearly, that is not the case when comparing the CV reported vs. Li/Li^+ in both cases; reading of the plot, E_{ox} for $[C_4mpyr][FTFSI]$ sits at around 5.5 V whereas for $[C_4mpyr][TFSAM]$ E_{ox} is around 4.5 V. This assessment is also in qualitative agreement with Shaplov's data where E_{ox} for $[C_3mpyr][TFSI]$ is about 0.5 V more positive than for $[C_3mpyr][TFSAM]$. Both reports are consistent in that the reductive stability of the $[TFSAM]^-$ salts are inferior to the $[TFSI]^-$ salts by around 1 V due to the commonly known electrochemical instability of the CN group.[86] Nevertheless, reversible lithium deposition and stripping could be demonstrated for $[C_4mpyr][TFSAM]$, albeit with low coulomb efficiency.[85]

Matsumoto et al.[87] synthesized and characterized a number of ILs consisting of the $[TSAC]^-$ anion, initially introduced by Armand and Muller[88] as an asymmetric analogue to $[TFSI]^-$ with only slightly lower molar mass. While maintaining a relatively high degree of charge delocalization by replacing the CF_3SO_2-group with a CF_3CO-group, the combined effects of asymmetric structure and slightly lower molar mass lead to an improved liquid range (lower m.p.) and good conductivities for a given aliphatic onium cation. (This trend does not hold for imidazolium ILs). Thermal stabilities for pyrrolidinium or piperidinium salts were not reported, neither by Matsumoto's group nor in the comprehensive review of Maton et al.[43b] on the thermal properties of ILs. However, according to data for the $[emim]^+$ analogues, the short term T_d of salts with this anion are around 300 °C, somewhat lower than or close to the most thermally stable $[TFSI]^-$ and $[FTFSI]^-$ analogues, respectively. Despite their attractive phase and transport behavior, the $[TSAC]^-$ ILs display inferior electrochemical stability at both, the cathodic and anodic limiting potentials for the ESW[18b] compared to ILs composed of either one of $[TFSI]^-$, $[FTFSI]^-$, $[FSI]^-$ anions. More particularly, the negative potential limit of $[TSAC]^-$ based pyrrolidinium ILs occurs well before values required to support deposition of lithium metal, thereby rendering these compounds unsuitable for lithium battery applications. Interestingly, lithium deposition and stripping was possible when Li[TFSI] was present in a $[TSAC]^-$ IL electrolyte solution. This emphasizes the special property displayed by anions like $[TFSI]^-$ in being able to stabilize the surface of lithium metal through the formation of an SEI with optimum properties.

The example of the $[MCTFSI]^-$ anion recently investigated by our group[16d] as its sodium and $[C_4mpyr]^+$ salts provide further insight into the effect of substituting trifluoro- and fluorosulfonyl groups on imide-type anions with carbonyl based functional groups. The solid–liquid phase transition behavior and short-term thermal stability for the sodium and pyrrolidinium carbimide salts, examined by DSC and TGA respectively, show values between the corresponding [cation][TFSI] and [cation][FSI] salts. With the aim of assessing the degree of charge delocalization, we calculated the proton affinity for $[MCTFSI]^-$ to be $-566\ kJ\cdot mol^{-1}$, indicating a lesser degree of charge delocalization compared to [TFSI]-($543\ kJ\cdot mol^{-1}$) but similar to $[TSAC]^-$ ($577\ kJ\cdot mol^{-1}$) with a maximum computational error of $11\ kJ\cdot mol^{-1}$.[17c] The conductivity of $[C_4mpyr][MCTFSI]$ is similar to that reported for the corresponding $[TFSI]^-$ IL despite an approximately 25% lower molar mass and a lower symmetry. While investigations are still in a preliminary stage and a lithium salt is not available yet, it has been shown that the ESWs are somewhat narrower compared to $[TFSI]^-$ salts but sodium plating and stripping is possible in solutions of 1 M Na[MCTFSI] in EC:PC.

According to this review of physico- and electrochemical data, the following (qualitative) order of respectively improving properties for the pyrrolidinium derivatives of imide-type anions can be given as follows:

Thermal stability:
$[TFSI]^- > [TSAC]^{-[a]} \approx [TFSAM]^{-[b]} \cong [FTFSI]^{-[b]} > [FSI]^-$

Melting points:
$[TFSI]^- > [FSI]^-$

$[FTFSI]^-$, $[TFSAM]^-$, $[TSAC]^-$,
no crystallization detected before T_g

Glass transition temperatures:
$[FTFSI] \leq [FSI] < [TFSAM] < [TFSI] \approx [TSAC]$

Conductivity:
$[FSI]^- \gg [FTFSI]^{-[a]} \approx [TFSAM]^- \approx [TSAC]^{-[c]} > [TFSI]^- \approx [MCTFSI]^-$

Electrochemical stability:
$[FTFSI]^- > [TFSI]^- > [FSI]^- > [TSAC]^- \approx [MCTFSI]^-$

[a] Anticipated, as comparative data are only available for $[TFSI]^-$ derivatives. [b] Order depends on $[C_xmpyr]^+$ series ($x = 3$ or 4). [c] Data available for $[C_3mpip]^+$ and since the conductivities of piperidinium ILs are typically lower than those of pyrrolidinium ILs it is likely that $\sigma[TFSAM]^- \approx \sigma[TSAC]^-$.

2.2.4. Triflate, $[TfO]^-$

Although not an imide type anion we include discussion of triflate anion based ILs in this section, since they feature both the sulfonyl group, and high fluorine content, which are clearly important contributors to the properties sought.[89] Also in

common with $[TFSI]^-$ and other anions discussed in this review, $[TfO]^-$ is the conjugate base of a strong organic acid, albeit the computed proton affinity of $-568.6\ kJ\cdot mol^{-1}$ is less than that of $[TFSI]^-$ (Table 3). Owing to the smaller size, fewer degrees of conformational freedom and the higher symmetry of the $[TfO]^-$ anion compared to imide anions, on heating, $[C_4mpyr][TfO]$ does not melt before 5.6 °C; below that an endothermic solid-solid phase transition is present at −96 °C.[89b] The thermal stability of $[C_4mpyr][TfO]$ is not included in the work by Moreno et al.[89b] nor in the comprehensive review by Xue et al.,[17a] but the onset decomposition temperature is above 300 °C (according to a graph in ref. [89a] and a T_d of 340 °C given in the specification of the commercial supplier, Solvionic). According to 24 h isothermal TGA measurements, the long term thermal stability is good with mass losses of 0.28 wt% at 200 °C and 2.8% at 250 °C.[89a] Once in its liquid state, the conductivity of $[C_4mpyr][TfO]$ is comparable to (or slightly less than) that of $[C_4mpyr][TFSI]$ despite its smaller size and molar mass.[89b] The reports on the electrochemical stability are inconsistent, while they are similar regarding E_{red} they differ significantly by 1.4 V (!) for E_{ox} (both *vs* Ag/Ag^+), 2.03 (on Pt)[89b] and 3.4 V (on GC) .[90] The experimental conditions for acquiring CV data were quite different: besides the differences in scan rates and electrode substrates, the data set obtained on GC was recorded in acetonitrile solution instead of analysing of the neat IL and no cutoff values for current density were given. Furthermore, the CV trace obtained for the $[C_4mpyr][TfO]$ sample in solution shows significant current at ~2.7 V, close to the limiting E_{ox} reported by Moreno et al. and before the bulk oxidation response at 3.4 V. It is not clear whether the response at 2.7 V is related to impurities since a major point of the work by Ignat'ev et al.[89a,90] was to establish an alternative synthetic procedure which avoids the difficulties in obtaining a very pure product from the commonly used silver salt ion-exchange method. Hence at this stage the ESW of 5.38 V reported by Moreno et al. appears to be the more realistic. The ESW of $[C_4mpyr][TfO]$ is approximately 200 mV narrower than its $[TFSI]^-$ counterpart recorded under the same conditions, mainly due to a lower cathodic stability of ~350 mV when considering the reported E_{ox} and E_{red} (We note that this must have been misrepresented in the text of the original literature[89b] where the authors referred to lower anodic stability by 200 mV compared to the $[TFSI]^-$ derivative,[20b] while the E_{ox} values stated in the respective tables are essentially the same). When taking into account the original E_{red} data obtained at two different current densities, the lowering in reductive stability between E_{red} at 0.1 and E_{red} at 0.05 $mAcm^{-2}$ is far more significant for the triflate salt (0.48 V) than for the $[TFSI]^-$ salt ($\Delta = 0.1$ V). The lesser reductive stability may be related to the strong electron withdrawing nature of a third oxygen as opposed to nitrogen in the imide anions combined with a better shielding. Although implied in both papers, the promising electrochemical properties of $[C_4mpyr][TfO]$ were neither explored in CV experiments with respect to reversible Li deposition and stripping nor in battery cycling regimes.

Table 3. Proton affinities of selected imide-type anions.[a]

$[TFSI]^-$	$[MCTFSI]^-$[b]	$[TfO]^-$	$[TSAC]^-$	$[DCA]^-$	$[CF_3CO_2]^-$
−542.7	−565.5	−568.6	−577.2	−590.4	−667.0

[a] All data taken from Ref. [17c], except [b], taken from Ref. [16d]. Calculations were performed using (MP2/aug-cc-pVTZ) method.

2.3. Borate-Type Anions

2.3.1. Chelatoborates $[BOB]^-$ and $[DFOB]^-$

The bis(oxalatoborate) anion[91] $[BOB]^-$, as a prominent example amongst a large group chelatoborates, was originally synthesized with the intention of introducing an anion that is weakly coordinating, like $[TFSI]^-$, $[FSI]^-$ and $[BF_4]^-$, but not fluorinated, thereby creating a lighter and possibly less expensive electrolyte component. Indeed, compared to $Li[PF_6]$, attractive properties were found for Li[BOB] and its solutions in organic molecular solvents, such as the far better thermal stability and an associated low rate of capacity fading when cycled at 50–70 °C in conventional lithium ion cells even when present in low concentrations.[91–92] However, the conductivities of 1 M solutions of this salt in common non-protic solvents are 8–9 $mS\cdot cm^{-1}$, somewhat less than those observed for even 2.0 M solutions of $Li[PF_6]$.[91,93] Xu et al.[94] and Lall-Ramnarine et al.[95] determined key physicochemical properties of bis(oxalatoborate) ($[BOB]^-$) and other related chelatoborates with a range of organic cations including $[C_4mpyr]^+$. Compared to the corresponding $[FSI]^-$ and $[TFSI]^-$ ILs, their glass temperatures and viscosities are relatively high, and therefore the orthoborate ionic liquids are much less conductive, just below $10^{-4}\ S\cdot cm^{-1}$ at 25 °C. Lall-Ramnarine et al.[95] found a m.p. of 55 °C in DSC measurements of this IL, but thermal and electrochemical stability data were not reported. Recognizing that the complete exclusion of fluorine may have ruled out some of the more desirable characteristics for BOB, researchers turned to partially fluorinated borates, in the hope of striking an optimized balance in electrolyte properties.

The unsymmetric hybrid anion difluorooxalatoborate, $[DFOB]^-$, was introduced by Zhang et al.[96] and Gao et al.[97] with the intention of combining the advantages of $[BOB]^-$ and $[BF_4]^-$, that is, excellent SEI formation on graphite anodes ($[BOB]^-$), better low temperature performance ($[BF_4]^-$) than that of $[PF_6]^-$, and protection against overcharge ($[BOB]^-$ and $[BF_4]^-$) (we have noticed an error in a reference given for the latter in the Zhang paper). Indeed, graphite/$LiNi_{1-x-y}M_xN_yO_2$ (M and N are metal atoms not further defined in the original literature) Li-ion cells assembled with Li[DFOB] PC/EC/EMC electrolytes showed excellent cycling behavior[96] over a wide temperature range and retained about 90% of the initial capacity after 200 cycles at 60 °C. Another property which made the anion very attractive for electrolyte formulations is its excellent SEI-forming nature at the additive level and on graphitic anodes.[98] Furthermore, it has been shown that even at low concentrations in conventional electrolytes this anion protects aluminum current collectors effectively from corrosion.[100] The

decomposition of Li[DFOB] ($T_d = 200\,°C$) appears to follow the combined pathways of $[BF_4]^-$ and $[BOB]^-$. The pyrrolidinium derivatives $[C_x mpyr][DFOB]$ (R = butyl, pentyl, hexyl) reported by Allen et al.[101] are similar to their $[TFSI]^-$ counterparts, RTILs with low melting points, high thermal stability and relatively wide ESW ($E_{ox} \sim 5$ V vs. Li/Li^+). However, in the cathodic scan they give rise to a partly reversible redox process between 0 and 1 V (vs. Li/Li^+) that was tentatively assigned to the oxalate ligand. This process was absent in CVs recorded for solutions of $[C_x mpyr][DFOB]$ ILs containing Li[DFOB] or Li[TFSI] and reversible lithium plating could be observed with 90% coulomb efficiency after the first cycle. Although it emerged from these studies that this IL has all the hallmarks of being suitable as an electrolyte medium, no conductivity or battery cycling data have been reported.

2.3.2. Non-chelate Homo and Heteroleptic Borate Anions

Anions in which ancillary groups other than oxygen chelates are linked to a boron center take a less prominent stage in the literature although they are very interesting not only because of the properties of their corresponding ILs but also with regards to their chemistry and synthesis. From the starting point of homoleptic borates $[BF_4]^-$, $[B(CN)_4]^-$, $[B(CF_3)_4]^-$ and $[BH_4]^-$, an impressive library of novel heteroleptic boron compounds has been added more recently, by successive exchange of the substituents, to the pool of anions suitable for forming ILs possessing the properties expected to be considered for ILEL formulations, with major contributions from the groups of Zhou and Matsumoto et al. and Finze et al. (in collaboration with the Merck company). Lowering symmetry and molar mass to further reduce viscosity (and increase conductivity) were a substantial part of the motivation to achieve the more complex synthesis of heteroleptic borate anions.[102] Sequential variation of the substitution pattern around the boron center was possible to a substantial degree and resulted in five classes of borate anions: perfluoroalkylhydrido,[54] $[C_nF_{2n+1}BH_3]^-$, cyanohydrido[102c] $[BH_n(CN)_{4-n}]^-$, perfluoroalkylfluorido[28,103] $[C_nF_{2n+1}BF_3]^-$, cyanofluorido[104] $[BF_x(CN)_{4-n}]^-$ and even examples of higher permutation perfluoroalkylcyano- and perfluoroalkylcyanofluoro borates[102b] $[C_nF_{2n+1}BF_x(CN)_{3-x}]$. A representation of these iterations is given in Figure 7. In the following we discuss the physicochemical properties of their pyrrolidinium cation based ILs; key data of their properties are listed in Table 4.

All these anions, once combined with an alkali metal ion or an organic cation, lead to salts with relatively high T_d, usually well above 200 °C and sufficient for applications in battery electrolytes. Positioned at the higher end of the temperature scale are the borates with cyano group substituents and at the lower end the perfluoroalkylhydrido borates. Amongst the latter, the Li-salts are somewhat unstable, for instance $Li[C_2F_5BH_3]^-$ decomposes at room temperature.[54] The destabilizing presence of hydrido substituents also manifests itself in the series of homologous cyanohydridoborates[102c] where T_d decreases from 330 °C in $[C_4mpyr][BH(CN)_3]$ to 225 °C in $[C_4mpyr][BH_3(CN)]$. A consistent observation in all groups is the superior thermal stability of the corresponding homoleptic anion salts, $[BF_4]^-$, $[BCN_4]^-$, and $[BH_4]^-$ though not $[B(CF_3)_4]^-$.

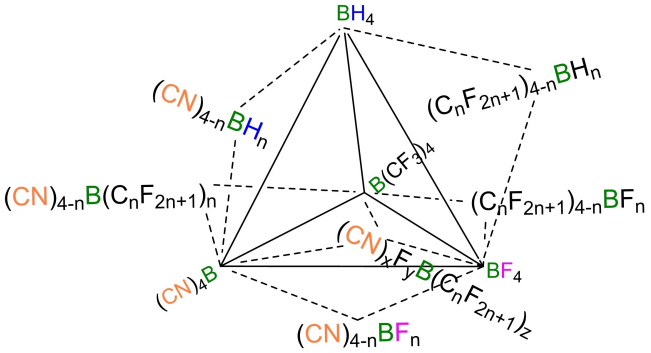

Figure 7. Permutation of homo- and heteroleptic borate anions.

As a result of a subtle interplay between factors such as size, symmetry and flexibility, the nature of the anion significantly affects the melting points of their (cyclic) QA salts. The homologous series of the $[R^FBF_3]^-$ ions[28,103] salts can serve to illustrate the point since many well characterized examples have been reported for variation in fluoroalkyl chain length ($R^F = C_mF_{2m+1}$, $m = 0$–4) and counter cations. For the ILs with the smaller anions ($R^F = CF_3$, C_2F_5) the melting points are usually lower than for those with the larger anions ($R^F = n\text{-}C_3F_7$, $n\text{-}C_4F_9$) and, notably, QA salts with the high-symmetry $[BF_4]^-$ anion (see section 2.1). This suggests that an anion with a low symmetry and a medium size favors a lowering of the melting point of its salt due to a reduced packing efficiency and without a significant increase of the van der Waals interactions in its salts, while the very large sized anions (in this series $m = 3$ and 4) or anions of high symmetry ($[BF_4]^-$) tend to increase the melting point owing to the increased van der Waals (London) interactions and ordered ion arrangement, respectively.[17b,29] To complement this picture, it must be pointed out here that all the QA salts with the large $[TFSI]^-$ anion exhibit low melting points; these results suggest that the high flexibility (conformational degree of freedom) and relative low symmetry in the $[TFSI]^-$ anion are dominant over its large size (i.e., van der Waals interactions).

The impact of symmetry of the anion on the melting point of its respective IL is further corroborated when considering the series of perfluoroalkylcyanoborates and perfluoroalkylcyanofluoro borates for a fixed chain length of the perfluoroalkyl group.[102b] The melting points of their $[emim]^+$ ILs ($C_x$mpyr ILs were not reported) decrease in the order $[R^fB(CN)_3]^- > [R^fBF(CN)_2]^- > [R^fBF_2(CN)]^-$ down to a surprisingly low −57 °C due to lowering symmetry and reducing the number in cyano donor moieties.[102b] A similar, but less consistent, trend was also observed for cyanohydridoborates.[102c]

For the latter group of ILs as well as the perfluoroalkylcyanoborate and perfluoroalkylcyanofluoroborate ILs some T_{gs} data are also available, whereas these were not observed or reported for the other borate anion ILs. Remarkably low T_g of −105 to −110° were found for the ILs with low symmetry

Table 4. Selected physicochemical properties of Li and pyrrolidinium salts of borate anions.

Salt	T_d [°C]	T_g [°C]	T_m [°C]	σ(25 °C) [mS cm^{-1}]	ΔE [V]	E_{ox} [V]	E_{red} [V]
Li[BOB]	293 (±4)[114]	n.r.	$>T_d$	8–9 dep. on solvent[91]	~4.5 (Pt)	n.r.	n.r.
[C_4mpyr][BOB]	n.r.	−37.8[94]	n.o.	0.1	n.r.	n.r.	n.r.
	~300[115] for [C_1mpyr][BOB]	−40[95]	55	0.06	4.79(GC)[115] for [C_1mpyr][BOB] In CH_3CN	3.13	−1.66
Li[DFOB]	200[48]	n.r.	265–271	0.4[96,116]			
[C_4mpyr][DFOB]	290[101]	−77	−5	n.r.	~5(Pt)	1.6	−3.4 to 2.4
	Perfluoroalkyl borates						
Li[B(CF_3)$_4$]	185[109]	n.r.	n.r.	10.1 (in EC/DEC/DMC)[108,117]	6.0(Pt)	n.r.	n.r.
	Perfluoroalkylfluoroborates: for ILs,[28] for Li-salt[112]						
[C_4mpyr][(CF_3)BF_3]	236	n.r.	−18	3.3	n.r.	n.r.	n.r.
Li[(C_2F_5)BF_3]	>100	n.r.	n.r.	~7 (in EC/EMC)	~5.5(Pt)	n.r.	n.r.
[C_4mpyr][(C_2F_5)BF_3]	311	n.r.	22	3.5	5.64 (GC	2.24	−3.41
	Perfluoroalkylhydrido-borates[54]						
Li[(C_2F_5)BH_3]	unstable at RT						
[C_4mpyr] [(CF_3)BH_3]	Only NMR data, synth. not reproducable						
[C_4mpyr] [(C_2F_5)BH_3]	200	n.r.	−1	2.9	3.9 (in CH_3CN)	0.6	−3.3
	Perfluoroalkylcyano(fluoro)-borates[102b]						
K[(C_2F_5)B($CN)_3$]	270	n.o.	n.r.	n.r.	n.r.	n.r.	n.r.
[emim][(C_2F_5)B($CN)_3$]	375	n.o.	−7	9.8	4.7(GC)	2.1	−2.4
K[(C_2F_5)B$F(CN)_2$]	310	n.r.	n.r.	n.r.	n.r.	n.r.	n.r.
[emim][(C_2F_5)B$F(CN)_2$]	330	−110	−21	13.1	4.8 (GC)	2.4	−2.4
K[(C_2F_5)BF_2(CN)]	260	n.o.	n.r.	n.r.	n.r.	n.r.	n.r.
[emim][(C_2F_5)BF_2(CN)]	260	n.o.	−57	15.3	5.8 (GC)	3.2	−2.6
	Cyanohydridoborates[102c]						
Na[BH_3(CN)]	340		250				
[C_4mpyr][BH_3(CN)]	225	n.o.	23	7.0	3.6 (GC)	0.5	−3.1
Na[$BH_2(CN)_2$]	350		175				
[C_4mpyr][$BH_2(CN)_2$]	290	−110	n.o.	10.2	3.8(GC)	0.6	−3.2
Na[BH$(CN)_3$]	380	330					
[C_4mpyr][BH $(CN)_3$]	330	−105	n.o.	8.1	5.2 (GC)	2.0	−3.2
	Tetracyanoborates, for Li salt [104a], for IL [102c]						
Li[B$(CN)_4$]	500	n.o.	n.o.				
[C_4mpyr][B$(CN)_4$]	350	−80[118]	20	4.1	5.8	2.7	−3.1

anions $[BH_2(CN)_2]^-$, $[BH_2(CN)_2]^-$ and $[C_2F_5BF(CN)]^-$, similar or slightly lower than the T_g of $[C_4mpyr]^+$ ILs of the asymmetric anion $[FTFSI]^-$. For the many examples of $QA[C_nF_{2n+1}BF_3]^-$ Zhou et al.[103] noticed as a general trend that for a common cation their T_g values are significantly lower than those of the corresponding $[TFSI]^-$ and $[BF_4]^-$ salts.

Depending on the symmetry of the anions $[BH_n(CN)_{4-n}]^-$, their $[C_4mpyr]^+$ salts[102c] possess one of the highest conductivities observed for ILs; they increase in the order $n=0<1<2<3$, then decreasing again. A direct comparison to ILs of the perfluoroalkylcyano(fluoro)borates cannot be made since no data are available for their $[C_4mpyr]^+$ salts.[102b] However, the latter can be expected to be lower since the conductivities of their imidazolium ILs are significantly lower than those of the corresponding cyanohydridoborates; e.g. $[emim][BH_2(CN)_2]$ possesses an almost three times higher conductivity at 20 °C than $[emim][C_2F_5BF(CN)_2]$ owing to a significantly lower molecular mass.[102b] Likewise, it can be reasonably assumed that the ionic conductivities of pyrrolidinium perfluoroalkylcyano(fluoro)borates will be in the order of 3 $mS\cdot cm^{-1}$, comparable to those measured for the other two series of perfluoroalkylborate ILs, $[C_nF_{2n+1}BH_3]^-$ and $[C_nF_{2n+1}BF_3]^-$. For the latter Zhou et al. observed a decreasing trend in the order of $([FSI]^-) \gg [C_2F_5BF_3]^- > [CF_3BF_3]^- > [TFSI]^- > [n\text{-}C_3F_7BF_3]^- > [BF_4]^- > [n\text{-}C_4F_9BF_3]^-$; ($[FSI]^-$) added by us based on our data survey.

Unfortunately, there are limited electrochemical data available for several of the heteroleptic borate anion alkali salts and ILs and the majority of these were established for their reductively (cathodic reaction) less stable imidazolium derivatives. Hence, considering the reported ESW (ΔE), a sound assessment of their true potential in battery applications cannot be made for several of these anions since the available E_{red} values are limited by the electrochemical stability of the imidazolium cation[7a,28] and therefore are very similar; −2.4 V on average.[102b] This is clearly the case when comparing, for example, electrochemical data of $[emim]^+$ and $[C_4mpyr]^+$ ILs of cyanohydrido[102c] and perfluoroalkyhydrido[54] borate anions where the E_{red} values of the $[C_4mpyr]^+$ derivatives are on average 0.7 V more negative, or even more so. This observation gives reason to believe that borate salts, for which data were reported only for the $[emim]^+$ derivatives, are suitable for lithium battery applications, unless they have limited chemical stability. For example, the K- and Cs-salts of $[C_2F_5BH_3]^-$ are highly shock sensitive in the solid state and the Li-salt undergoes slow decomposition in ether solution whereas the organic cation salts are unprecedentedly stable.[54] No reference was made to the stability and solubility of the alkali metal salts in their corresponding IL derivatives.

Amongst cyanoborates, the largest ESWs were reported for ILs with the homoleptic TCB anion, $[C_4mpy][B(CN)_4]$ with $\Delta E=5.8$ V[102c,104a,105] A clear trend in electrochemical stability was observed in cyanohydridoborate ILs, $[C_4mpyr][BH_n(CN)_{4-n}]$[102c] where, considering oxidative stability (E_{ox}), decreases with a decreasing number of cyano groups from 2.0 to 0.5 V for the $[C_4mpy]^+$ ILs as a result of the increasing hydridic nature of the BH moieties (vide infra) following the same order. Similarly, the oxidative stability of the perfluoroalkylhydridoborate, $[C_4mpy][C_2F_5BH_3]$ is also low but overall its ΔE is 300 mV larger owing to the stabilizing effect of the pentafluoroethyl group.[54] For the two other anions, $[(C_2F_5)_3BH]^-$[106] and $[(CF_3)_3BH]^-$,[107] electrochemical data were not reported. The relatively low oxidative stability of hydridoborate anions raises concerns about their applicability as electrolyte components in high voltage battery systems. As in the case of cycanoborates, the best stability was observed for $[B(CF_3)_4]^-$ ILs. A very wide ESW of 6 V was disclosed in EP 1205480[108] and Bernardt et al.[109] demonstrated that the alkali salts of this anion are remarkably resistant towards both strong oxidizing and reducing agents. It is not affected by normal nucleophiles (e.g. $[C_2H_5O]^-$) or electrophiles (such as Li^+ or H_3O^+). For 0.96 M solutions of $Li[B(CF_3)_4]$ in EC:DEC:DMC (2:1:2) very attractive ionic conductivities of 10.1 $mS\cdot cm^{-1}$ were measured,[108] slightly higher than 9.6 $mS\cdot cm^{-1}$ for 1.0 M $Li[PF_6]$ in the same solvent medium.

Electrochemical data have been reported for $[emim]^+$ ILs of cyanofluoroborate anions, so their E_{red} hardly exceed −2.3 V and their E_{ox} are approximately 2.0 V;[21b] there are no electrochemical data reported in WO2004072089.[110]

Electrochemical stability data for perfluoroalkyltricyanoborate $[C_nF_{2n+1}B(CN)_3]^-$ and perfluoroalkylcyanofluoroborate anions $[C_nF_{2n+1}BF(CN)_2]^-$, $[C_nF_{2n+1}BF_2(CN)]^-$ were only reported for their respective $[emim]^+$ ILs[102b] and hence the limiting reduction potentials are around −2.4 V (±0.2 V). Nevertheless, wide ESWs were found, up to +5.8 V in the case of $[C_nF_{2n+1}BF_2(CN)]^-$, owing to very high E_{ox}, e.g. $[C_4F_9BF_2(CN)]$ and $[C_2F_5BF_2(CN)]$, 3.0 and 3.2 V, respectively. While there is little variability of the E_{ox} with the perfluoroalkyl chain length, they vary appreciably with the F, CN substitution pattern: at opposite poles are $[C_nF_{2n+1}BF_3]^-$ with $E_{ox}=2.1$ V and $[C_2F_5BF_2(CN)]^-$ with $E_{ox}=3.2$ V. It is reasonable to expect that the ESWs of $[C_4mpyr]^+$ derivatives could be more than 0.5 V wider, rendering these salts some of the electrochemically most stable ILs available.

Surprisingly, important physicochemical properties (i.e., σ, E, solubility) for the evaluation of metal (lithium) salt solutions of cyanofluoroborate, perfluoroalkyltricyanoborate and perfluoroalkylcyanofluoroborate anions in solution of their corresponding ILs for application as battery electrolytes have not been reported; notably the absence of any cyclic voltammetric data confirming reversible plating and stripping of respective battery metals (i.e. Li^+ or Na^+) as a bare minimum (we assume that this is not related to negligence but to commercial interest; a significant number of patents appearing prior to publication of individual works).

The physicochemical properties for a range of ILs of the simpler $[C_nF_{2n+1}BF_3]^-$ (n=1-4) anions with various organic cations has been reported by Zhou et al.,[28,103,111] and a limited data set of their redox potentials is available confirming that the E_{red} for the $[C_4mpyr]^+$ derivatives are, as expected, significantly more stable than the corresponding $[emim]^+$ salts; in the case of $n=2$ by 0.9 V. Due to the absence of stabilizing CN groups in perfluoroalkyltrifluoroborate ILs, the E_{ox} of the perfluoroalkyltrifluoroborate ILs are up to 1 V less positive than those of their CN containing counterparts. Electrochemical data have also been estimated for solutions of $Li[C_2F_{2n+1}BF_3]$ in a common carbonate solvent mixture, EC:EMC (3:7 v/v) with

$\Delta E \sim 5.5$ V, and Li cycling was demonstrated in Li | Graphite half cells.[112] The corresponding $[C_4mpy]^+$ ILELs are discussed in the following section.

2.4. Comparison of IL Anions for Application in Electrolytes for Li Batteries

Matsumoto drew together much of the literature on 'alternative' anions for lithium-compatible ionic liquids in a book chapter published in 2014.[113] The overall impression conveyed by that survey is that several new anions, when combined with common small quaternary ammonium cations, yield ionic liquids with excellent liquid properties (reviewed above). Most however proved to have electrochemical properties that were inferior to those of the corresponding $[TFSI]^-$ ILs. As a first example, a series of ILs based on a fluoroalkylborate ($[FAB]^-$) was examined.[28] The only information provided on any lithium electrochemistry was for a mixture of 0.3 M $Li[BF_4]$ in $[C_4mpyr][F_5C_2BF_3]$ for which lithium plating and stripping was found to be reversible, though the degree of reversibility was not quantified.

As described earlier, the anion known as $[TSAC]^-$ also confers impressive liquid properties when combined with small organic cations.[87] The electrochemical properties of $[TSAC]^-$ are however possibly the least favorable of all of the recently developed anions. Matsumoto et al.[87b] show that lithium reduction potentials are only accessible when the salt added is Li[TFSI]. Here it is highly likely that SEI formation courtesy of the latter provides the electrode surface conditions required for reversible lithium plating-stripping to take place. A later study[18a] confirmed the relative instability of $[TSAC]^-$ at negative potentials, by comparison with other fluorinated anions, where the same cation was present.

The other anions reviewed by Matsumoto[113] are the group of species that are closely related to $[TFSI]^-$: (i) the direct (symmetrical) analogues $[FSI]^-$ and $[BETI]^-$ (bis[pentafluoroethanesulfonyl]imide); (ii) the asymmetrical analogues $[FTFSI]^-$ (half [FSI], half [TFSI]), 'C1 C2' (half [TFSI], half [BETI]) and $[FBETI]^-$ (half [FSI], half [BETI]). In general terms, all of the asymmetrical anions support reversible lithium electrochemistry to some extent although the liquid properties with the same cation are inferior to the comparable $[TFSI^-$ IL. RTILs based on $[BETI^-$ can also be categorized in this way. As described earlier, $[FSI]^-$ ILs quickly set new benchmarks in performance as electrolytes, not only with Li[FSI] as the source of lithium ions, but also with a range of other lithium salts.

In one of the few studies that allowed direct comparison of many of the anions discussed, Matsumoto et al.[14] were able to make some important comparisons of the corresponding ILs, in terms of their physicochemical, electrochemical, and battery-electrolyte properties. The comparison was based on RTILs in which the cation was the quaternary ammonium species $[N_{1221O2}]^+$ (diethyl-,methyl-,methoxy-ethyl-ammonium, 'DEME'). Most significant were the results from a comparison of full cell performance when these ionic liquids were used as electrolytes in Li–$LiCoO_2$ coin cells. Figure 8 is a summary of the results.

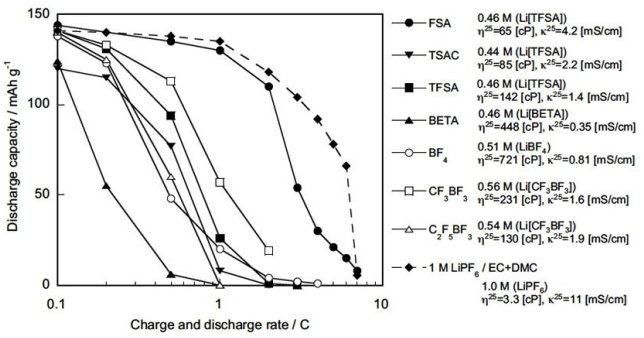

Figure 8. Charge-discharge rate property of Li/LiCoO2 cell using $N_{122.1O2}$-ILs-ILs. $T = 25\,°C$, $1\,C = 0.2\,mA\,cm^{-2}$. The physical properties of lithium electrolytes at 25 °C used were also indicated. [Originally appears as Figure 5 in Matsumoto et al., *ECS* Trans, 2009]. Reprinted with permission from Ref. [14]. Copyright 2009, The Electrochemical Society.

It is noted that Li[TFSI] was the salt employed for the $[FSI]^-$, $[TSAC]^-$ and $[TFSI]^-$ IL-based electrolytes, with the respective anion salts being used for the remainder (namely, $[BETI]^-$, $[BF_4]^-$ and the two fluoroalkyl derivatives). The results clearly show that the only electrolyte that outperformed the $[TFSI]^-$ benchmark, based on an evaluation of discharge capacity vs. discharge rate, was that based on $[FSI]^-$. While $[FAB]^-$ and $[TSAC]^-$ have low viscosity and good conductivity, as noted earlier, both gave rise to inferior battery performance. Interestingly, Matsumoto et al.[14] recorded EIS spectra for all cells and assigned the two-semicircle responses to a contribution of one semicircle each for cathode and anode. Given that SEI formation on lithium-ion cathodes is still a matter of conjecture and has never been shown to be nearly as prolific as on anode materials, it seems likely that the EIS response was completely due to the interaction of the lithium anode with the electrolyte. In this light, their results are consistent with the proposition that the group of new anions (with the clear exception of $[FSI]^-$) forms SEI layers at lithium that are thicker and/or more resistant to lithium ion movement than those derived from $[TFSI]^-$.

The key to understanding battery electrochemistry is the electrode/electrolyte interface, as it is where a Li-ion combines with an electron followed by storage in the electrode. The interface, which is further complicated by a solid passivation layer on the electrode is commonly referred to as the solid electrolyte interface (SEI). An efficient SEI film is responsible for the better performance and longer life of a battery. A good review including comprehensive literature references on the topic was recently published by Wang et al.[119] Generally, the functionalities of the SEI should: block the interaction between electrons (from the electrode) and the electrolyte to avoid continuous electrolyte reduction reactions, not impede Li-ion transport from the electrolyte to the electrode, be chemically stable (not reacting with or dissolving into the electrolyte) and be mechanically stable. Although the SEI is regarded as one of the most important components in rechargeable Li-ion batteries, it is also still one of the least understood areas. This can be attributed to the complexity of the chemical and electrochemical reactions involved in its formation and, although

highly desirable, to difficulties in quantifying the chemistry-structure vs. property relationship of SEI films, due to its thinness and lack of suitable analytical methods. However, new computational modelling methods combined with precise surface coating methods helped to deconvolute structure-property relationships of SEI layers. Combined experimental surface and modelling studies, mainly performed on conventional electrolytes, provide insight into factors associated with the formation and performance of SEIs and therefore guide the exploration of candidates for alternative formulations for new battery chemistries, i.e. boron-based anion receptors and ILs.

From these studies it follows that the initial formation process of an SEI film, which plays an important role in the SEI composition, is the reduction of an electrolyte on the anode surface. While the reduction potential of an individual electrolyte component can be readily calculated from its LUMO in the gas phase, the situation is much more complex in a multi-component solution environment where the reduction potential depends on concentration, solvent polarity and notably the M^{n+} solvation complexes. For example, the order of first electron reduction for carbonate solvents changes significantly when coordinated to Li^+. While the latter pertains to traditional carbonate electrolytes, the situation in ILs (absence of neutral molecular solvent molecules) is very different. Since anions can participate in overall electrolyte reduction processes, they play an important role in SEI formation processes in ILELs (see also next section 2.5). Moreover, the coordination (solvation) sphere of M^{n+} is composed of one or more anion species, depending on the IL and metal salt present in multicomponent ILELs (a more detailed discussion of $M_x[anion]_y$ structures and coordination chemistry is presented in section 4). The coordination number in $M_x[anion]_y$ species depends on DNs, structure and geometry of the anion and therefore the reduction potential can vary significantly. Data of E_{red} are available for several Lithium salts. For example, the $Li[PF_6]$ reduction potential (1.61 V) is higher than that of $Li[BF_4]$ (0.2–0.3 V) and therefore impacts passivation layer formation more significantly than $Li[BF_4]$ (higher E_{red} imply greater ease of reduction). In comparison, the E_{red} potentials of two prominent borate salts, Li[BOB] (1.5–1.8 V) and Li[DFOB] (1.57 V; 2.12 V dimer), are also higher than that of $Li[BF]_4$ and similar to $Li[PF_6]$. The imide salts Li[TFSI] (2.1–2.9 V LiF contact) and Li[FSI] (1.6–2.3 V) compare favorably with the two borates, particularly in presence of LiF which has been shown to increase the reduction potential once formed. Furthermore, it is expected that the changes in the chemistry, morphology, and properties of the SEI, such as the density, cohesive energy, solubility, and porosity are much larger compared to conventional carbonate electrolytes because of the much greater variation in chemical composition of the various available anions. This has major implications on the electron insulating properties and ion conductivity of the SEI layer. It has been shown for carbonate electrolytes that of the two principal inorganic compounds present, LiF is a much better electron insulator than Li_2CO_3. In case of ILELs, the composition of the SEI and hence its conducting properties are quite different due to the presence of several other elements in the ion structures. In terms of M-ion transport from the electrolyte to the electrode, the coordination (solvation) structure of the M-ion and the M-ion binding energy are important since the transport process involves M-ion desolvation at the electrolyte/SEI interface and diffusing through the SEI. Again, while in traditional mixed carbonate solvent/$Li[PF_6]$ electrolytes the M-ion species are solvated mainly by EC (unless PC is present), in ILELs $M_x[anion]_y$ species are present with entirely different transport properties.

In the time since many of the comparative studies referred to were conducted, ILs based on $[FSI]^-$ have gained increasing prominence in the literature related to lithium batteries, particularly that concerned with lithium metal anodes. This also applies to the parallel investigations that employ very high concentrations of Li[FSI] in a range of solvents, most notably the ethers used in lithium-sulfur battery development. A recent example of how this information translates to improved battery performance comes from Suo et al.[120] who demonstrated extended cycling behavior for lithium-sulfur cells configured with lithium metal electrodes and electrolyte containing 7 M Li[FSI].

2.5. Role of Anion in Lithium Plating and Stripping

For many metal ions, electroplating involves a reasonably simple mechanism, namely transport of the metal species to the electrode surface, electron transfer and subsequent phase change. The stripping process is then the reverse of the plating reaction. When considering lithium metal, the electroplating mechanism is significantly more complex. Firstly, the species transport, in the context of ILs, is complicated by the negatively charged species formed upon dissolution of Li^+ in the IL through coordination to the IL anions. Upon reaching the electrode surface, the electron transfer process can occur which also includes a phase change. However, this is not straightforward due to the high reactivity of lithium metal, which interacts with the electrolyte with formation of the SEI layer. Therefore, any Li^+ solution species also has to navigate through an SEI layer, which is typically formed from non-conducting passivation products prior to electron transfer occurring. The SEI formation can also occur with two distinctly different mechanisms – electrochemical and chemical. All of these reactions typically proceed simultaneously, and the overall effect translates into the generalised electrical response of lithium metal batteries.

Looking firstly at the chemical reactions with the reactive lithium metal to form the SEI, Liang et al.[121] (as summarised in Ref. [122]) have shown a facile chemical interaction route to obtaining different SEI layers through in situ deposition of metallic alloys. The different SEI layers formed demonstrated differing cycling ability. In the context of this manuscript, the chemical interaction would arise from use of different IL anions, hence the role of anions should be accounted for in the design of electrolytes for lithium metal batteries, as they will have a direct influence on the SEI nature formed during the chemical interaction process. This effect has been utilised by Wang et al.[123] through chemical interaction of [bdmim][BF_4] and

lithium metal to form LiF layers. The resultant SEI enabled high current cycling of the lithium electrode at 5 mA/cm^2 and cycling of NMC-Li batteries at a charge/discharge rate of 1 hour (1 C).

Probing the composition effects of organic electrolytes utilising Li[TFSI], Hayashi et al.[124] and Crowther and West[125] have demonstrated onset of lithium dendrite formation can be delayed upon reducing the organic solvent component and increasing the ionic concentration (in this case Li[TFSI]). In a review of lithium metal electrodes Lin et al.[126] discuss the use of high Li salt concentrations to retard dendrite formation. Utilising the $[TFSI]^-$ and $[FSI]^-$ anions, use of salt concentrations of 4 M or 7 M results in retarded dendrite formation and high current ability.[120,127] Further work in this area by Qian et al.[127a] showed that using low salt concentrations (1 M) of Li[PF_6], Li[FSI] or Li[TFSI] in PC resulted in dendrite formation. However, increasing concentration to 1–5 M for Li[FSI] in DME, showed deposition of nodule like structures as compared to the needle like dendrites in the PC solvent. Optimising this discovery, the authors showed that 6000 cycles can be obtained using the 4 M Li[FSI]-DME solution. These literature sources identify two important points, firstly, the anion type will affect the chemical SEI composition and secondly, higher ionic concentrations are suitable for dendrite suppression. The latter is inherent in any IL, thus the role of the anion is now discussed further.

In conventional carbonate based solvents, significant studies by Zinigrad et al. have identified formation of a range of complexes. Typically, the carbonate electrolytes breakdown to form compounds such as Li_2O, LiF, Li_2CO_3 amongst others. For ILs, the SEI layer formed through chemical interaction with Li metal can form a range of compounds dependent on the IL cation and anion. Basile et al.[128] have used X-ray photoelectron spectroscopy (XPS) and observed that for Li[FSI]/[C_3mpyr][FSI] electrolytes, the anion breakdown forms compounds such as LiF, LiOH, Li_2O and SO_2F. Further, the data found evidence for surface confined cation and anions.[129] This chemical reaction was observed over a time period of hours to several days. Upon introduction of a third anion through use of salts such as Li[BF_4], Li[PF_6] or Li[AsF_6] rather than Li[FSI], similar chemical interactions occur, thought the end result is formation of different SEI components. For example, the $[BF_4]^-$ salt contains an SEI with surface confined Li[BF_4] after a period of 7 days.[130] The subtle differences introduced due to the third anion from the lithium salt affect the final surface morphology of the lithium metal electrode,[128] which will lead to influences on the electrochemical cycling during battery applications. This morphological effect has also been noted by Yao et al.[131] where the use of Li[FSI] in [bmim][NO_3] allowed the exposure of lithium metal to $[FSI]^-$ and $[NO_3]^-$ anions to form stable SEI layers and morphologies. These in turn enabled relatively good cycling ability for the LiS cells. Cycling of [C_3mpyr][FSI] containing either Li[PF_6], Li[AsF_6] or Li[FSI] after a period of chemical interaction (12 days) showed that the average CEs were 99.96%, 99.93% and 99.42% for cells containing Li[FSI], Li[PF_6] and Li[AsF_6], respectively. These differences were attributed to the formation of different decomposition products, which can be directly related to the Li-salt anion changes. The different products on the macro scale tend to form differing surface morphologies. Interestingly, this chemical interaction was found to be beneficial rather than detrimental. Li/LFP cells used for the study were stored for 1 year and cycled. The cycling data showed a similar performance to that of freshly constructed cells. The synergistic effect of the cation-anion combination has also been studied by Yoo et al.[132] Through change of the cation, the beneficial properties of the $[FSI]^-$ breakdown can be enhanced by use of cations with long aliphatic chains to form an electrostatic shield on the lithium surface which translates to dendrite suppression in battery cycling. One of the findings of Yoo was that the use of long aliphatic chains formed flexible SEI layers in contrast to those formed with short chain cations. Taking these bodies of work together, it can be possible to use the tailoring ability of ILs for stable and flexible SEI layers which can lead to stable, dendrite free cycling and the ongoing chemical reaction can lend itself to long storage times.

Turning to the electrochemical SEI formation, the vast majority of literature sources focus on cation changes for stabilising lithium plating and stripping. This is unsurprising as utilising different cations, different ESWs can be obtained. However, as discussed above, the solvated Li^+ species predominantly exist in negatively charged aggregates or complexes. Hence the role of the anion cannot be discounted. Work by Basile et al.[133] showed that by fixing the IL cation and only changing the lithium salt anion different effects on cycling and SEI stability can be observed. Using CV data, an order for the SEI formation rate was determined and found to be Li[BF_4] > Li[AsF_6] > Li[PF_6] > Li[TFSI] > Li[FSI]. Moving away from the imide type anion, the electrochemical SEIs formed can become complex. For example, work by Yoon et al.[45] has demonstrated that the $[DCA]^-$ is a poor choice for SEI formation, unless a small quantity of water is present. Inferred from the data presented, the SEI formation was retarded when the water content is less than 100 ppm resulting in poor cycling behavior. However, a beneficial SEI forms when sufficient water is present.

These studies demonstrate that the role of anions on SEI formation and lithium surface morphologies cannot be discounted. Although to a large degree, plating/stripping behavior of lithium is dependent on the choice of IL cation, the anion also plays a crucial role in SEI stabilisation. Use of appropriate cation and anion combinations can lead to utilisation of high current densities in IL batteries[76a] compared to traditional EC/PC/Li[PF_6] systems or commercially viable cycle lifetimes.[128]

3. Transport Properties

Transport properties such as self- and inter-diffusion coefficients, conductivity and transport numbers of ILs and ILELs are important descriptors because they determine the ease of ion (charge carrier) movements in electrolyte solutions on which the rate of battery charge/discharge operation depends. Apart from quantifying these properties, measurement of transport properties, for example ion self-diffusion by spin-echo NMR, can provide some insight regarding the size charge state and

the disruption-formation mechanism of the coordination shell of $[M]^{n+}$ on which the transport properties depend.

For a binary electrolyte system there are six transport properties describing mass and charge flow in addition to the viscosity describing momentum flow, the thermal conductivity describing heat flow and the thermal diffusion coefficient describing the flows of mass, and hence charge, due to temperature gradients. While not the topic of this review, it is noteworthy that the latter two properties have been little studied as yet in ionic liquid systems, though the thermal conductivity is of considerable importance in the design of chemical engineering process reactors and thermal diffusion needs to be considered wherever temperature gradients produce concentration gradients or vice versa.

There are three phenomenological treatments of mass and charge flow in solutions: two are based on non-equilibrium thermodynamics, employing either mobility or resistance coefficients, and one is based on statistical mechanics, employing velocity cross-correlation coefficients.

Mobility coefficients, (not to be confused with ion mobility in an electric field and sometimes called Onsager coefficients), have not been examined in any detail in molten salts or their mixtures. The necessary equations for the calculation of resistance and velocity cross-correlation coefficients exist only for one component systems and two-component systems with a common ion and do not yet extend to reciprocal mixtures of two different salts (technically a three component system). However, they do allow some insight into ion transport in molten electrolytes that is not biased by notions of ionicity (i.e., ion association) or assumptions based on Stokes-Einstein-Sutherland hydrodynamics, both of which are extensively used in the literature.

It is beyond the scope of this review to examine the great many single component ionic liquid systems that have been studied. Rather we first show how phenomenological treatments can be applied to such systems and used as a guide to dealing with salt-ionic liquid mixtures with a common anion together with the types of experimental methods required to determine phenomenological mass and charge transport coefficients. Experimental diffusion studies on ionic liquid mixtures of lithium and sodium salts of interest as models for alkali battery electrolytes are then summarized.

3.1. Single Component Systems

In a single component system there are only three independent mass and charge transport properties, the conductivity and the two ion self-diffusion coefficients. Despite common belief, no transport number is measurable, as is explained below.

3.1.1. Mobility Coefficients

For two ion constituents, *c* and *a*, the ion fluxes J_i can be expressed as linear functions of the forces X_i causing the flux, that is, gradients in the electrochemical potential [Eqs. (2)–(3)].

$$J_c = l_{cc}X_c + l_{ca}X_a \tag{2a}$$

$$J_a = l_{ac}X_c + l_{aa}X_a \tag{2b}$$

$$X_i = -(\nabla\mu_i + z_iF\nabla\phi) \tag{3}$$

where μ_i.and z_i are the chemical potential and charge number, including the sign, of the ion constituent, *F* is the Faraday and ϕ is the electric potential.[134] The l_{ij} are the mobility coefficients. By the Onsager reciprocal relationship, $l_{ca}=l_{ac}$. The molar conductivity is given by Equation (4):

$$\frac{\Lambda}{v_cz_cF^2} = \frac{|z_c|l_{cc}}{c_c} + \frac{|z_a|l_{aa}}{c_a} - \frac{2|z_c|l_{ca}}{c_a} \tag{4}$$

where the v_i are stoichiometric coefficients and *c* is the amount concentration or molarity.[134a] The self- or intra-diffusion coefficient [D_{Si}, Eq. (5)] requires a more subtle approach. This are determined by measurement of the inter-diffusion of distinguishable species of the ion which are identical in every other respect. For example, in NMR spin-echo measurements the distinguishable difference is the energy of the resonant nucleus in the applied magnetic field gradient. This introduces another pair of mobility coefficients, $l_{cc'}$ and $l_{aa'}$ where the prime indicates the labelled species. Thus,

$$D_{Sc} = RT\left(\frac{l_{cc}}{c_c} - \frac{l_{cc'}}{c_{c'}}\right) \tag{5}$$

To simplify these expressions and to so obtain three mobility coefficients from three experimental properties, Laity made the reasonable assumption that [Eq. (6)]:

$$l_{cc'} = l_{aa'} = 0 \tag{6}$$

Hence [Eq. (7)],

$$\Lambda = \frac{F^2}{RT}\left(v_c{z_c}^2D_{Sc} + v_a{z_a}^2D_{Sa} - \frac{2|z_c|l_{ca}}{c_a}\right) \tag{7}$$

Comparison with the Nernst-Einstein equation [Eq. (8)],[135]

$$\Lambda = \frac{F^2}{RT}(v_c{z_c}^2D_{Sc} + v_a{z_a}^2D_{Sa})(1-\Delta) \tag{8}$$

shows that the NE deviation parameter Δ is another form of the cation-anion cross-term mobility coefficient describing the interaction of the cation and anion flows [Eq. (9)].

$$\Delta = \frac{F^2}{RT}\frac{z_cl_{ca}}{c_a(v_c{z_c}^2D_{Sc} + v_a{z_a}^2D_{Sa})} = \frac{F^2}{RT}\frac{|z_a|l_{ca}}{c_c(v_c{z_c}^2D_{Sc} + v_a{z_a}^2D_{Sa})} \tag{9}$$

where the relations $c_i=v_i\ c_{salt}$ and $z_cc_c+z_ac_a=1$ have been employed. Note that in the equations above there is no need to specify a frame of reference as a) in this case the mass and volume-fixed frames are identical, and b) Λ and the D_{Si} are independent of the frame of reference.[134b]

Misunderstanding of the definition of a transport number (t_i) in a single component system has caused controversy.[135–136] It was shown long ago that any particular choice of a reference frame for a single component system is arbitrary.[137] For instance, in the mass-fixed frame, it is given by the ratio of the ion molar mass to the salt molar mass as a result of the law of momentum conservation.[137a,b] Laity's assumption [Eq. (6)] leads to an alternative form, independent of any frame of reference [Eq. (10)]:

$$t_c = 0.5 + \frac{F^2}{2RT\Lambda}(z_c D_{Sc} - |z_a| D_{Sa}) \tag{10}$$

This is rather different from the commonly used but inappropriate approximation based on the Nernst-Hartley equation for infinitely dilute electrolyte solutions:

$$t_c = v_c {z_c}^2 D_{Sc} / (v_c {z_c}^2 D_{Sc} + v_a {z_a}^2 D_{Sa}) \tag{11}$$

This equation can be obtained by combining [Eq. (6)] and [Eq. (10)], again with Δ set equal to zero, but for ionic liquids and molten salts [Eq. (11)] can never apply, as $1 > \Delta > 0$.[135] It should be noted that t_i for a single component system is not a measurable quantity, but a derived one, contrary to claims in the literature.[138] Unlike self-diffusion coefficients or the molar conductivity, it cannot be written directly in terms of statistical mechanical expressions using linear response theory without making arbitrary assumptions.

3.1.2. Laity Resistance Coefficients (LRC)

The Laity resistance coefficients (r_{ik}) are non-equilibrium thermodynamic quantities that are a generalization of the familiar Stokes-Einstein-Sutherland (SES) friction coefficient that can be applied to molten salts and solutions away from the constraint of infinite dilution (tracer diffusion). They are obtained from the measurable transport properties and are independent of any model.

They are defined by

$$X_i \equiv -(\text{grad}\ \mu_i)_T = \sum_{k=1}^{N} r_{ik} x_k (\boldsymbol{v}_i - \boldsymbol{v}_k) \tag{12}$$

where X_i is again the thermodynamic or generalized frictional force on ion species i in an electrochemical potential gradient, $\boldsymbol{v}_i$ its velocity in a given frame of reference (e.g. mass-fixed, volume-fixed etc.) and x_k is the mole fraction of k. As [Eq. 12] contains velocity differences, the resistance coefficients are independent of the frame of reference, unlike the mobility coefficients (in other than one-component systems). The Onsager reciprocity relation here takes the form $r_{ik} = r_{ki}$. For a single salt [Eqs. (13)–(14)],[139]

$$r_{ca} = z_c v_c (z_c + |z_a|) F^2 / \Lambda \tag{13}$$

and

$$r_{ii} = \frac{1}{|z_j|}\left[\frac{(z_c + |z_a|)RT}{D_{Si}} - |z_i| r_{ca}\right],\ i = c, a; j \neq i \tag{14}$$

r_{ca} is necessarily positive, but the two r_{ii} may be positive or negative, unlike a necessarily positive SES friction coefficient. Hence the use of the terminology "resistance", rather than "friction".

The Nernst-Einstein deviation parameter can be written in terms of the Laity resistance coefficients [Eq. (15)][140]

$$\Delta = \frac{z_c |z_a| r_{ca} (1 - r_{cc} r_{aa} / r_{ca}^2)}{(2 z_c |z_a| r_{ca} + z_c^2 r_{aa} + z_a^2 r_{cc})} \tag{15}$$

If

$$r_{ca}^2 = r_{cc} r_{aa} \tag{16}$$

that is, the cation-anion resistance coefficient is the geometric mean of the cation and anion resistance coefficients, then Δ is zero.[140–141] Δ approaches 0.5 as r_{cc} and r_{aa} approach zero (from positive values).[140b] The self-diffusion coefficients are given by Equation (17):

$$D_{Si} = \frac{(z_c + |z_a|)RT}{(|z_j| r_{ii} + |z_i| r_{ca})},\ j \neq i \tag{17}$$

so, under these circumstances, the cation-anion resistance term dominates, and for a 1:1 salt, the cation and anion self-diffusion coefficients are then, formally, equal.

For single component systems, the main value of the calculation of resistance coefficients is that both like-ion r_{ii} are found to be negative in systems where ion association occurs, such as $ZnCl_2$.[142] This occurs much less frequently for ionic liquids than is commonly argued from so-called "ionicities" based on the comparison of conductivities with values calculated from the Nernst-Einstein equation. This is a flawed argument (see below, Section 3.1.4). To date, the only known examples appear to be the protic 1-methyl-2-oxopyrrolidinium tetrafluoroborate, [PyrOMe][BF_4], 1,8-diazabicyclo-[5,4,0]-udec-7-eneium methanesulfonate, [DBUH][CH_3SO_3],[142b] (which both need experimental confirmation given some uncertainties in the quality of the data), the pseudo-protic ionic liquid *N*-methylimidazolium acetate where association is more certain,[143] and certain lithium salts[144] (see discussion below, Section 3.2.2). Normal aprotic ionic liquids all have positive like-ion r_{ii} that increase with increasing viscosity and decrease with increasing temperature.[76c,140a,145] Examples include 1-alkyl-3-methylimidazolium bis(trifluoromethanesulfonyl)amides, [Rmim][TFSI],[145a] tetrafluoroborates, [Rmim][BF_4] and hexafluorophosphates, [Rmim][PF_6],[140a] *N*-methyl-*N*-propylpyrrolidinium bis(fluorosulfonyl)imide, [Pyr_{13}][FSI],[76c] triethylpentylphosphonium [TFSI], [$P_{222,5}$][TFSI],[145b] and *N*-butyl-*N*-methylpyrrolidinium [TFSI], [Pyr_{14}][TFSI], (calculated from the published transport properties).[58] For all these examples, the Nernst-Einstein parameter Λ is less than 0.5. On the other hand, in the few

cases where association does occur, Δ lies between 0.5 and 1.[140b,142b]

3.1.3. Velocity Cross-Correlation Coefficients (VCC)

The use of VCC for molten salts is due to Schönert (theory)[146] and to Trullás and Padrò (molecular dynamics simulations),[147] following earlier applications to electrolyte solutions.[148] Schönert related the transport properties to the Onsager mobility coefficients and Green-Kubo linear response theory expressions for the VCC. The cation-cation VCC is given in terms of the cation self-diffusion coefficient and the conductivity by Equation (18):

$$f_{cc} \equiv \frac{N_A V}{3}\int_0^\infty \langle \mathbf{v}_{c\alpha}(0)\cdot\mathbf{v}_{c\beta}(t)\rangle \mathrm{d}t = RT\kappa\left(\frac{M_a}{z_a FcM}\right)^2 - \frac{D_{Sc}}{\nu_c C} \qquad (18)$$

where c is the salt amount concentration (molarity), M is the molar mass, M_a is the molar mass of the anion, t is time, and N_A, R and F are Avogadro's number, the gas constant and the Faraday respectively. There is an analogous expression for the anion-anion velocity cross-correlations, f_{aa}. The cation-anion VCC depends only on the conductivity, κ [Eq. (19)],

$$f_{ca} \equiv \frac{N_A V}{3}\int_0^\infty \langle \mathbf{v}_{c\alpha}(0)\cdot\mathbf{v}_{a\beta}(t)\rangle \mathrm{d}t = RT\kappa\frac{M_c M_a}{z_c z_a (FcM)^2} \qquad (19)$$

The cross or "distinct" correlation is between the velocity v of a given ion, α, and that of a different ion β, of like or unlike charge, averaged over the whole ensemble contained in volume V. The integral represents the time evolution of the cross-correlation function due to ion collisions and interactions. These expressions can be compared to the more familiar velocity auto- (or "self-") correlation in the expression for the self-diffusion coefficient [Eq. (20)].

$$D_{Sc} = \frac{1}{3}\int_0^\infty \langle \mathbf{v}_{c\alpha}(0)\cdot\mathbf{v}_{ca}(t)\rangle \mathrm{d}t \qquad (20)$$

It is often useful to employ distinct diffusion coefficients (DDC) [Eq. (21)]:[149]

$$D^d_{ij} = cf_{ij}(v_c + v_a) = vcf_{ij},\ i,j = c,a \qquad (21)$$

Note that both the VCC and DDC are negative quantities for single component systems, that is, they represent <u>anti</u>-correlations between the ion velocities, even for oppositely charged ions. This counter-intuitive behavior is a result of the law of conservation of momentum.[148a,150] Put at its simplest, movement of one ion requires movement of the rest of the ensemble in directions such that the total momentum remains fixed. Positive correlations on the other hand can occur in electrolyte solutions and binary salt mixtures where momentum can also be exchanged with solvent molecules or a third ion species. These separate effects have been confirmed in molecular dynamics simulations of salts, electrolyte solutions and polymeric ionic liquids.[150–151]

It is well known that self-diffusion coefficients of both molecular and ionic liquids obey a fractional Stokes-Einstein-Sutherland relationship when plotted against the fluidity or reciprocal viscosity, ($\phi = 1/\eta$), with high-pressure isotherms falling on a common line for all but strongly H-bonded substances such as alcohols and water [Eq. (22)],[152]

$$D_S/T \propto (1/\eta)^t \qquad (22)$$

Ionic liquids similarly obey a fractional Walden relation [Eq. (23)],

$$\Lambda \propto (1/\eta)^t \qquad (23)$$

where t is found by experiment to have the same value for all three properties.[58,76c,140a,145,153] (This is a good test of the quality and consistency of experimental data).

DDC, when plotted as [$-D^d_{ij}/T$] against the fluidity (Figure 9), have the same slope t, as is to be expected from [Eqs. (18), (19), and (21)], but there are patterns evident for different ionic liquid families with different anions.[153b] In the examples studied to date, cation-anion f_{ca} are always smaller in magnitude (less negative) than cation-cation and anion-anion f_{ii}, due no doubt to coulombic attractions moderating the momentum conservation effect (or "momentum buffering").[150] For $[BF_4]^-$ and $[PF_6]^-$ salts (three examples of each),[140a] $f_{cc} < f_{aa}$ (more negative, that is the anti-correlations are stronger for the cation-cation case) but for $[FSI]^-$ (one example) and $[TFSI]^-$ salts

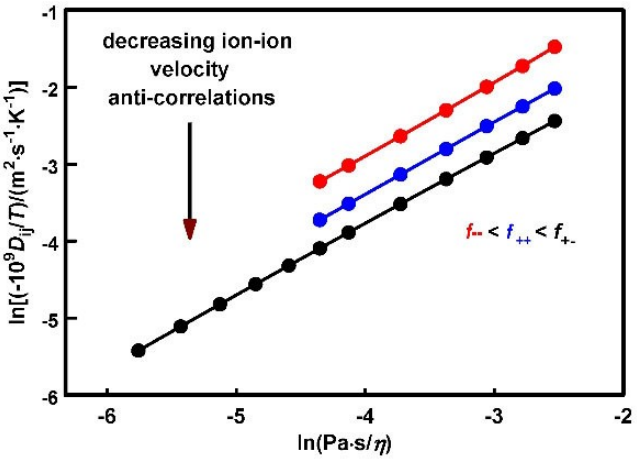

Figure 9. Plot of ln[($-D^d_{ij}/T$)/(10^{-9} $m^2 \cdot s^{-1} \cdot K^{-1}$)] vs. ln[(Pa·s)/$\eta$] for $[Pyr_{14}][TFSI]$. Redrawn from Figure 5 of Ref. [58], with corrected x-axis labelling. The D^d_{ij} are distinct diffusion coefficients, and η is the viscosity. This is analogous to a Stokes-Einstein-Sutherland plot of ln(D_{Si}/T) or a Walden plot of ln Λ against ln ($1/\eta$). The slopes are 0.96, 0.94, and 0.93 for D^d_{i-}, D^d_{++} and D^d_{+-} respectively. Symbols: blue, cation-cation; red, anion-anion; black, cation-anion. [FSI]- salts behave similarly, but for imidazolium $[BF_4]^-$and $[PF_6]^-$ salts the positions of the cation-cation and anion-anion D^d_{ij} are interchanged, that is the velocity anti-correlations are strongest for the cation-cation case.[140a,153b] High pressure isotherms (where measured) overlap with the atmospheric pressure isobar: that is, the D^d_{ij} are functions of the viscosity, not T and p per se. Reprinted with permission from Ref. [58] Copyright 2011 American Chemical Society.

(13 examples)[145,154] the order is reversed, and the anti-correlations are stronger for the anion-anion case. [emim][CH_3SO_3], [emim][CF_3SO_3], and [emim][TCB] (tetracyanoborate) also have more negative cation-cation VCC.[155] These anion effects seem to be independent of the nature of the cation.

3.1.4. Ionicity

Some authors have argued that comparison of experimental molar conductivities with those calculated from the simple Nernst-Einstein equation [Eq. (8) without the deviation parameter, Δ] is a measure of the "ionicity" of the salt, $Y = \Lambda/\Lambda_{NE} = (1-\Delta)$, that is, the degree to which it is dissociated into its component ions.[156] This hypothesis assumes that paired ions cannot contribute to the conductivity whereas self-diffusion coefficients are the sum of contributions from both paired and unpaired ions.

VCC analysis[135,146,150,153a,157] however shows that Δ is given by the departure of the cation-anion VCC from the arithmetic mean of the cation-cation and anion-anion VCC (compare [Eq. (16)]).

$$\Delta = -\frac{c\left(2\nu_c\nu_a z_c z_a f_{ca} + \nu_c^2 z_c^2 f_{cc} + \nu_a^2 z_a^2 f_{aa}\right)}{\left(\nu_c^2 z_c^2 D_{Sc} + \nu_a^2 z_a^2 D_{Sa}\right)} = \frac{c(2f_{ca} - f_{cc} - f_{aa})}{(D_{Sc}/\nu_c + D_{Sa}/\nu_a)} \quad (24)$$

So ion-pairing is not required as an explanation, as shown long ago by the molecular dynamics simulations of Hansen and MacDonald for molten NaCl where Δ is non-zero and NaCl is clearly not associated.[158] The matter is dealt with in detail in Ref. [142b].

An interesting case example is that of lithium fluorosulfonyl (trifluoromethanesulfonyl)amide (lithium [*N*-trifluoromethylsulfonyl]-sulfamoylfluoride), a component of some newly suggested battery electrolytes.[159] Kubota et al. claim (see their Figure 5) that this is truly superionic, based on self-diffusion measurements at 150 °C, that is, that the conductivity is larger than that predicted by the NE equation and hence Δ in [Eq. (8)] is negative. Unfortunately, the conductivity is not directly reported. From [Eq. (24)], this means that the VCC f_{ca} is less (more negative) than the mean of f_{cc} and f_{aa}, or, in other words, unlike-ion velocity anti-correlations override the like ion interactions. Alternatively, from [Eq. (16)], $r_{ca} < \sqrt{r_{cc} r_{aa}}$. This could be interpreted as the clustering of either ion, but structural studies are required to test this hypothesis.

An alternative approach to the calculation of "ionicity" from the Nernst-Einstein equation, used when self-diffusion coefficients are unavailable, is to compare a Walden molar-conductivity-viscosity plot with an arbitrary reference line passing through the value for aqueous KCl at 1 mol/L concentration with unit slope for units of $S \cdot cm^2 \cdot mol^{-1}$ and dPa·s (non-SI P).[160] Again it is argued that if association occurs, plots will be displaced downwards from the "ideal" line. This approach has been criticized on a number of grounds, primarily for its arbitrary nature, there being no clear reason why 1 mol/L aqueous KCl should be a model for molten salts.[161] The method incorrectly predicts that a number of molten alkali halides are "superionic", as their Walden plots lie above the KCl reference line, when they have normal Δ values lying between 0 and 0.5.[140b] Clearly this method can lead to misleading conclusions and its use should be discontinued.

3.2. Two Component Systems with a Common Anion

In such three-ion systems (cations c1 and c2, anion a) there are six transport properties describing mass and charge flow: the three self-diffusion coefficients, the inter-diffusion coefficient of the two salts (reference frame dependent), the conductivity and one independent transport number (two are defined relative to the flow of the common ion, but sum to unity). The determination of all these properties for a given system is a challenging task though advances have been made with block co-polymer electrolyte systems.[162]

Schönert[146] has given expressions for calculating the corresponding mobility and velocity cross-correlation coefficients. Activity coefficients are required in addition to the transport properties. Laity[139a] and Richter[163] have given the corresponding equations for the resistance coefficients. The cross-coefficients r_{c1a}, r_{c2a} *and* r_{c1c2} are determined by the inter-diffusion coefficient, the transport number(s) and the conductivity alone; the diagonal terms r_{c1c1}, r_{c2c2} and r_{aa} can then be determined from the self-diffusion coefficients and the cross-coefficients.

However, the limiting forms for infinite dilution of one component are simpler and may be useful. For the limiting tracer diffusion of cation c2 in salt c1a Richter found that

$$^2D_{T,c2} = \frac{2RT}{(^2r_{c1c2} + {}^2r_{c1a})} \quad (25)$$

where the preceding superscript indicates infinite dilution of ion species 2, and the subscript T indicates tracer diffusion, using Dunlop's notation.[164] As $^2r_{c1a}$ is just r_{c1a} for the pure salt and is calculable from the molar conductivity, $^2r_{c1c2}$ can be obtained as a measure of the cation-cation interactions. This approach has yet to be employed in experimental studies.

3.2.1. Experimental Measurements

The measurement of the transport properties for ionic liquids is not straightforward. Due to their high viscosity, many techniques developed for low viscosity solutions cannot be applied or must be substantially modified.

Hayamizu has recently reviewed NMR spin-echo techniques for self-diffusion measurements, also summarizing her and her colleagues' measurements on lithium salt mixtures with ionic liquids.[165] The main things to be considered are the linearity of the applied gradient; its calibration; consistency of the results with variation of the pulse parameters and the removal of eddy current effects; sample temperature homogeneity and temperature measurement; the avoidance of convection; and the

removal of any background DC bias current in the detector. Self-diffusion coefficients can also be obtained with broadband dielectric spectroscopy.[166]

As yet, inter-diffusion does not seem to have been directly measured in ionic liquid mixtures, though new dynamic light scattering techniques have been applied to mixtures of gases and molecular liquids with ionic liquids[167] and a restricted diffusion method has been applied to poly(ethylene oxide) electrolytes containing lithium salts.[168]

Conductivities are best determined by electrochemical impedance spectroscopy (EIS).[169] Measurements made with AC conductance bridges should be corrected for the frequency dependence due to polarization at the electrodes, and capacitance and inductive effects, though this is not always done.[157,170]

The determination of transport numbers is somewhat controversial. The commonly used methods are a) potentiostatic polarization[171] and galvanostatic polarization.[172] Electrophoretic NMR,[138,173] very low frequency impedance spectroscopy[174] and anion-exchange concentration cells,[175] a variant of the classical emf method,[170] have been introduced more recently. However there are doubts over the reference frames specified for some of these methods,[136,138c] care must be taken to apply the appropriate corrections,[174–176] and a comparative study[176] shows there are discrepancies yet to be properly resolved.

Very recent molecular dynamics studies by Molinari et al.[177] have attempted to include velocity cross-correlations in determining transport numbers in lithium and sodium salt mixtures with $[FSI]^-$, $[TFSI]^-$, $[BF_4]^-$ and other examples as the common anion. In each case, the transport number of the alkali cation was found to be small but negative, in the mass-fixed frame of reference, below $x(\text{Li salt}) < 0.2$, becoming positive and larger in magnitude above this value. Kubisiak et al.[177c] have published very similar molecular dynamics calculations for some of the same systems, Li/Na-[EMIM][TFSI]. However, these results appear to be subject to the same criticisms made regarding electrophoretic NMR measurements of transport numbers[136] in that it is unclear whether "external" t_i or "internal" t_i are computed. Only one ion transport number can be independently determined in a three-ion (two-component) system:[136,146,163] one defines the reference mobility (even where velocities are set relative to the that of the center of mass of the system),[142] and the other two sum to unity.

Molecular dynamics studies[178] are increasingly being used to complement experimental studies. Lorenço et al.[178f] have examined twelve lithium salt-IL mixtures based on 1-ethyl-3-methylimidazolium, (methyloxymethyl)triethylphosphonium, and tri-ethylbutylphosphonium cations, and 2-(cyano)pyrrolide, 3-(cyano)pyrrolide, 1,2,3-triazolide and 1,2,4-triazolide anions. Lithium always diffused more slowly than the IL cation and the common anion. They concluded that phosphonium triazolide based ILs showed the best potential for electrolyte applications due to higher apparent transport numbers [as given by the approximation, Eq. (11)].

Experimental diffusion studies for lithium containing systems are summarized in the Electronic Supporting Information (ESI) in Tables S1 (pyrrolidinium salts),[15b, 76c,d,178a,179] S2 (imidazolium salts),[178a,180] and S3 (phosphonium and other salts)[105,180f, g,181] Sodium containing systems[182] are listed in Table S4. Ion abbreviations used below are listed in the Table footnotes.

3.2.2. Lithium-Containing Systems

3.2.2.1. Pyrrolidinium Ionic Liquids

With increasing lithium concentration, the conductivities and ion self-diffusion coefficients decrease and the viscosity increases. The lithium ion appears to act as a "defect" in the liquid structure, analogous to an interstitial atom in an alloy. Whether SES and Walden slopes are consistent or not and the constancy or otherwise of the NE deviation parameter have been checked for only a few examples.

In almost every case, the self-diffusion coefficient of the lithium ion is less than that of the ionic liquid cation and of the common anion. This is usually attributed to solvation by the anion with lithium ion exchange between anionic complexes, giving so-called "structural diffusion"[15b,179d,e] as opposed to "vehicular diffusion" of stable complexed Li species. There is spectroscopic and other evidence for the formation of complexes,[183] though to what degree and on what timescale is less certain.[184] The (directly measured) transport number for Li^+ is quite low, around 0.15 to 0.18 in $[Pyr_{13}][FSI]$ and $[Pyr_{13}][TFSI]$.[185] One explanation advanced is that these anions and lithium can also form contact ion pairs owing to a large degree of covalency in the bonding between them.[186]

It is noteworthy that where D_s(cation) is greater than D_s(anion) in the pure ionic liquid, as in $[TFSI]^-$ and $([FTFSI]^-)$ salts (or vice versa, as in $[FSI]^-$ salts), then this order is retained in the mixtures. In many neat ionic liquids, small anions, such as $[BF_4]^-$, $[PF_6]^-$,[157] or $[B(CN)_4]^-$,[155] diffuse more slowly than the much larger cations, suggesting caging and back-scattering effects, well-known in liquid dynamics,[187] and Li^+ appears to behave in the same way. The molecular dynamics studies of the Kirchner group[178c,d] are consistent with this picture, showing "that the ionic liquids largely retain their structure upon salt addition", and that Li^+ ions are trapped in cages by the anions in the cases and compositions examined. The molecular dynamics study by Kiyobayashi et al.[188] of self-diffusion coefficients and conductivities for the mixtures $(Li_{1-x}Cs_x)CO_3$ and $(Li_{1-x}K_x)CO_3$ at 1223 K also reinforces this conclusion. In these systems $D_S(CO_3^{2-})$ is less than the self-diffusion coefficients of the cations, but with $D_S(Li^+) > D_S(Cs^+)$ or $D_S(K^+)$ only below $x(Li^+) \sim 0.6$. (This crossover is an example of the Chemla effect[189]). The analysis of the contributions of velocity cross-correlations to the conductivities in this region support the argument that the Li^+ ion is trapped by enclosing (common) anions when the lithium salt is mixed with another salt with a larger cation, which is of course, also the case in ionic liquid electrolytes.

This situation contrasts with that of neat lithium molten salts,[159,190] including Li[FSI] and Li[FTFSI],[159] where Li^+ diffuses more quickly than the anions, though the order is reversed in

rather complex borates substituted with 1,1,1,3,3,3-hexafluoro-2-propoxy or pentafluorophenoxy radicals[144a] where the high NE Δ values reported (as Watanabe "ionicities") suggest ion association. This has been confirmed by calculation of like-ion Laity resistance coefficients, which are large and negative.[144b] Similarly, in mixtures, where the cations have ether linkages in the alkyl radicals linked to the nitrogen of the pyrrolidinium, there is some evidence for the formation of aggregates containing more than one Li^+ ion.[15b,179d,e]

3.2.2.2. Imidazolium Ionic Liquids

A number of imidazolium based systems have been investigated, largely owing to the extensive database for the pure ionic liquids. Again lithium ion is always found to diffuse more slowly in the mixtures than the IL cation and the common anion. The results of Hayamizu et al.[180a] for Li[FSI]-[emim][FSI] and Li[TFSI]-[emim][TFSI] seem anomalous as the NE Δ parameter increases strongly with increasing temperature, whereas it is constant in other studies of imidazolium systems (Table S2). A number of studies[180f,g,191] have stressed that the presence of the acidic proton at the C2 position between the nitrogen atoms in the imidazolium ring makes 1,3-dialkylimidazolium salts unsuitable for use with metallic lithium[191] and suggested a number of alternatives where the C2 position is occupied by other groups. Of these, $[EtO(CH_2)_2MMI][TFSI]$ had the lowest viscosity and highest conductivity at $x(Li[TFSI]) = 0.24$.

3.2.2.3. Phosphonium Ionic Liquids

Shah et al.[181a] have examined the Li[BSCB]-$[P_{4448}]$[BScB] as a function of temperature and composition to $x = 0.2$. ^{7}Li NMR spectroscopy suggests the possibility of two Li-containing species at the highest compositions.

The work of Martins et al.[181b] on triethylpentylphosphonium ($[P_{2225}]^+$) and (2-methoxyethyl)trimethylphosphonium ($[P_{222(2O1)}]^+$) bis(trifluoromethanesulfonyl)amide mixtures with Li[TFSI] is of great interest as direct measurement of the lithium transport number by potentiostatic polarization[171] yielded the large values of 0.44 and 0.55 respectively at 25 °C. For the first mixture, the Li^+ self-diffusion coefficients are higher than the IL cation and anion coefficients, which are approximately equal at $x(Li^+) = 0.25$.

For the second, there is some scatter over the temperature range, but $D_s(Li^+)$ is generally the largest at two compositions, $x(Li^+) = 0.25$ and 0.39, with $D_s([P_{222(2O1)}]^+)$slightly larger than $D_s([TFSI]^-)$. Molecular dynamics simulations were consistent with solvation of lithium by the anion, as in other systems, but also that there was interaction between the lithium and the ether oxygen on the $[P_{222(2O1)}]^+$ cation. However, Walden plots showed that increasing lithium concentration at a fixed viscosity produced lower conductivities, more so for the $[P_{222(2O1)}]^+$ containing mixture.

The high Li^+ transport numbers and self-diffusion coefficients in these systems are very different from what is observed for other lithium salt - ionic liquid mixtures and deserve confirmation by other workers and further investigation. Chen and Forsyth[192] have argued on the basis of molecular dynamics simulations that these effects are due to "dynamic heterogeneity" with lithium atoms associated with the anions have higher electrical and diffusive mobilities than free lithium ions. However, it is unclear why this should be promoted by the presence of phosphonium cations.

3.2.2.4. Other Mixtures

Of these studies (listed in Table 2), that of Umecky et al.[181c] on Li[TFSI] + $[C_8DABCO][TFSI]$ is of interest as they showed by NMR spectroscopy and comparison with Li[TFSI] + [OMIM][TFSI] that the cation interacts with the lithium, as well as the anion. Despite this the NE Δ parameter was not altered by dissolution of Li[TFSI], ($x = 0.1$), suggesting that the lithium ion is labile.

The Torresi group[181b] have compared three tetracyanoborate systems, each at a single, dilute composition, 0.1 mol/L. Here, the anion is reported as diffusing more quickly than the IL cation in each case (contrast Ref. [155] but compare Ref. [193] the ratio appears to depend on cation size): again the Li^+ ion diffuses more slowly than either, but as there is no strong interaction with the anion, the rate is higher than in systems where there is such interaction, such as $[TFSI]^-$ salts.

Nasrabadi and Ganesan[178i] have compared Li[TFSI] salt solutions in the protic [triethylammonium][TFSI] and aprotic [triethylammonium][TFSI] in molecular dynamics simulations. They interpreted their results in terms of Li^+-anion aggregation. The Li self-diffusion coefficient was higher in the less viscous aprotic IL. They did not calculate the Li^+ transport number directly, but relied on Eq. (11), so their conclusions regarding ion mobility lack validity.

One reciprocal (three-component mixture), with four ions, $[Pyr_{13}][FSI]$ + Li[TFSI] has been examined over the composition range $0.023 < x(Li[TFSI]) < 0.42$.[194] The Walden plots were composition dependent, with the molar conductivity decreasing with increasing x(Li[TFSI]. No SES analysis was made. The NE Δ parameter was 0.5 or larger in the mixtures. Directly measured lithium transport numbers were low, consistent with the literature results for $[Pyr_{13}][FSI]$ and $[Pyr_{13}][TFSI]$ mixtures with the corresponding lithium salts.

A molecular dynamics study has been made of Li[TFSI] dissolved in a mixture of $[Pyr_{13}][TFSI]$ and 1-ethyl-3-methylimidazolium dicyanamide ([emim][DCA]).[178g]

3.2.3. Sodium-Containing Systems

Sodium-containing systems[182] are listed in Table S4. Short T_2 spin-spin relaxation times make it very difficult to measure sodium ion self-diffusion coefficients by spin-echo NMR.[182b]

Molecular dynamics studies suggest strong correlation of the sodium ion with $[FSI]^-$,[177b,195] $[TFSI]^-$,[194,196] $[FTFSI]^-$[195] and

$[PF_6]^{-}$[197] ions on the timescale of the simulations. However such simulations are very dependent on the force fields employed.[198] On the other hand, the lower solubility of sodium salts in ionic liquids in comparison with the corresponding lithium salts is argued to derive from a lesser contribution of covalent interactions between the sodium ion and the IL anions.

3.3. Summary

In brief, in the great majority of systems examined experimentally, the self-diffusion coefficient of lithium is lower than those of the ionic liquid cation and common anion. This generally taken as being due to complexation of the lithium with both structural and vehicular mechanisms, or a combination of the two, but molecular dynamics studies suggest that this is probably secondary to the effects of caging and backscattering of a very small ion surrounded by the larger anions and cations of the ionic liquid. If so, one would expect a lesser effect for sodium systems, but self-diffusion of sodium is much harder to measure. In any event, the transport of charge by lithium is constrained. Phosphonium containing systems are the major exception to this behavior and warrant further investigation.

Complementing the standard self-diffusion, viscosity and conductivity measurements by inter-diffusion and more rigorous transport number measurements should help clarify our general understanding of charge and mass transport in lithium salt -ionic liquid mixtures.

4. Structural Characterisation of Neat M(anion)$_n$ (M = Li, Na) Salts and their Binary IL Mixtures

In order to develop effective electrolyte systems, it is not only important to assess the dynamic behavior of the charge carrier species but also to learn about its static properties. It is therefore of fundamental importance to understand the state of coordination (solvation) of the electroactive species, lithium and sodium in this review, because it is correlated to the conductivity and M^+ transport number in a given electrolyte solvent system.[183a,d] A number of the traditional Li[PF_6] electrolyte systems have been characterized with regards to the coordination state of Li^+ in a molecular solvent environment commonly composed of alkyl carbonates such as EC, DMC and the like.[15a,199] A good account of these efforts was presented by Han et al.[15a] showing that, for isolated solid materials characterized by single crystal structure analysis, ionic interactions can be classified as either solvent-separated ion pair (SSIP), contact ion pair (CIP), or aggregate (AGG) coordination depending upon whether the anions form coordinate bonds with zero, one, or more than one Li^+ cations, respectively. Which kind of coordination environment is adopted by Li^+ is determined by the nature of the solvent present in the electrolyte system. Compared to conventional electrolytes, the situation in Li-salt ILELs is significantly more complex since the solvent itself is ionized and the interactions between the solute and solvent ions are strongly dependent on their relative concentrations as well as the chemical nature of the anion.[15b,183d,200] The dependency on the latter is somewhat simpler in the case of $[PF_6]^-$ compared to when sulfonylimide anions such as $[TFSI]^-$ and others are present which can act as mono- and bidentate or bridging ligands.[7b,201] This complicated situation in ILELs hampers the identification of the structural identity of Li species, and thus the factors responsible for ion mobility.[200] Saito et al.[183d,200] showed, based on NMR diffusion and computational evidence, the presence of $[Li(TFSI)_{n+1}]^{n-}$ in Li[TFSI]/[alkylmethylimidazolium][TFSI] mixed electrolytes, with the major Li species having the coordination number $(n+1)$ ~3–4. For example, Lassègues et al.[183a] concluded $CN < 2$ for the same system at mole fractions above 0.2, which is not in agreement with other studies. According to a single crystal structure analysis by Matsumoto et al.,[202] Li is coordinated by 3 and 4 anions in two different Li environments observed in solid $Li_2(emim)(TFSI)_2)_3$. Hence, it is important to emphasize that spectroscopic methods can provide insight into, but do not have the ability to directly discern, the type of Li complexes that form and their distribution.[7b,15a]

Apart from these structural considerations and owing to the anionic solvent component, the overall charge of the Li-complex in ILELs will be negative if the coordination environment constitutes more than one anion, i.e. in $[Li(TFSI)_3]^{2-}$. From an electrostatic point of view, the overall negative charge implies that such anion species would resist moving towards a negatively polarized electrode in a battery.[183d] If this picture of Li coordination is true, then a further requirement would arise at the cathode during discharge which is the process of Li leaving its coordination environment whilst moving into the electrode structure and should be facilitated by a weakly coordinating ligand environment. The notion of a weakly coordinating ligand environment would also agree with a charge transport model developed on the basis of molecular dynamics simulations by Borodin et al.,[203] where Li^+ transport in C_1mpyr-TFSI primarily occurred via TFSI-ligand exchange in the first coordination shell of Li^+ (structural-diffusion mechanism) while diffusion of whole $[Li(TFSI)_n]^{(n-1)-}$ complexes (vehicular mechanism) contribute only very little.

In the following we review structural examples of Li^+ and Na^+ coordination with a focus on imide-type anions since they display a rich coordination chemistry owing to their structure and flexibility, and because they are currently the most prevalent anions encountered in ILELs. Na^+ complexes are also considered here as intriguing examples for the breadth of coordination geometries possible as a function of the cation species which has implications for future battery chemistries beyond Li^+. Selected bond length of five Li-salts are listed in Table 5. Further, we first discuss $[M(TFSI)_n]^{(n-1)-}$ complexes before moving to the corresponding metal complexes in IL solution where remarkable changes in the coordination geometry around the metal center can occur. Although the properties of salts derived from six different imide-type anions are presented in section 2.2, our discussion of coordination environments around M^+ is confined to the salts of $[TFSI]^-$,

Table 5. Selected bond length in lithium salts of various anions.

Bond[a]	[FSI]$^-$	[TFSI]$^-$	[TfO]$^-$	[DFOB]$^-$	[BOB]$^-$
Li–O	2.12	1.95	1.82–1.89	2.02	1.94–2.1
N–S	1.556	1.557	–	–	–
S–O	1.39–1.413	1.429–1.451	1.472–1.44	–	–

[a] Bond lengths in Å.

[FSI] $^-$, [TfO]$^-$ and [MCTFSI]$^-$ anions due to the lack of other structurally characterized examples.

Before discussing $[M(TFSI)_n]^{(n-1)-}$ structures it is instructive to note that this anion can adopt two low energy conformations regarding the orientation of the two CF_3 groups, trans and cis of C2 and C1 symmetry, respectively, with the latter being significantly more prevalent when coordinated to a metal center in a chelating manner. In Li[TFSI], the Li^+ is coordinated in a slightly distorted tetrahedral fashion, but not involving chelating by the anion, instead monodentate contacts with four O atoms of four different *trans*-[TFSI]$^-$ anions are made.[204] Determination of the crystal structure for this salt also provides clear evidence for the already mentioned high degree of charge delocalization across the S–N-S backbone. The relatively short N–S distances as well as the S–N-S bond angle of 129 ° are a reflection of a high degree of double-bond character and hence the negative charge is distributed, via the double bonds, to the SO_2-CF_3 moieties, rather than being localized at the central N. Therefore, coordination involving the N-atom is rarely encountered. In terms of potential water content in ILELs it is important to note that a significant change in the coordination environment was found in the crystal structure of Li[TFSI]···H_2O where all of the six crystallographically independent Li^+ atoms are octahedrally coordinated by four O atoms from two chelating *cis*-[TFSI]$^-$ anions and one or two O atoms from H_2O molecules.[205] The crystal structure of the sodium salt of [TFSI]$^-$ consists of two crystallographically independent but similar Na^+ (Na1 and Na2) coordination environments, where the Na^+ cation has primary contacts with five O atoms and for the secondary contacts the rather rare coordination with one O atom and one N atom was found.[206] The larger sodium ion is surrounded by five [TFSI]$^-$ and two of them are coordinated in a bidentate fashion resulting in a distorted pentagonal bipyramidal environment.

By comparison, in the structure of Li[FSI] the rather uncommon, coordination number (CN) of six is adopted via oxygen coordination only but the geometry is different in the three independent Li environments.[207] Li1 displays three chelating anions in a trigonal prismatic environment. Six anions create a distorted octahedral environment around the cations in both Li2 and Li3 by acting in a mono-dentate manner. The high CN of six can be explained by the absence of bulky CF_3-groups which prevent the formation of chelates in the [TFSI]$^-$ salt.

In terms of charge delocalization and coordination strength it is interesting to compare structural data of Li–O and S–O distances as well as S–N-S distances and bond angles in Li[FSI] and Li[TFSI]. Considering the Li–O bond lengths, TFSI (1.95 Å) appears to be more strongly coordinated to Li than FSI (2.12 Å). In turn, the S–O distances are longer in Li[TFSI] (1.451-1.429 Å) and hence have less double bond character compared to the respective distances in Li[FSI] (1.39–1.413 Å). The N–S bond lengths observed in the two salts, albeit similar, are slightly shorter in Li[FSI]. The narrower S–N–S bond angle in Li[FSI] vs. Li[TFSI] is most likely related to the anion acting as a chelating ligand in Li1 combined with the absence of bulky CF_3-groups rather than small differences in S–N distances. The comparison of the crystallographic data clearly supports the notion that, with respect to Li, [FSI]$^-$ is a more weakly coordinating ligand than [TFSI]$^-$. It is unfortunate (and surprising) that single crystal structure data are not available for the Li-salts of the asymmetric anions [FTFSI]$^-$, [TSAC]$^-$ and [TFSAM]$^-$ to further elucidate the influence the relationship between structural and electronic properties of imide type anions have on their coordination behavior towards M^+. As for anhydrous Li[TFSI], a crystal structure for anhydrous Li[TfO] was determined from powder diffraction data that show Li surrounded by three anions, one of which coordinating in a bidentate fashion via two of the SO_3 group oxygens, so that Li is placed in a pseudo-tetrahedral environment.[208] Notably, two of the Li–O distances involving chelation are significantly shorter than those found in Li[TFSI], indicating the stronger coordination of Li in Li[TfO].

The single crystal structure of anhydrous Li[DCA] revealed two independent environments for Li where the ion is coordinated in an octahedral (Li1) and tetrahedral (Li2) fashion, respectively (Figure 10).[209] In Li1, coordination is afforded by two terminal and four bridging N-atoms, while in Li(2) the anion binds only via its bridging N-atom. According to bond distance and angle data, the anion, for which three Lewis structures (sp, sp^2, sp^3) are possible, exhibits a high degree of charge delocalization by adopting the sp^2 mode, where the bond character of the terminal N–C is between two and three and the bond between the central N and C is intermediate between two and one. As expected for a sp^2 mode, the bond angle at the central N is 120.6°. We note that the Li–N contacts

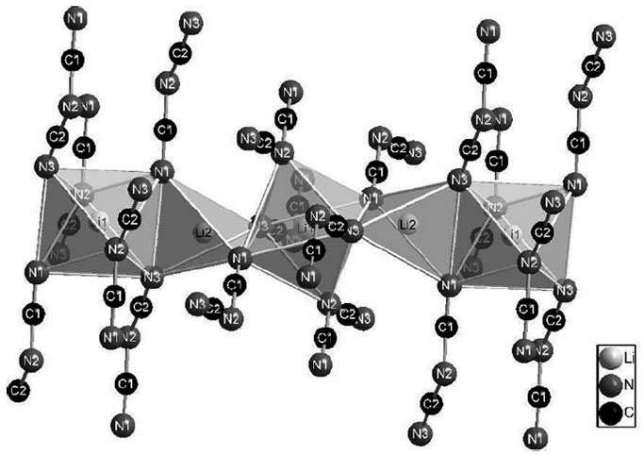

Figure 10. View perpendicular to the *c* axis at the columns built up by alternating $[(Li_1)N_6]_{17}$-octahedra and $[(Li_2)N_4]_{11}$-tetrahedra sharing common trans-oriented edges. Reprinted with permission from Ref. [209]. Copyright 2014 Wiley-VCH.

differ significantly between octahedral (2.22 Å) and tetrahedral (2.05 Å) coordination environments.

An assessment of the coordination environment of the recently reported[16d] [MCTFSI]$^-$ anion in its Li salt cannot be made because crystallographic data are not available. A comparison of Na[MCTFSI] with its [TFSI]$^-$ equivalent shows that replacement of one tetrahedral O_2S-CF_3 group by a trigonal and less electron withdrawing OC–OCH_3 group leads to significant differences in the Na coordination environment (Figure 11). Three crystallographically independent environments (Na(1), Na(2), Na(3); Figure 11, Figure S1–S3) show the unique co-ordination behavior of the anion in this salt. Na(1) is coordinated by three anions in a less-common bidentate N–O fashion via the methoxy O(4).

The geometry of the Na(1) environment is highly distorted octahedral. The S(1)–N–C(2) bond angle is a few degrees smaller than the equivalent S–N–S angle observed in Na[TFSI], due to the shorter C–O distance (1.221(3) Å) compared to S–O (1.440-(2) Å). The conformation of the anions arising from the N–O coordination in Na(1) then defines the environment in Na (2) as O–O, involving the carbonyl oxygen atom and one sulfonyl oxygen atom. Six anions are engaged in a monodentate co-ordination of the Na(3) through either the second sulfonyl oxygen or the carbonyl O(3) in an alternating fashion.

The Na–O/N coordination bonds in Na[MCTFSI] follow the order *N*-$O_{sulfonyl}$, chelate < Na-$O_{sulfonyl}$, monodentate < Na-$O_{carbonyl}$ < Na–N < Na-O_{methyl}. All of these distances are shorter than related distances in Na[TFSI], hence reflecting stronger coordination bonds and basicity for the [MCTFSI]$^-$ anion. Notably, while the distances are very similar with respect to one N-sulfonyl group, the distances in the mixed donor (N–O) chelates are significantly shorter than the secondary chelate contacts found for the less basic 5-sulfonyl moiety in Na[TFSI].

Important for the understanding of ILELs, the metal ion coordination environment undergoes significant changes when the metal salt is used to formulate binary ILELs with the same anion. This process is complex and the determination of the number of anions and their mode of interaction with the solute is further complicated by factors such as concentration and temperature dependence[7b,15b,83c,183a] and by the unresolved debate around the transport mechanism of charge carrier, vehicular vs. structure diffusion mechanism.[178a,210] While the unambiguous identification of the true nature of the metal species in solution may be difficult to achieve, a small number of reports have described the isolation of crystalline materials suitable for single crystal X-ray diffraction.[7b,202,211] It can be argued that these solids are not representative of the real solution speciation, but they are still accurately characterized compounds demonstrating what could be possible in solution; additionally, solid-state structural studies are complemented by spectroscopic analyses. The crystal structure[7b] of (1-*x*) [$C_y$mpyr][TFSI]-*x* Li[TFSI] ($x = 0.67$; $y = 4$ or 5) shows the Li coordinated by either three or four anions (Figure 12). In the former, Li adopts an all oxygen CN of 5 where two anions are chelating in their *trans* (C2-[TFSI]$^-$) and *cis* form (C1-[TFSI]$^-$), respectively and the third-[TFSI]$^-$ is acting as a monodentate ligand. In the second environment Li is tetrahedrally coordinated by oxygen atoms of four-[TFSI]$^-$ anions, two of which are in their trans and two in their cis conformation. A very different coordination environment involving bidentate oxygen coordination by two [TFSI]$^-$ in either *trans* or *cis* conformation has been proposed for more dilute solutions of Li[TFSI] in this ILEL, however based

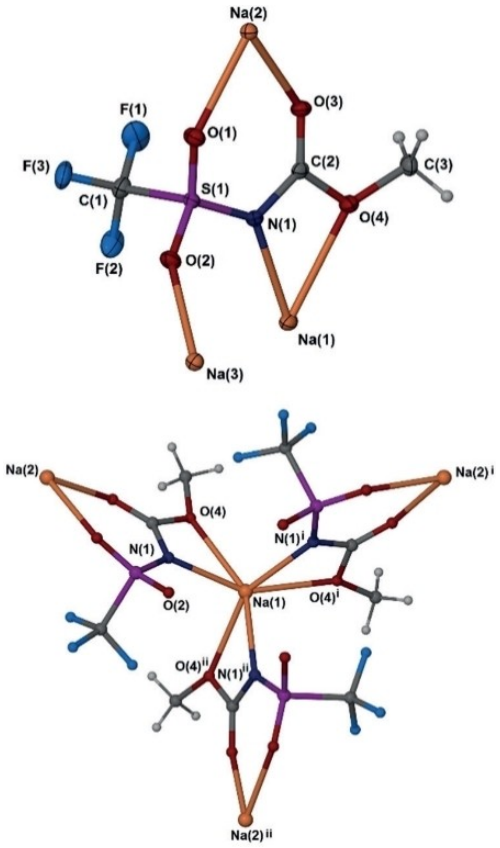

Figure 11. Top: diagram of the asymmetric unit (ASU) contents of Na[MCTFSI] with non-hydrogen atoms represented by 50% displacement ellipsoids and hydrogen atoms as spheres of arbitrary size. Note each Na atom resides on a crystallographic three-fold axis. Bottom: the coordination environment of Na(1) showing N–O chelating for each coordinating anion. Reprinted with permission from Ref. [16d]. Copyright 2019 Wiley-VCH. Representations of coordination environments Na(2) and Na(3) are provided in the Supporting Information.

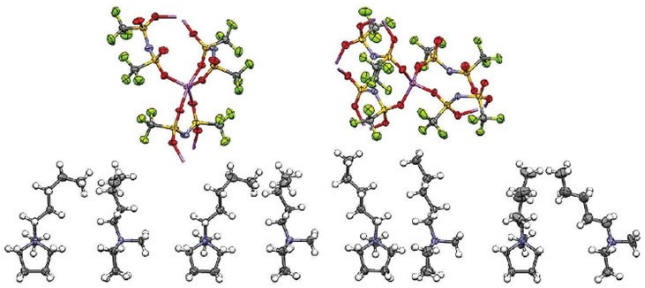

Figure 12. Examples of Li^+ cation coordination by [TFSI]$^-$ anions and the $[Pyr_{15}]^+$ cation conformations (2 views shown for each) in the crystal structure of the (1-*x*) $[Pyr_{15}][TFSI]$ – *x* Li[TFSI] ($x = 0.67$) phase (Li, purple; O, red; S, yellow; N, blue; F, green). Reprinted with permission from Ref. [7b]. Copyright 2011 American Chemical Society.

on vibrational spectroscopic data only. Two crystallographically independent Li cations were also found in Li_2[emim][N$(SO_2CF_3)_2)_3$].[202] In one environment, Li is, similar to the pyrrolidinium case, but with trigonal bipyramidal (CN 5) oxygen coordinated by two chelating $[TFSI]^-$ anions in cis conformation and one monodentate anion. In the second environment (CN 5) involving four anions only one is behaving in a bidentate *cis* conformation manner.

Crystal structures for lithium salts with the $[FSI]^-$ anion crystallized from pyrrolidinium ILs have not been reported but a structure is available[211] for Li[emim][$FSI]_2$ where Li is in an octahedral oxygen environment composed of two bidentate and two monodentate anions.

Crystal structures of lithium salts with the simple anion $[BF_4]^-$[212] as well as the chelatoborates Li[BOB][199a] and Li [DFOB][48] have been solved (Figure 13). It is interesting to see, in comparison, that Li in Li[BF_4] is only tetrahedrally coordinated by one fluorine of four $[BF_4]^-$ anions whereas it adopts higher CNs in $[BOB]^-$ (CN 5, involving four anions by three oxygens from three oxalates and two oxygens from one chelating oxalate) and $[DFOB]^-$ (CN 6, involving five anions by two fluorines from two DFOB and two oxygens from two oxalates and two oxygens from one chelating oxalate) despite the larger size of the chelatoborate anions. The lower CN in Li[BF_4] can be related to the lower basicity of the fluorine ligands compared to the more basic oxygen donor centers in the oxalate ligands. Although $[DFOB]^-$ constitutes of two F centers of low basicity, the CN in its Li salt is still higher than in Li[BOB], probably because the two oxalate rings adopt a spiro orientation in the latter which creates steric constraints on placing additional $[BOB]^-$ anions. The oxygen atoms of the spiro oriented rings are linking upper and lower lithium oxalate chains and thus occupy apical positions in the square pyramidal Li-oxygen environment of Li[BOB].[1] The bond distances between Li and the chelating carbonyl oxygens in Li [BOB] (1.94-2.1 Å) are similar to those in Li[TFSI] and slightly shorter than the respective distances in the fluoro derivative Li[DFOB] (2.02 Å), indicative of a more weakly coordinating behavior of the latter.

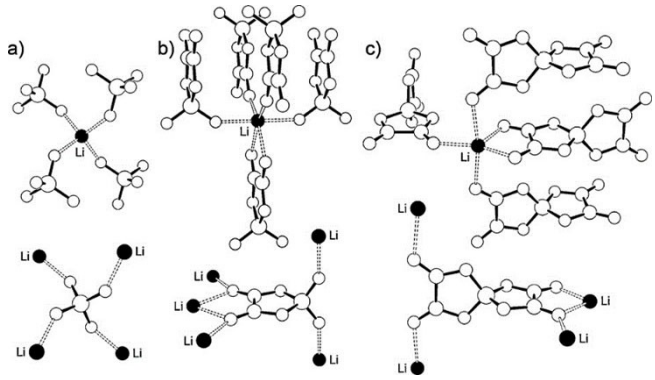

Figure 13. Li^+ cation (top) and anion (bottom) coordination in the crystal structures of (a) L[iBF_4], (b) Li[DFOB] and (c) Li[BOB]. Reprinted with permission from Ref. [48]. Copyright 2011 Elsevier.

[1] There is some confusion in the report by Allen et al.[48] where their citation [41] in the caption of their Figure 3 is intended to refer to Li[BOB] whereas it in fact cites a paper by Sharpataya et al.[213] which describes the calorimetric investigation of Li[BF_4] and its solvates. The correct reference would be Zavalij et al.[199] (their [40]). Further, the Zavalij study reports the crystal structure of Li[BOB] based on powder diffraction studies but the authors also refer to a yet to be published single crystal structure which, however, we could not find in the publication record list of M.S. Whittigham; we note that a subsequent 2004 paper was published by the same group on single crystal structures of Li[BOB]·solvates.[214]

5. Conclusions

In choosing a compound as an electrolyte in an electrochemical storage device, a number of critical constraints are placed on the physicochemical properties of that compound, with chemical and thermal stability essential, along with the promotion of high ionic conductivity. With devices featuring metallic lithium electrodes, further constraints arise in maintaining stability at extreme negative potentials. Since their first uses in this challenging domain, room temperature ionic liquids have attracted extensive consideration, with a wide variety of organic cations and anions interchanged in search of optimum performance. Two key principles that have emerged, which provided the premise for this review, are that: (i) only a small number of organic cations have characteristics at lithium reduction potentials that allow stable negative electrode behavior; (ii) the ionic liquid anion exerts the major influence over the important properties, i.e., those of most interest to battery electrochemists. Accordingly, we have focused this review on the bisalkyl pyrrolidinium compounds of the relatively small group of anions which has dominated this part of the literature.

Our initial survey of pyrrolidinium-anion ILs highlighted the significance of a combination of factors, including: low symmetry, high degree of charge delocalization, low donor number, weakly coordinating behavior, large redox potential limits, and a tendency to allow a SEI of favorable properties to form. In addition, the eventual mixture of IL and salt must prioritize the transport of lithium ions so as to maximize battery charge/discharge rate capability. Clear evidence for these property determining factors is nicely provided when examining pyrrolidinium salts derived from a series of six trifluorosulfonyl imide salts where one side of the imide anion has been systematically altered, spanning a wide range of substitutions.

The search for improved electrolyte properties has led to the creation of a number of 'sophisticated' anions, often based on simpler progenitors, and with the aim of introducing some of the characteristics known to be important. For example, the heteroleptic borate anions add asymmetry and/or more extensive charge-delocalization to simple tetrafluoroborate, to give promising candidates such as perfluoroalkylcyanofluoroborate and tetrakis(trifluromethyl)borate. These salts possess high ionic conductivity and exceptionally wide ESWs, but detailed studies on battery cycling remain to be published.

By comparison, the research effort that has been directed at the pyrrolidinium salts derived from the family of fluorosulfonyl imide anions has yielded results that have in many ways

defined the use of IL-based electrolytes in batteries. Beginning with $[TFSI]^-$, followed by systematic variation of substituents (involving $[FSI]^-$ and $[FTFSI]^-$, amongst others), research has generated some of the best battery cycling performance to date. In so doing, these studies have highlighted not only the improvements made in fundamental physicochemical properties, but have also established the crucial chemical role of the sulfonyl- and fluoro-functionalities, which underpin the formation of a stable SEI on the electrode surface. Detailed combined XPS, SEM and electrochemical studies of SEI layers formed as a result of chemical and electrochemical ion decomposition have provided good insight into their chemical composition, morphology and stability. While the garnered insight is mainly pertaining to $[PF_6]^-$, $[BF_4]^-$, $[chelatoborate]^-$ and $[imide]^-$ type anions, there is little or no information concerning other anions, notably the very interesting heteroleptic borate anions discussed in this review. The SEI formation and its nature are strongly dependent on the structure and substituents present in a given anion and therefore future research should be directed towards studies of SEI layers derived from other anion families.

While the impact of changing the structural nature of substituents of anions on the resulting properties of the respective ILs can be anticipated to some degree, the situation becomes far more complex (literally) in the presence of an electroactive cation, i.e. Li^+ and Na^+, due to their propensity of forming complexes with the anion component of the IL solvent medium. Complexation of these metals also occurs in common molecular organic solvents, which typically feature donor centers, yet in this case coordination does not change the overall charge of the resulting metal complex. The net negative charge of IL-anion – metal-ion complexes ultimately influences key electrolyte properties.

For several examples of imide and chelate-borate anions, structural characterization of metal salt complexes isolated from electrolyte mixtures has shown that the variation in coordination (solvation) around the metal center depends on both the anion structure and the original concentration of the metal salt in solution. Solvation structure and dynamics impact the rates of charge/discharge and thus the rate of the redox reactions at the solid-electrolyte interfaces in batteries. Although an important aspect of transport properties in ILELs, the structural and dynamical changes in the solvation shell surrounding M^{n+} in a multi-anion environment are poorly understood. Combined NMR diffusion, molecular dynamics simulations and Raman studies, however, suggest that the true nature of the coordination sphere of the metal ion in solution may be different from what is found in the solid state and the identification of the metal ion species in ILEL solutions is subject of debate. The solvation and transport properties of charge carriers in ILs can be modified via the presence of multiple ions with varying degrees of coordination, which provides an approach to impact the performance in electrochemical processes. Despite the macroscopic effects (conductivity, viscosity, T_g, etc.) of a changing coordination environment being measurable, there is more controversy then agreement regarding the actual mechanism by which the charge carrier is transported through the electrolyte; vehicular vs. exchange mechanism (see below). For example, the same group which initially advocated for an exchange mechanism later revised their opinion, all based on MD studies. It appears from the literature that agreement cannot be achieved based on MD studies and that experimental evidence cannot be gained from Raman studies alone since the obtained spectral patterns are too complex to be interpreted with sufficient confidence due to the structural and conformational complexity of many anion candidates. From a coordination chemistry point of view and considering that the 'top-candidate' anions are all weakly coordinating, ligand exchange processes involving free and binding anions appears to play an important role as already suggested by Niu et al. In this regard and as discussed at the outset of this review, we suggest to determine donor numbers in ILs of already existing anions (few data are currently available) and further developments. In almost all transport studies of lithium salt-based ILELs it has been shown that the self-diffusion coefficient of the lithium ion is less than that of the ionic liquid cation and of the common anion. This is usually attributed to a mechanism involving solvation by the anion with lithium ion exchange between anionic complexes, termed "structural diffusion" as opposed to a "vehicular" mechanism where Li moves with the whole coordination sphere. However caging of such a small ion by bulkier IL solvent ions also needs to be considered. Deeper investigation of coordination chemistry occurring in ionic liquid electrolyte formulations is needed as there is presently no coherent picture of the solvation/desolvation mechanism. How this can be achieved depends on the availability of suitable spectroscopic methods that are element sensitive and can distinguish between various coordination modes at the metal center, preferably on a time-resolved basis in the likely case that ligand exchange processes are involved. Ideally, such methodology could also be designed to probe, in situ, processes occurring at the electrode electrolyte interface when disruption of the solvation sphere must occur upon insertion of the electroactive species into the electrode structure.

One of the properties limiting the application of ILELs in battery devices is their low temperature conductivity. Although several anions have been developed which, in combination with sufficiently stable cations such as pyrrolidinums and phosphoniums, give ILs with much improved conductivities, there is still much debate about the accurate measurement of transport numbers for the charge carrier.

Another barrier for the adoption of ILELs may be simply economics. Currently, the price for Li[FSI] (from China, approx. \$US 300–500 kg^{-1}) does not compare favorably with that of Li $[PF_6]$ (99% grade from China, approx. \$US 50 kg^{-1}). Therefore, it would be desirable to develop more economic synthetic procedures for imide-type and other salts. However, the market price may change once patent families have expired.

To date the most promising anions for ionic liquid electrolyte formulations are the imides $[TFSI]^-$, $[FSI]^-$ and, notably the respective asymmetric hybrid anion $[FTFSI]^-$ which, by combining the benefits of its sister anions, gives ILs with exceptional properties. Amongst heteroleptic borate anions, the perfluor-

ocyanofluroborates have outstanding properties. Their performance in battery cycling remains to be seen.

Acknowledgements

Many thanks go to Dr Marzieh Barghamadi for expertly revising the manuscript. We also like to thank other researchers in our group and collaborators for their great efforts and research contributions over the years: Drs. Marzieh Barghamadi, Andrew Basil, Junhua Huang, Mitsuhiro Kanakubo (AIST, Japan), George H. Lane, Jansen Lauw, Peter Mahon (Swinburne University, Australia), Mustafa Musameh, Youssof Shekibi, T. J. Simons, Graeme Snook, Theo Rodopoulos, Jean-Pierre Veder the late Lawrie Woolf (UNSW, Australia), H. Yoon and Mr(s) Kaitlyn Gunderson-Briggs, Mike Horne, Thuy D. Huynh, Pon Kao, Arek P. Levandowski, Oliver Pohl. Financial support for our research from several CSIRO Business Units, is greatly acknowledged.

Conflict of Interest

The authors declare no conflict of interest.

[1] J. S. Wilkes, M. J. Zaworotko, *J. Chem. Soc. Chem. Commun.* **1992**, 965–967.
[2] P. Walden, *Bull. Acad. Imp. Sci. St.-Petersbourg* **1914**, *8*, 405–422.
[3] N. V. Plechkova, K. R. Seddon, *Chem. Soc. Rev.* **2008**, *37*, 123–150.
[4] a) J. L. Anthony, J. D. Holbrey, E. J. Maginn, R. A. Mantz, R. D. Rogers, P. C. Trulove, A. E. Visser, T. Welton, in *Ionic Liquids in Synthesis*, (Eds.: P. Wassersheid, T. Welton), Wiley-VCH Verlag GmbH & Co. KGaA, Weinheim, **2003**, Chapt. 3; b) H. Ohno, *Bull. Chem. Soc. Jpn.* **2006**, *79*, 1665–1680; c) M. C. Buzzeo, R. G. Evans, R. G. Compton, *ChemPhysChem* **2004**, *5*, 1106–1120.
[5] a) D. R. MacFarlane, N. Tachikawa, M. Forsyth, J. M. Pringle, P. C. Howlett, G. D. Elliott, J. H. Davis, M. Watanabe, P. Simon, C. A. Angell, *Energy Environ. Sci.* **2014**, *7*, 232–250; b) G. Gebresilassie Eshetu, M. Armand, B. Scrosati, S. Passerini, *Angew. Chem. Int. Ed.* **2014**, *53*, 13342–13359; *Angew. Chem.* **2014**, *126*, 13558–13576.
[6] K. Xu, *Chem. Rev.* **2004**, *104*, 4303-4418.
[7] a) M. Watanabe, M. L. Thomas, S. Zhang, K. Ueno, T. Yasuda, K. Dokko, *Chem. Rev.* **2017**, *117*, 7190–7239; b) Q. Zhou, P. D. Boyle, L. Malpezzi, A. Mele, J.-H. Shin, S. Passerini, W. A. Henderson, *Chem. Mater.* **2011**, *23*, 4331–4337.
[8] G. A. Giffin, A. Moretti, S. Jeong, K. Pilar, M. Brinkkotter, S. G. Greenbaum, M. Schönhoff, S. Passerini, *ChemSusChem* **2018**, *11*, 1981–1989.
[9] M. D. Tikekar, S. Choudhury, Z. Tu, L. A. Archer, *Nat. Energy* **2016**, *1*, 16114.
[10] a) M. Barghamadi, A. S. Best, A. I. Bhatt, A. F. Hollenkamp, M. Musameh, R. J. Rees, T. Rüther, *Energy Environ. Sci.* **2014**, *7*, 3902–3920; b) M. Barghamadi, A. S. Best, A. I. Bhatt, A. F. Hollenkamp, P. J. Mahon, M. Musameh, T. Rüther, *J. Power Sources* **2015**, *295*, 212–220; c) S. Xiong, M. Regula, D. Wang, J. Song, *Electrochem. Energy Rev.* **2018**, *1*, 388–402.
[11] J. Christensen, P. Albertus, R. S. Sanchez-Carrera, T. Lohmann, B. Kozinsky, R. Liedtke, J. Ahmed, A. Kojic, *J. Electrochem. Soc.* **2011**, *159*, R1-R30.
[12] a) S.-J. Tan, X.-X. Zeng, Q. Ma, X.-W. Wu, Y.-G. Guo, *Electrochem. Energy Rev.* **2018**, *1*, 113–138; b) H. Zhang, J. Zhang, J. Ma, G. Xu, T. Dong, G. Cui, *Electrochem. Energy Rev.* **2019**, *2*, 128–148; c) B. P. Thapaliya, C.-L. Do-Thanh, C. J. Jafta, R. Tao, H. Lyu, A. Y. Borisevich, S. -Z Yang, X.-G. Sun, S. Dai, *Batteries & Supercaps* **2019**, *2*, 985–991; d) B. P. Thapaliya, I. Popov, S. Dai, *ACS Appl. Energy Mater.* **2020**, *3*, 1265–1270.
[13] J. M. Slattery, C. Daguenet, P. J. Dyson, T. J. S. Schubert, I. Krossing, *Angew. Chem. Int. Ed.* **2007**, *46*, 5384–5388; *Angew. Chem.* **2007**, *119*, 5480–5484.
[14] H. Matsumoto, H. Sakaebe, K. Tatsumi, *ECS Trans.* **2009**, *16*, 59–66.
[15] a) S.-D. Han, S.-H. Yun, O. Borodin, D. M. Seo, R. D. Sommer, V. G. Young, W. A. Henderson, *J. Phys. Chem. C* **2015**, *119*, 8492–8500; b) F. Castiglione, E. Ragg, A. Mele, G. B. Appetecchi, M. Montanino, S. Passerini, *J. Phys. Chem. Lett.* **2011**, *2*, 153–157; c) C. Zhang, K. Ueno, A. Yamazaki, K. Yoshida, H. Moon, T. Mandai, Y. Umebayashi, K. Dokko, M. Watanabe, *J. Phys. Chem. B* **2014**, *118*, 5144–5153.
[16] a) A. Ponrouch, D. Monti, A. Boschin, B. Steen, P. Johansson, M. R. Palacín, *J. Mater. Chem. A* **2015**, *3*, 22–42; b) R. Younesi, G. M. Veith, P. Johansson, K. Edström, T. Vegge, *Energy Environ. Sci.* **2015**, *8*, 1905–1922; c) E. Jónsson, M. Armand, P. Johansson, *Phys. Chem. Chem. Phys.* **2012**, *14*, 6021–6025; d) K. E. Gunderson-Briggs, T. Rüther, A. S. Best, M. Kar, C. Forsyth, E. I. Izgorodina, D. R. MacFarlane, A. F. Hollenkamp, *Angew. Chem. Int. Ed.* **2019**, *58*, 4390–4394; e) P. Johansson, L. E. Fast, A. Matic, G. B. Appetecchi, S. Passerini, *J. Power Sources* **2010**, *195*, 2074–2076.
[17] a) Z. Xue, L. Qin, J. Jiang, T. Mu, G. Gao, *Phys. Chem. Chem. Phys.* **2018**, *20*, 8382–8402; b) A. B. Rupp, I. Krossing, *Acc. Chem. Res.* **2015**, *48*, 2537–2546; c) E. I. Izgorodina, M. Forsyth, D. R. MacFarlane, *Aus. J. Chem.* **2007**, *60*, 15–20.
[18] a) H. Matsumoto, N. Terasawa, T. Umecky, S. Tsuzuki, H. Sakaebe, K. Asaka, K. Tatsumi, *Chem. Lett.* **2008**, *37*, 1020–1021; b) H. Matsumoto, H. Sakaebe, K. Tatsumi, *J. Power Sources* **2005**, *146*, 45–50; c) A. I. Bhatt, P. Kao, A. S. Best, A. F. Hollenkamp, *J. Electrochem. Soc.* **2013**, *160*, A1171-A1180; d) A. Basile, A. I. Bhatt, A. P. O'Mullane, *Electrochim. Acta* **2016**, *215*, 19–28.
[19] P. C. Howlett, D. R. MacFarlane, A. F. Hollenkamp, *Electrochem. Solid-State Lett.* **2004**, *7*, A97-A101.
[20] a) D. R. MacFarlane, P. Meakin, J. Sun, N. Amini, M. Forsyth, *J. Phys. Chem. B* **1999**, *103*, 4164–4170; b) G. B. Appetecchi, M. Montanino, D. Zane, M. Carewska, F. Alessandrini, S. Passerini, *Electrochim. Acta* **2009**, *54*, 1325–1332; c) H. Sakaebe, H. Matsumoto, *Electrochem. Commun.* **2003**, *5*, 594–598.
[21] a) N. V. Ignat'ev, U. Welz-Biermann, A. Kucheryna, G. Bissky, H. Willner, *J. Fluorine Chem.* **2005**, *126*, 1150–1159; b) N. V. Ignat'ev, M. Finze, J. A. P. Sprenger, C. Kerpen, E. Bernhardt, H. Willner, *J. Fluorine Chem.* **2015**, *177*, 46–54; c) D. Bejan, N. Ignat'ev, H. Willner, *J. Fluorine Chem.* **2010**, *131*, 325–332.
[22] a) P. Johansson, *Phys. Chem. Chem. Phys.* **2007**, *9*, 1493–1498; b) J. Golding, N. Hamid, D. R. MacFarlane, M. Forsyth, C. Forsyth, C. Collins, J. Huang, *Chem. Mater.* **2001**, *13*, 558–564; c) D. R. MacFarlane, S. A. Forsyth, J. Golding, G. B. Deacon, *Green Chem.* **2002**, *4*, 444–448.
[23] K. Seppelt, *Angew. Chem. Int. Ed.* **1993**, *32*, 1025–1027.
[24] S. H. Strauss, *Chem. Rev.* **1993**, *93*, 927–942.
[25] a) M. Schmeisser, P. Illner, R. Puchta, A. Zahl, R. van Eldik, *Chem. Eur. J.* **2012**, *18*, 10969–10982; b) M. Holzweber, R. Lungwitz, D. Doerfler, S. Spange, M. Koel, H. Hutter, W. Linert, *Chem. Eur. J.* **2013**, *19*, 288–293.
[26] Y. Marcus, *Chem. Soc. Rev.* **1993**, *22*, 409–416.
[27] S. Bulut, P. Klose, M. M. Huang, H. Weingartner, P. J. Dyson, G. Laurenczy, C. Friedrich, J. Menz, K. Kummerer, I. Krossing, *Chem. Eur. J.* **2010**, *16*, 13139–13154.
[28] Z. B. Zhou, H. Matsumoto, K. Tatsumi, *Chem. Eur. J.* **2006**, *12*, 2196–2212.
[29] O. J. Curnow, M. I. J. Polson, K. J. Walst, R. Yunis, *RSC Adv.* **2018**, *8*, 28313–28322.
[30] S. Forsyth, J. Golding, D. R. MacFarlane, M. Forsyth, *Electrochim. Acta* **2001**, *46*, 1753–1757.
[31] O. Stolarska, H. Rodríguez, M. Smiglak, *Fluid Phase Equilib.* **2016**, *408*, 1–9.
[32] a) D. R. MacFarlane, M. Forsyth, *Adv. Mater.* **2001**, *13*, 957–966; b) J. M. Pringle, P. C. Howlett, D. R. MacFarlane, M. Forsyth, *J. Mater. Chem. A* **2010**, *20*, 2056–2062; c) J. M. Pringle, *Phys. Chem. Chem. Phys.* **2013**, *15*, 1339–1351.
[33] A. M. O'Mahony, D. S. Silvester, L. Aldous, C. Hardacre, R. G. Compton, *J. Chem. Eng. Data* **2008**, *53*, 2884–2891.
[34] L. Jin, P. Howlett, J. Efthimiadis, M. Kar, D. MacFarlane, M. Forsyth, *J. Mater. Chem.* **2011**, *21*, 10171-10178 .
[35] Y. Shekibi, T. Rüther, J. Huang, A. F. Hollenkamp, *Phys. Chem. Chem. Phys.* **2012**, *14*, 4597–4604.
[36] a) J. Kalhoff, G. Gebresilassie Eshetu, D. Bresser, S. Passerini, *ChemSusChem* **2015**, *8*, 2154–2175; b) V. Sharova, A. Moretti, T. Diemant, A. Varzi, R. J. Behm, S. Passerini, *J. Power Sources* **2018**, *375*, 43–52.
[37] a) M. Stich, M. Göttlinger, M. Kurniawan, U. Schmidt, A. Bund, *J. Phys. Chem. C* **2018**, *122*, 8836–8842; b) C. G. Barlowz, *Electrochem. Solid-State Lett.* **1999**, *2*, 362–364.

[38] a) L. Terborg, S. Weber, F. Blaske, S. Passerini, M. Winter, U. Karst, S. Nowak, *J. Power Sources* **2013**, *242*, 832–837; b) J. Vetter, P. Novák, M. R. Wagner, C. Veit, K. C. Möller, J. O. Besenhard, M. Winter, M. Wohlfahrt-Mehrens, C. Vogler, A. Hammouche, *J. Power Sources* **2005**, *147*, 269–281.
[39] H. Yang, G. V. Zhuang, P. N. Ross, *J. Power Sources* **2006**, *161*, 573–579.
[40] K. S. Gavritchev, G. A. Sharpataya, A. A. Smagin, E. N. Malyi, V. A. Matyukha, *J. Therm. Anal. Calorim.* **2003**, *73*, 71–83.
[41] A. Mauger, C. M. Julien, A. Paolella, M. Armand, K. Zaghib, *Mater. Sci. Eng. R* **2018**, *134*, 1–21.
[42] S. P. Ong, O. Andreussi, Y. Wu, N. Marzari, G. Ceder, *Chem. Mater.* **2011**, *23*, 2979–2986.
[43] a) M. C. Kroon, W. Buijs, C. J. Peters, G.-J. Witkamp, *Thermochim. Acta* **2007**, *465*, 40–47; b) C. Maton, N. De Vos, C. V. Stevens, *Chem. Soc. Rev.* **2013**, *42*, 5963–5977.
[44] T. J. Simons, P. M. Bayley, Z. Zhang, P. C. Howlett, D. R. MacFarlane, L. A. Madsen, M. Forsyth, *J. Phys. Chem. B* **2014**, *118*, 4895–4905.
[45] H. Yoon, G. H. Lane, Y. Shekibi, P. C. Howlett, M. Forsyth, A. S. Best, D. R. MacFarlane, *Energy Environ. Sci.* **2013**, *6*, 979-986.
[46] a) S. M. Ivanova, B. G. Nolan, Y. Kobayashi, S. M. Miller, O. P. Anderson, S. H. Strauss, *Chem. Eur. J.* **2001**, *7*, 503–510; b) S. Tsujioka, B. G. Nolan, H. Takase, B. P. Fauber, S. H. Strauss, *J. Electrochem. Soc.* **2004**, *151*, A1418-A1423.
[47] I. Raabe, K. Wagner, K. Guttsche, M. Wang, M. Grätzel, G. Santiso-Quinones, I. Krossing, *Chem. Eur. J.* **2009**, *15*, 1966–1976.
[48] J. L. Allen, S.-D. Han, P. D. Boyle, W. A. Henderson, *J. Power Sources* **2011**, *196*, 9737–9742.
[49] H.-B. Han, S.-S. Zhou, D.-J. Zhang, S.-W. Feng, L.-F. Li, K. Liu, W.-F. Feng, J. Nie, H. Li, X.-J. Huang, *J. Power Sources* **2011**, *196*, 3623–3632.
[50] T. Schedlbauer, U. C. Rodehorst, C. Schreiner, H. J. Gores, M. Winter, *Electrochim. Acta* **2013**, *107*, 26–32.
[51] L. Qiao, Z. Cui, B. Chen, G. Xu, Z. Zhang, J. Ma, H. Du, X. Liu, S. Huang, K. Tang, S. Dong, X. Zhou, G. Cui, *Chem. Sci.* **2018**, *9*, 3451–3458.
[52] K. Hayamizu, *J. Chem. Eng. Data* **2012**, *57*, 2012–2017.
[53] R. Kalb, A. Kraynov, in *WO 2013/113452 Al* (Ed.: W. I. P. Organization), **2013**.
[54] P. T. Hennig, J. A. P. Sprenger, L. N. Schneider, N. V. Ignat'ev, M. Finze, *Chem. Commun.* **2019**, *55*, 6110–6113.
[55] J. Foropoulos, D. D. DesMarteau, *Inorg. Chem.* **1984**, *23*, 3720–3723.
[56] D. Benrabah, D. Baril, J.-Y. Sanchez, M. Armand, G. G. Gard, *J. Chem. Soc. Faraday Trans.* **1993**, *89*, 355–359.
[57] a) Y. Choquette, G. Brisard, M. Parent, D. Brouillette, G. Perron, J. E. Desnoyers, M. Armand, D. Gravel, N. Slougui, *J. Electrochem. Soc.* **1998**, *145*, 3500–3507; b) L. A. Dominey, V. R. Koch, T. J. Blakley, *Electrochim. Acta* **1992**, *37*, 1551–1554; c) A. Webber, *J. Electrochem. Soc.* **1991**, *138*, 2586–2590.
[58] K. R. Harris, L. A. Woolf, M. Kanakubo, T. Rüther, *J. Chem. Eng. Data* **2011**, *56*, 4672–4685.
[59] R. E. Del Sesto, T. M. McCleskey, C. Macomber, K. C. Ott, A. T. Koppisch, G. A. Baker, A. K. Burrell, *Thermochim. Acta* **2009**, *491*, 118–120.
[60] a) J. G. Huddleston, A. E. Visser, W. M. Reichert, H. D. Willauer, G. A. Broker, R. D. Rogers, *Green Chem.* **2001**, *3*, 156–164; b) W. H. Awad, J. W. Gilman, M. Nyden, R. H. Harris, T. E. Sutto, J. Callahan, P. C. Trulove, H. C. DeLong, D. M. Fox, *Thermochim. Acta* **2004**, *409*, 3–11; c) H. L. Ngo, K. LeCompte, L. Hargens, A. B. McEwen, *Thermochim. Acta* **2000**, *357–358*, 97–102.
[61] T. J. Wooster, K. M. Johanson, K. J. Fraser, D. R. MacFarlane, J. L. Scott, *Green Chem.* **2006**, *8*, 691–696.
[62] Y. Katayama, T. Morita, M. Yamagata, T. Miura, *Electrochemistry* **2003**, *71*, 1033–1035.
[63] H. Matsumoto, H. Kageyama, Y. Miyazaki, *Electrochemistry* **2003**, *71*, 1058–1060.
[64] a) P. C. Howlett, N. Brack, A. F. Hollenkamp, M. Forsyth, D. R. MacFarlane, *J. Electrochem. Soc.* **2006**, *153*, A595-A606; b) L. Zhao, J.-I. Yamaki, M. Egashira, *J. Power Sources* **2007**, *174*, 352–358.
[65] a) H. Sakaebe, H. Matsumoto, K. Tatsumi, *Electrochim. Acta* **2007**, *53*, 1048–1054; b) S. Seki, Y. Mita, H. Tokuda, Y. Ohno, Y. Kobayashi, A. Usami, M. Watanabe, N. Terada, H. Miyashiro, *Electrochem. Solid-State Lett.* **2007**, *10*, A237-A240; c) J.-H. Shin, W. A. Henderson, S. Passerini, *Electrochem. Solid-State Lett.* **2005**, *8*, A125-A127; d) J. H. Shin, W. A. Henderson, G. B. Appetecchi, F. Alessandrini, S. Passerini, *Electrochim. Acta* **2005**, *50*, 3859–3865.
[66] a) F. N. Sayed, M.-T. F. Rodrigues, K. Kalaga, H. Gullapalli, P. M. Ajayan, *ACS Appl. Mater. Interfaces* **2017**, *9*, 43623–43631; b) K. Matsumoto, K. Inoue, K. Nakahara, R. Yuge, T. Noguchi, K. Utsugi, *J. Power Sources* **2013**, *231*, 234–238.
[67] B. Garcia, M. Armand, *J. Power Sources* **2004**, *132*, 206–208.
[68] R. Appel, G. Eisenhauer, *Chem. Ber.* **1962**, *95*, 246-248..
[69] M. Beran, J. Příhoda, *Z. Anorg. Allg. Chem.* **2005**, *631*, 55–59.
[70] K. Kubota, T. Nohira, T. Goto, R. Hagiwara, *Electrochem. Commun.* **2008**, *10*, 1886–1888.
[71] M. Kerner, N. Plylahan, J. Scheers, P. Johansson, *RSC Adv.* **2016**, *6*, 23327–23334.
[72] J. Huang, A. F. Hollenkamp, *J. Phys. Chem. C* **2010**, *114*, 21840–21847.
[73] C. Michot, M. Armand, M. Gautier, N. Ravet, in *WO 99/40025* (Ed.: PCT), **1999**.
[74] H. Matsumoto, H. Sakaebe, K. Tatsumi, M. Kikuta, E. Ishiko, M. Kono, *J. Power Sources* **2006**, *160*, 1308–1313.
[75] Q. Zhou, W. A. Henderson, G. B. Appetecchi, M. Montanino, S. Passerini, *J. Phys. Chem. B* **2008**, *112*, 13577–13580.
[76] a) A. I. Bhatt, A. S. Best, J. Huang, A. F. Hollenkamp, *J. Electrochem. Soc.* **2010**, *157*, A66-A74; b) A. S. Best, A. I. Bhatt, A. F. Hollenkamp, *J. Electrochem. Soc.* **2010**, *157*, A903-A911; c) T. Rüther, M. Kanakubo, A. S. Best, K. R. Harris, *Phys. Chem. Chem. Phys.* **2017**, *19*, 10527–10542; d) H. Yoon, A. S. Best, M. Forsyth, D. R. MacFarlane, P. C. Howlett, *Phys. Chem. Chem. Phys.* **2015**, *17*, 4656–4663.
[77] M. Kunze, S. Jeong, G. B. Appetecchi, M. Schönhoff, M. Winter, S. Passerini, *Electrochim. Acta* **2012**, *82*, 69–74.
[78] G. B. Appetecchi, M. Montanino, A. Balducci, S. F. Lux, M. Winterb, S. Passerini, *J. Power Sources* **2009**, *192*, 599–605.
[79] H.-B. Han, K. Liu, S.-W. Feng, S.-S. Zhou, W.-F. Feng, J. Nie, H. Li, X.-J. Huang, H. Matsumoto, M. Armand, Z.-B. Zhou, *Electrochim. Acta* **2010**, *55*, 7134–7144.
[80] K. Liu, Y.-X. Zhou, H.-B. Han, S.-S. Zhou, W.-F. Feng, J. Nie, H. Li, X.-J. Huang, M. Armand, Z.-B. Zhou, *Electrochim. Acta* **2010**, *55*, 7145–7151.
[81] I. A. Shkrob, T. W. Marin, Y. Zhu, D. P. Abraham, *J. Phys. Chem. C* **2014**, *118*, 19661–19671.
[82] A. Basile, A. F. Hollenkamp, A. I. Bhatt, A. P. O'Mullane, *Electrochem. Commun.* **2013**, *27*, 69–72.
[83] a) J. Reiter, S. Jeremias, E. Paillard, M. Winter, S. Passerini, *Phys. Chem. Chem. Phys.* **2013**, *15*, 2565–2571; b) A. Moretti, S. Jeong, G. A. Giffin, S. Jeremias, S. Passerini, *J. Power Sources* **2014**, *269*, 645–650; c) G. A. Giffin, N. Laszczynski, S. Jeong, S. Jeremias, S. Passerini, *J. Phys. Chem. C* **2013**, *117*, 24206–24212.
[84] A. S. Shaplov, E. I. Lozinskaya, P. S. Vlasov, S. M. Morozova, D. Y. Antonov, P.-H. Aubert, M. Armand, Y. S. Vygodskii, *Electrochim. Acta* **2015**, *175*, 254–260.
[85] J.-P. Hoffknecht, M. Drews, X. He, E. Paillard, *Electrochim. Acta* **2017**, *250*, 25–34.
[86] A. Lewandowski, A. Świderska-Mocek, *J. Power Sources* **2009**, *194*, 601–609.
[87] a) H. Matsumoto, H. Kageyama, Y. Miyazaki, *Chem. Commun.* **2002**, 1726–1727; b) H. Matsumoto, H. Sakaebe, K. Tatsumi, *J. Power Sources* **2005**, *146*, 45–50.
[88] M. Armand, M. Gauthier, D. Muller, *WO88/03331* **1988**.
[89] a) N. V. Ignat'ev, P. Barthen, A. Kucheryna, H. Willner, P. Sartori, *Molecules* **2012**, *17*, 5319-5338 ; b) M. Moreno, M. Montanino, M. Carewska, G. B. Appetecchi, S. Jeremias, S. Passerini, *Electrochim. Acta* **2013**, *99*, 108–116.
[90] N. M. Ignatyev, M. Schulte, K. Kawata, T. Goto, E. Bernhardt, V. Bernhardt-Pitchougina, H. Willner, *WO 2012/163489 A* **2012**.
[91] W. Xu, C. A. Angell, *Electrochem. Solid-State Lett.* **2001**, *4*, E1-E4.
[92] K. Xu, U. Lee, S. S. Zhang, T. R. Jow, *J. Electrochem. Soc.* **2004**, *151*, A2106-A2112.
[93] K. Xu, S. Zhang, T. R. Jow, W. Xu, C. A. Angell, *Electrochem. Solid-State Lett.* **2002**, *5*, A26-A29.
[94] W. Xu, L.-M. Wang, R. A. Nieman, C. A. Angell, *J. Phys. Chem. B* **2003**, *107*, 11749–11756.
[95] S. I. Lall-Ramnarine, J. Hatcher, A. Castano, M. Thomas, J. Wishart, *ECS Trans.* **2010**, *33*, 659–665.
[96] S. Shui Zhang, *Electrochem. Commun.* **2006**, *8*, 1423–1428.
[97] H. Gao, Z. Zhang, Y. Lai, J. Li, Y. Liu, *J. Cent. South Univ. Technol.* **2008**, *15*, 830-834.
[98] a) Z. Chen, J. Liu, K. Amine, *Electrochem. Solid-State Lett.* **2007**, *10*, A45-A47; b) A. Xiao, L. Yang, B. L. Lucht, S.-H. Kang, D. P. Abraham, *J. Electrochem. Soc.* **2009**, *156*, A318-A327; c) S. S. Zhang, *J. Power Sources* **2007**, *163*, 713–718; d) S. H. Kang, D. P. Abraham, A. Xiao, B. L. Lucht, *J. Power Sources* **2008**, *175*, 526–532.

[99] M. Kunze, S. Jeong, E. Paillard, M. Winter, S. Passerini, *J. Phys. Chem. C* **2010**, *114*, 12364–12369.
[100] a) A. Lex-Balducci, R. Schmitz, R. W. Schmitz, R. A. Müller, M. Amereller, D. Moosbauer, H. J. Gores, M. Winter, *ECS Trans.* **2010**, *25*, 13–17; b) S. Zugmann, D. Moosbauer, M. Amereller, C. Schreiner, F. Wudy, R. Schmitz, R. Schmitz, P. Isken, C. Dippel, R. Müller, M. Kunze, A. Lex-Balducci, M. Winter, H. J. Gores, *J. Power Sources* **2011**, *196*, 1417–1424.
[101] J. L. Allen, D. W. McOwen, S. A. Delp, E. T. Fox, J. S. Dickmann, S.-D. Han, Z.-B. Zhou, T. R. Jow, W. A. Henderson, *J. Power Sources* **2013**, *237*, 104–111.
[102] a) Z.-B. Zhou, M. Takeda, M. Ue, *J. Fluorine Chem.* **2003**, *123*, 127–131; b) J. Landmann, J. A. P. Sprenger, P. T. Hennig, R. Bertermann, M. Grüne, F. Würthner, N. V. Ignat'ev, M. Finze, *Chem. Eur. J.* **2018**, *24*, 608–623; c) L. A. Bischoff, M. Drisch, C. Kerpen, P. T. Hennig, J. Landmann, J. A. P. Sprenger, R. Bertermann, M. Grüne, Q. Yuan, J. Warneke, X. B. Wang, N. V. Ignat'ev, M. Finze, *Chem. Eur. J.* **2019**, *25*, 3560–3574.
[103] Z. B. Zhou, H. Matsumoto, K. Tatsumi, *Chem. Eur. J.* **2005**, *11*, 752–766.
[104] a) E. Bernhardt, M. Finze, H. Willner, *Z. Anorg. Allg. Chem.* **2003**, *629*, 1229–1234; b) J. A. P. Sprenger, C. Kerpen, N. Ignat'ev, M. Finze, *J. Fluorine Chem.* **2018**, *206*, 54–60.
[105] N. Sanchez-Ramirez, V. L. Martins, R. A. Ando, F. F. Camilo, S. M. Urahata, M. C. C. Ribeiro, R. M. Torresi, *J. Phys. Chem. B* **2014**, *118*, 8772–8781.
[106] G. Pawelke, H. Willner, *Z. Anorg. Allg. Chem.* **2005**, *631*, 759–762.
[107] J. Geier, G. Pawelke, H. Willner, *Inorg. Chem.* **2006**, *45*, 6549–6554.
[108] M. K. Schmidt, A. Kühner; H. Willner, E. Bernhardt, in EP 1 205 480 A2, **2002**.
[109] E. Bernhardt, G. Henkel, H. Willner, G. Pawelke, H. Bürger, *Chem. Eur. J.* **2001**, *7*, 4696–4705.
[110] U. Welz-Biermann, N. Ignat'ev, E. Bernhardt, M. Finze, H. Willner, in *WO 2004/072089A1*.
[111] Z.-B. Zhou, H. Matsumoto, K. Tatsumi, *Chem. Lett.* **2004**, *33*, 1636–1637.
[112] Z.-B. Zhou, M. Takeda, T. Fujii, M. Ue, *J. Electrochem. Soc.* **2005**, *152*, A351-A356.
[113] H. Matsumoto, in *Electrolytes for Lithium and Lithium-Ion Batteries* (Ed.: R. T. Jow, K. Xu, O. Borodin, M. Ue), Springer, **2014**, pp. 209-225..
[114] E. Zinigrad, L. Larush-Asraf, G. Salitra, M. Sprecher, D. Aurbach, *Thermochim. Acta* **2007**, *457*, 64–69.
[115] H. V. T. Nguyen, S. Lee, K. Kwak, K.-K. Lee, *Electrochim. Acta* **2019**, *321*, 134649.
[116] S. Zugmann, M. Fleischmann, M. Amereller, R. M. Gschwind, M. Winter, H. J. Gores, *J. Chem. Eng. Data* **2011**, *56*, 4786–4789.
[117] M. K. Schmidt, A. Kühner; H. Willner, E. Bernhardt, in EP 1 205 480 A2, **2002**.
[118] J. Scheers, J. Pitawala, F. Thebault, J.-K. Kim, J.-H. Ahn, A. Matic, P. Johansson, P. Jacobsson, *Phys. Chem. Chem. Phys.* **2011**, *13*, 14953–14959.
[119] A. Wang, S. Kadam, H. Li, S. Shi, Y. Qi, *NPJ Comput. Mater.* **2018**, *4*, 15.
[120] L. Suo, Y.-S. Hu, H. Li, M. Armand, L. Chen, *Nat. Commun.* **2013**, *4*, 1481.
[121] Q. P. X. Liang, I. R. Kochetkov, M. S. Sempere, H. Huang, X. Sun, *Nat. Energy* **2017**, *2*, 17119–17124.
[122] N. Delaporte, Y. Wang, K. Zaghib, *Front. Mater.* **2019**, *6*, 267.
[123] G. Wang, X. Xiong, D. Xie, X. Fu, Z. Lin, C. Yang, K. Zhang, M. Liu, *ACS Appl. Mater. Interfaces* **2019**, *11*, 4962–4968.
[124] K. Hayashi, Y. Nemoto, S.-i. Tobishima, J.-i. Yamaki, *Electrochim. Acta* **1999**, *44*, 2337–2344.
[125] O. Crowther, A. C. West, *J. Electrochem. Soc.* **2008**, *155*, A806-A811.
[126] D. Lin, Y. Liu, Y. Cui, *Nat. Nanotechnol.* **2017**, *12*, 194–206.
[127] a) J. Qian, W. A. Henderson, W. Xu, P. Bhattacharya, M. Engelhard, O. Borodin, J.-G. Zhang, *Nat. Commun.* **2015**, *6*, 6362; b) J. Qian, B. D. Adams, J. Zheng, W. Xu, W. A. Henderson, J. Wang, M. E. Bowden, S. Xu, J. Hu, J.-G. Zhang, *Adv. Funct. Mater.* **2016**, *26*, 7094–7102.
[128] A. Basile, A. I. Bhatt, A. P. O'Mullane, *Nat. Commun.* **2016**, *7*, 11794.
[129] A. Budi, A. Basile, G. Opletal, A. F. Hollenkamp, A. S. Best, R. J. Rees, A. I. Bhatt, A. P. O'Mullane, S. P. Russo, *J. Phys. Chem. C* **2012**, *116*, 19789–19797.
[130] A. Basile, A. I. Bhatt, A. P. O'Mullane, *Aus. J. Chem.* **2012**, *65*, 1534–1541.
[131] Y.-X. Yao, X.-Q. Zhang, B.-Q. Li, C. Yan, P.-Y. Chen, J.-Q. Huang, Q. Zhang, *InfoMat* **2019**, *2*, 379-388/a.
[132] D.-J. Yoo, K. J. Kim, J. W. Choi, *Adv. Energy Mater.* **2018**, *8*, 1702744.
[133] A. Basile, A. I. Bhatt, A. P. O'Mullane, *Electrochim. Acta* **2016**, *215*, 19–28.
[134] a) R. W. Laity, *Discuss. Faraday Soc.* **1961**, *32*, 172–180; b) H. J. V. Tyrrell, K. R. Harris, *Diffusion in Liquids*, Butterworths, London, **1984**, chapt. 8.3.
[135] K. R. Harris, *J. Phys. Chem. B* **2010**, *114*, 9572–9577.
[136] K. R. Harris, *Phys. Chem. Chem. Phys.* **2018**, *20*, 30041–30045.
[137] a) C. Sinistri, *J. Phys. Chem.* **1962**, *66*, 1600–1601; b) B. R. Sundheim, *J. Chem. Phys.* **1964**, *40*, 27–32; c) R. Haase, *Thermodynamics of Irreversible Processes*, Addison-Wesley, Reading, Mass., **1969**; corrected ed., Dover Publications Inc, New York, **1990**, chapt. 4.16; d) S. K. Ratkje, H. Rajabu, T. Førland, *Electrochim. Acta* **1993**, *38*, 415–423.
[138] a) M. Gouverneur, J. Kopp, L. van Wüllen, M. Schönhoff, *Phys. Chem. Chem. Phys.* **2015**, *17*, 30680–30686; b) M. Gouverneur, F. Schmidt, M. Schönhoff, *Phys. Chem. Chem. Phys.* **2018**, *20*, 7470–7478; c) M. Schönhoff, C. Cramer, F. Schmidt, *Phys. Chem. Chem. Phys.* **2018**, *20*, 30046–30052.
[139] a) R. W. Laity, *J. Chem. Phys.* **1959**, *30*, 682–691; b) R. W. Laity, *J. Phys. Chem.* **1959**, *63*, 80–83.
[140] a) K. R. Harris, M. Kanakubo, *J. Phys. Chem. B* **2016**, *120*, 12937–12949; b) K. R. Harris, *J. Phys. Chem. B* **2019**, *123*, 7014–7023.
[141] R.. Takagi, K. Kawamura, *Bull. Tokyo Inst. Technol.* **1975**, *127*, 57–62.
[142] a) R. W. Laity, *Ann. N. Y. Acad. Sci.* **1960**, *79*, 997–1022; b) K. R. Harris, *J. Phys. Chem. B* **2016**, *120*, 12135–12147.
[143] H. Watanabe, T. Umecky, N. Arai, A. Nazet, T. Takamuku, K. R. Harris, Y. Kameda, R. Buchner, Y. Umebayashi, *J. Phys. Chem. B* **2019**, *123*, 6244–6252.
[144] a) H. Shobukawa, H. Tokuda, S.-I. Tabata, M. Watanabe, *Electrochim. Acta* **2004**, *50*, 1–5; b) K. R. Harris, *Electrochim. Acta* **2020**, *337*, 135806.
[145] a) K. R. Harris, M. Kanakubo, *Phys. Chem. Chem. Phys.* **2015**, *17*, 23977–23993; b) K. R. Harris, M. Kanakubo, D. Kodama, T. Makino, Y. Mizuguchi, M. Watanabe, T. Watanabe, *J. Chem. Eng. Data* **2018**, *63*, 2015–2027.
[146] H. Schönert, *J. Phys. Chem.* **1984**, *88*, 3359–3363.
[147] a) J. A. Padró, J. Trullàs, G. Sesé, *Mol. Phys.* **1991**, *72*, 1035–1049; b) J. Trullàs, J. A. Padró, *Phys. Rev. B* **1997**, *55*, 12210–12217.
[148] a) H.-G. Hertz, *Ber. Bunsen-Ges.* **1977**, *81*, 656–664; b) L. A. Woolf, K. R. Harris, *J. Chem. Soc. Faraday Trans. 1* **1978**, *74*, 933–947; c) D. G. Miller, *J. Phys. Chem.* **1981**, *85*, 1137–1146.
[149] H. L. Friedman, R. Mills, *J. Solution Chem.* **1986**, *15*, 69–80.
[150] H. K. Kashyap, H. V. R. Annapureddy, F. O. Raineri, C. J. Margulis, *J. Phys. Chem. B* **2011**, *115*, 13212–13221.
[151] Z. Zhang, B. K. Wheatle, J. Krajniak, J. R. Keith, V. Ganesan, *ACS Macro Lett.* **2020**, *9*, 84–89.
[152] a) K. R. Harris, *J. Chem. Phys.* **2009**, *131*, 054503; b) K. R. Harris, *J. Mol. Liq.* **2016**, *222*, 520–534.
[153] a) K. R. Harris, M. Kanakubo, N. Tsuchihashi, K. Ibuki, M. Ueno, *J. Phys. Chem. B* **2008**, *112*, 9830–9840; b) K. R. Harris, M. Kanakubo, *Faraday Discuss.* **2012**, *154*, 425–438.
[154] a) T. Rüther, K. R. Harris, M. D. Horne, M. Kanakubo, T. Rodopoulos, J.-P. Veder, L. A. Woolf, *Chem. Eur. J.* **2013**, *19*, 17733–17744; b) K. R. Harris, T. Makino, M. Kanakubo, *Phys. Chem. Chem. Phys.* **2014**, *16*, 9161–9170.
[155] K. R. Harris, M. Kanakubo, *J. Chem. Eng. Data* **2016**, *61*, 2399–2411.
[156] a) H. Tokuda, S. Tsuzuki, M Abu Bin Hassan Susan, K. Hayamizu, M. Watanabe, *J. Phys. Chem. B* **2006**, *110*, 19593–19600; b) K. Ueno, H. Tokuda, M. Watanabe, *Phys. Chem. Chem. Phys.* **2010**, *12*, 1649–1658.
[157] M. Kanakubo, K. R. Harris, N. Tsuchihashi, K. Ibuki, M. Ueno, *J. Phys. Chem. B* **2007**, *111*, 2062–2069.
[158] a) J. P. Hansen, I. R. McDonald, *J. Phys. C* **1974**, *7*, L384-L386; b) J. P. Hansen, I. R. McDonald, *Phys. Rev. A* **1975**, *11*, 2111–2123.
[159] K. Kubota, Z. Siroma, H. Sano, S. Kuwabata, H. Matsumoto, *J. Phys. Chem. C* **2018**, *122*, 4144–4149.
[160] a) W. Xu, C. A. Angell, *Science* **2003**, *302*, 422; b) W. Xu, E. I. Cooper, C. A. Angell, *J. Phys. Chem. B* **2003**, *107*, 6170–6178; c) M. Yoshizawa, W. Xu, C. A. Angell, *J. Am. Chem. Soc.* **2003**, *125*, 15411–15419.
[161] C. Schreiner, S. Zugmann, R. Hartl, H. J. Gores, *J. Chem. Eng. Data* **2010**, *55*, 1784–1788.
[162] M. D. Galluzzo, W. S. Loo, A. A. Wang, A. Walton, J. A. Maslyn, N. P. Balsara, *J. Phys. Chem. B* **2020**, *124*, 921–935.
[163] a) J. Richter, *Ber. Bunsen-Ges.* **1974**, *78*, 972–977; b) J. Richter, *Ber. Bunsen-Ges.* **1974**, *78*, 977–981.
[164] P. J. Dunlop, *J. Phys. Chem.* **1965**, *69*, 1693–1699.
[165] K. Hayamizu, in *Annual Reports on NMR Spectroscopy, Vol. 98* (Ed.: G. A. Webb), Academic Press, London, **2019**, chapt. 2.

[166] J. R. Sangoro, C. Iacob, S. Naumov, R. Valiullin, H. Rexhausen, J. Hunger, R. Buchner, V. Strehmel, J. Kärger, F. Kremer, *Soft Matter* **2011**, *7*, 1678–1681.
[167] a) M. H. Rausch, J. Lehmann, A. Leipertz, A.-P. Fröba, *Phys. Chem. Chem. Phys.* **2011**, *13*, 9525–9533; b) T. M. Koller, A. Heller, M. H. Rausch, P. Wasserscheid, I. G. Economou, A.-P. Fröba, *J. Phys. Chem. B* **2015**, *119*, 8583–8592.
[168] D. M. Pesko, K. Timachova, R. Bhattacharya, M. C. Smith, I. Villaluenga, J. Newman, N. P. Balsara, *J. Electrochem. Soc.* **2017**, *164*, E3569-E3575.
[169] a) *Impedance Spectroscopy; Theory, Experiment, and Applications*, Eds.: E. Barsoukov, J. R. Macdonald), Wiley Interscience Publications New York, **2005**, 2nd ed.; b) M. Kanakubo, K. R. Harris, N. Tsuchihashi, K. Ibuki, M. Ueno, *J. Chem. Eng. Data* **2015**, *60*, 1495–1503.
[170] M. Spiro, in *Physical Methods of Chemistry, Electrochemical Methods, Vol. 2*, 2nd ed. (Ed.: B. W. H. Rossiter, J. F. Hamilton), John Wiley and Sons Inc, New York, **1986**, chapt. 8.
[171] a) P. G. Bruce, C. A. Vincent, *J. Electroanal. Chem. Interfacial Electrochem.* **1987**, *225*, 1–17; b) J. Evans, C. A. Vincent, P. G. Bruce, *Polymer* **1987**, *28*, 2324–2328.
[172] a) Y. Ma, M. Doyle, T. F. Fuller, M. M. Doeff, L. C. De Jonghe, J. Newman, *J. Electrochem. Soc.* **1995**, *142*, 1859–1868; b) D. M. Pesko, S. Sawhney, J. Newman, N. P. Balsara, *J. Electrochem. Soc.* **2018**, *165*, A3014-A3021.
[173] M. Holz, O. Lucas, C. Müller, *J. Magn. Reson.* **1984**, *58*, 294–305.
[174] F. Wohde, M. Balabajew, B. Roling, *J. Electrochem. Soc.* **2016**, *163*, A714-A721.
[175] N. Craig, S. A. Mullin, R. Pratt, G. B. Crane, *J. Electrochem. Soc.* **2019**, *166*, A2769-A2775.
[176] S. Zugmann, M. Fleischmann, M. Amereller, R. M. Gschwind, H. D. Wiemhöfer, H. J. Gores, *Electrochim. Acta* **2011**, *56*, 3926–3933.
[177] a) N. Molinari, J. P. Mailoa, B. Kozinsky, *J. Phys. Chem. Lett.* **2019**, *10*, 2313–2319; b) N. Molinari, J. P. Mailoa, N. Craig, J. Christensen, B. Kozinsky, *J. Power Sources* **2019**, *428*, 27–36; c) P. Kubisiak, P. Wróbel, A. Eilmes, *J. Phys. Chem. B* **2020**, *124*, 413–421.
[178] a) J. B. Haskins, W. R. Bennett, J. J. Wu, D. M. Hernández, O. Borodin, J. D. Monk, C. W. Bauschlicher, J. W. Lawson, *J. Phys. Chem. B* **2014**, *118*, 11295–11309; b) V. Lesch, Z. Li, D. Bedrov, O. Borodin, A. Heuer, *Phys. Chem. Chem. Phys.* **2016**, *18*, 382–392; c) P. Ray, T. Vogl, A. Balducci, B. Kirchner, *J. Phys. Chem. B* **2017**, *121*, 5279–5292; d) P. Ray, A. Balducci, B. Kirchner, *J. Phys. Chem. B* **2018**, *122*, 10535–10547; e) H. Liu, E. J. Maginn, *J. Chem. Phys.* **2013**, *139*, 114508-1–114508-10; f) T. C. Lourenço, Y. Zhang, L. T. Costa, E. J. Maginn, *J. Chem. Phys.* **2018**, *148*, 193834-1–193834-9; g) Q. Huang, T. C. Lourenço, L. T. Costa, Y. Zhang, E. J. Maginn, B. Gurkan, *J. Phys. Chem. B* **2019**, *123*, 516–527; h) J. Tong, X. Xiao, X. Liang, N. von Solms, F. Huo, H. He, S. Zhang, *Phys. Chem. Chem. Phys.* **2019**, *21*, 19216–19225; i) A. T. Nasrabadi, V. Ganesan, *J. Phys. Chem. B* **2019**, *123*, 5588–5600.
[179] a) C. J. F. Solano, S. Jeremias, E. Paillard, D. Beljonne, R. Lazzaroni, *J. Chem. Phys.* **2013**, *139*, 034502; b) K. Hayamizu, S. Tsuzuki, S. Seki, K. Fujii, M. Suenaga, Y. Umebayashi, *J. Chem. Phys.* **2010**, *133*, 194505-1–194505-13; c) J. M. Vicent-Luna, J. M. Ortiz-Roldan, S. Hamad, R. Tena-Zaera, S. Calero, J. A. Anta, *ChemPhysChem* **2016**, *17*, 2473–2481; d) F. Castiglione, M. Moreno, G. Raos, A. Famulari, A. Mele, G. B. Appetecchi, S. Passerini, *J. Phys. Chem. B* **2009**, *113*, 10750–10759; e) F. Castiglione, A. Famulari, G. Raos, S. V. Meille, A. Mele, G. B. Appetecchi, S. Passerini, *J. Phys. Chem. B* **2014**, *118*, 13679–13688; f) M. Kunze, E. Paillard, S. Jeong, G. B. Appetecchi, M. Schönhoff, M. Winter, S. Passerini, *J. Phys. Chem. C* **2011**, *115*, 19431–19436; g) T. Frömling, M. Kunze, M. Schönhoff, J. Sundermeyer, B. Roling, *J. Phys. Chem. B* **2008**, *112*, 12985–12990; h) T. Vogl, S. Menne, R.-S. Kühnel, A. Balducci, *J. Mater. Chem. A* **2014**, *2*, 8258–8265; i) G. A. Giffin, A. Moretti, S. Jeong, K. Pilar, M. Brinkkötter, S. G. Greenbaum, M. Schönhoff, S. Passerini, *ChemSusChem* **2018**, *11*, 1981–1989; j) P. Nürnberg, E. I. Lozinskaya, A. S. Shaplov, M. Schönhoff, *J. Phys. Chem. B* **2020**, *124*, 861–870.
[180] a) K. Hayamizu, S. Tsuzuki, S. Seki, Y. Umebayashi, *J. Chem. Phys.* **2011**, *135*, 084505; b) H. Srour, M. Traikia, B. Fenet, H. Rouault, M. F. Costa Gomes, C. C. Santini, P. Husson, *J. Solution Chem.* **2015**, *44*, 495–510; c) S. Duluard, J. Grondin, J.-L. Bruneel, I. Pianet, A. Grélard, G. Campet, M.-H. Delville, J.-C. Lassègues, *J. Raman Spectrosc.* **2008**, *39*, 627–632; d) T.-Y. Wu, Y.-H. Wang, S.-G. Su, Y.-C. Lin, C.-W. Kuo, J.-K. Chang, I. W. Sun, *J. Chem. Eng. Data* **2015**, *60*, 471–483; e) T.-Y. Wu, L. Hao, P.-R. Chen, J.-W. Liao, *Int. J. Electrochem. Sci.* **2013**, *8*, 2606–2624; f) F. F. C. Bazito, Y. Kawano, R. M. Torresi, *Electrochim. Acta* **2007**, *52*, 6427–6437; g) M. J. Monteiro, F. F. Camilo, M. C. C. Ribeiro, R. M. Torresi, *J. Phys. Chem. B* **2010**, *114*, 12488–12494.
[181] a) F. U. Shah, O. I. Gnezdilov, A. Filippov, *Phys. Chem. Chem. Phys.* **2017**, *19*, 16721–16730; b) V. L. Martins, N. Sanchez-Ramirez, M. C. C. Ribeiro, R. M. Torresi, *Phys. Chem. Chem. Phys.* **2015**, *17*, 23041–23051; c) T. Umecky, K. Suga, E. Masaki, T. Takamuku, T. Makino, M. Kanakubo, *J. Mol. Liq.* **2015**, *209*, 557–562; d) C.-W. Kuo, L. Hao, P.-L. Kuo, P.-R. Chen, T.-Y. Wu, *J. Inst. Chem.* **2014**, *45*, 1270–1279; e) Y.-C. Lin, C.-W. Kuo, P.-L. Kuo, L. Hao, L.-Y. Tseng, T.-Y. Wu, *J. Inst. Chem.* **2015**, *53*, 22–31; f) T.-Y. Wu, S.-G. Su, Y.-H. Wang, Y.-C. Lin, J.-K. Chang, C.-W. Kuo, I. W. Sun, *J. Inst. Chem.* **2016**, *60*, 138–150.
[182] a) C. R. Pope, M. Kar, D. R. MacFarlane, M. Armand, M. Forsyth, L. A. O'Dell, *ChemPhysChem* **2016**, *17*, 3187–3195; b) M. Forsyth, H. Yoon, F. Chen, H. Zhu, D. R. MacFarlane, M. Armand, P. C. Howlett, *J. Phys. Chem. C* **2016**, *120*, 4276–4286; c) F. S. Oliveira, E. J. Cabrita, S. Todorovic, C. E. S. Bernardes, J. N. Canongia Lopes, J. L. Hodgson, D. R. MacFarlane, L. P. N. Rebelo, I. M. Marrucho, *Phys. Chem. Chem. Phys.* **2016**, *18*, 2756–2766.
[183] a) J.-C. Lassègues, J. Grondin, C. Aupetit, P. Johansson, *J. Phys. Chem. A* **2009**, *113*, 305–314; b) Y. Umebayashi, H. Hamano, S. Seki, B. Minofar, K. Fujii, K. Hayamizu, S. Tsuzuki, Y. Kameda, S. Kohara, M. Watanabe, *J. Phys. Chem. B* **2011**, *115*, 12179–12191; c) K. Fujii, H. Hamano, H. Doi, X. Song, S. Tsuzuki, K. Hayamizu, S. Seki, Y. Kameda, K. Dokko, M. Watanabe, Y. Umebayashi, *J. Phys. Chem. C* **2013**, *117*, 19314–19324; d) Y. Saito, T. Umecky, J. Niwa, T. Sakai, S. Maeda, *J. Phys. Chem. B* **2007**, *111*, 11794–11802.
[184] J. B. Haskins, C. W. Bauschlicher, J. W. Lawson, *J. Phys. Chem. B* **2015**, *119*, 14705–14719.
[185] Q. Huang, Y.-Y. Lee, B. Gurkan, *Ind. Eng. Chem. Res.* **2019**, *58*, 22587–22597.
[186] S. Chen, J. Ishii, S. Horiuchi, M. Yoshizawa-Fujita, E. I. Izgorodina, *Phys. Chem. Chem. Phys.* **2017**, *19*, 17366–17372.
[187] E. G. D. Cohen, *Physica A* **1993**, *194*, 229–257.
[188] T. Kiyobayashi, T. Kojima, H. Ozaki, K. Kiyohara, *J. Chem. Phys.* **2019**, *151*, 074503.
[189] I. Okada, *J. Mol. Liq.* **1999**, *83*, 5–22.
[190] a) R. Lenke, W. Uebelhack, A. Klemm, *Z. Naturforsch. A* **1973**, *28*, 881–884; b) V. Sarou-Kanian, A.-L. Rollet, M. Salanne, C. Simon, C. Bessada, P. A. Madden, *Phys. Chem. Chem. Phys.* **2009**, *11*, 11501–11506.
[191] P. Schmitz, R. Jakelski, M. Pyschik, K. Jalkanen, S. Nowak, M. Winter, P. Bieker, *ChemSusChem* **2017**, *10*, 876–883.
[192] F. Chen, M. Forsyth, *Phys. Chem. Chem. Phys.* **2016**, *18*, 19336–19344.
[193] T. M. Koller, J. Ramos, P. S. Schulz, I. G. Economou, M. H. Rausch, A.-P. Fröba, *J. Phys. Chem. B* **2017**, *121*, 4145–4157.
[194] V. Chaudoy, J. Jacquemin, F. Tran-Van, M. Deschamps, F. Ghamouss, *Pure Appl. Chem.* **2019**, *91*, 1361-1381.
[195] S. Tsuzuki, K. Kubota, H. Matsumoto, *J. Phys. Chem. B* **2013**, *117*, 16212–16218.
[196] O. Borodin, G. A. Giffin, A. Moretti, J. B. Haskins, J. W. Lawson, W. A. Henderson, S. Passerini, *J. Phys. Chem. C* **2018**, *122*, 20108–20121.
[197] T. Méndez-Morales, J. Carrete, S. Bouzón-Capelo, M. Pérez-Rodríguez, Ó. Cabeza, L. J. Gallego, L. M. Varela, *J. Phys. Chem. B* **2013**, *117*, 3207–3220.
[198] P. Kubisiak, A. Eilmes, *J. Phys. Chem. B* **2017**, *121*, 9957–9968.
[199] a) P. Y. Zavalij, S. Yang, M. S. Whittingham, *Acta Crystallogr. Sect. B* **2003**, *59*, 753–759; b) T. Afroz, D. M. Seo, S.-D. Han, P. D. Boyle, W. A. Henderson, *J. Phys. Chem. C* **2015**, *119*, 7022–7027.
[200] T. Umecky, Y. Saito, Y. Okumura, S. Maeda, T. Sakai, *J. Phys. Chem. B* **2008**, *112*, 3357–3364.
[201] W. A. Henderson, F. McKenna, M. A. Khan, N. R. Brooks, V. G. Young, R. Frech, *Chem. Mater.* **2005**, *17*, 2284–2289.
[202] K. Matsumoto, R. Hagiwara, O. Tamada, *Solid State Sci.* **2006**, *8*, 1103–1107.
[203] O. Borodin, G. D. Smith, W. Henderson, *J. Phys. Chem. B* **2006**, *110*, 16879–16886.
[204] J. L. Nowinski, P. Lightfoot, P. G. Bruce, *J. Mater. Chem.* **1994**, *4*, 1579–1580.
[205] L. Xue, C. W. Padgett, D. D. DesMarteau, W. T. Pennington, *Solid State Sci.* **2002**, *4*, 1535–1545.
[206] K. Matsumoto, T. Matsui, T. Nohira, R. Hagiwara, *J. Fluorine Chem.* **2015**, *174*, 42–48.
[207] M. Beran, J. Příhoda, Z. Žák, M. Černík, *Polyhedron* **2006**, *25*, 1292–1298.
[208] M. Tremayne, P. Lightfoot, M. A. Mehta, P. G. Bruce, K. D. M. Harris, K. Shankland, C. J. Gilmore, G. Bricogne, *J. Solid State Chem.* **1992**, *100*, 191–196.

[209] O. Reckeweg, F. J. DiSalvo, A. Schulz, B. Blaschkowski, S. Jagiella, T. Schleid, *Z. Anorg. Allg. Chem.* **2014**, *640*, 851–855.
[210] F. S. Gittleson, D. K. Ward, R. E. Jones, R. A. Zarkesh, T. Sheth, M. E. Foster, *Phys. Chem. Chem. Phys.* **2019**, *21*, 17176–17189.
[211] K. Matsumoto, E. Nishiwaki, T. Hosokawa, S. Tawa, T. Nohira, R. Hagiwara, *J. Phys. Chem. C* **2017**, *121*, 9209–9219.
[212] K. Matsumoto, R. Hagiwara, Z. Mazej, E. Goreshnik, B. Žemva, *J. Phys. Chem. B* **2006**, *110*, 2138–2141.
[213] G. A. Sharpataya, K. S. Gavrichev, V. N. Plakhotnik, *Zh. Neorg. Khim.* **1997**, *42*, 649-654 .
[214] P. Y. Zavalij, S. Yang, M. S. Whittingham, *Acta Crystallogr. Sect. B* **2004**, *B60*, 716-724.

Manuscript received: January 30, 2020
Revised manuscript received: March 23, 2020
Accepted manuscript online: March 25, 2020
Version of record online: April 29, 2020